EXPERIMENTAL DETERMINATION OF THE SOLUBILITIES OF ETHANE IN SELECTED N-PARAFFIN SOLVENTS

By

AARON MICHAEL RAFF II

Bachelor of Science in Chemical Engineering

Oklahoma State University

Stillwater, Oklahoma

1986

Submitted to the faculty of the
Graduate College of the
Oklahoma State University
in partial fulfillment of
the requirements for
the Degree of
MASTER OF SCIENCE
May, 1989

EXPERIMENTAL DETERMINATION OF THE SOLUBILITIES OF ETHANE IN SELECTED N-PARAFFIN SOLVENTS

Thesis Approved:

Robert Robinson Jr
Thesis Adviser

Arland H. Johannes

Luther C. Glaser

Norman N. Durham
Dean of the Graduate College

PREFACE

An existing solubility apparatus was modified for the continuation of study on binary mixtures. The systems run for this study include carbon dioxide in benzene, and ethane in n-hexane, n-eicosane, n-hexatriacontane, and n-tetratetracontane at temperatures ranging from 40 C to 150 C and pressures up to 1800 psi. The interaction parameters in the Soave and Peng-Robinson equations of state were regressed from the solubility data and comparisons were made with previous investigators. The data was also added to a current data base of ethane + paraffins and used to determine interaction parameters. The significance of these results are discussed.

I would like to thank my advisor, Professor Robert L. Robinson, for the guidance and help he so readily donated to this project. I believe his demands for work in excess of normal requirements will prove beneficial to me in the future.

I would also like to thank Dr. K. A. M. Gasem for his persistence and support in several facets of this investigation.

I must also acknowledge the assistance of Mr. J. L. Mapes, Mr. M. H. Hraban, and Ms. L. R. Martin for their efforts in obtaining experimental data.

Special thanks are due Mr. P. B. Dulcamara and Mr. T. P. Seagraves for their aid, and for their friendship, which has made my time spent in lab enjoyable, as well as educational.

Financial support was gratefully received from Texas Eastman and project funding from the Department of Energy.

Finally my greatest appreciation, thanks, and love go to my family, Dr. L. M. Raff, Mrs. M. J. Raff, and Ms. L. D. Griffin, who wanted this as much or more than I.

TABLE OF CONTENTS

LIST OF TABLES

LIST OF FIGURES

Figure page

CHAPTER I

INTRODUCTION

In recent years there has been a growing interest in enhanced oil recovery from petroleum reservoirs, as well as alternate sources of energy such as the conversion of coal to fluid fuels. In such processes, multiphase fluids are present in all stages of operation, yet data are scarce concerning phase equilibrium in these areas. However, models can be developed to represent multiphase, multicomponent mixtures based on data taken on binary systems of similar compounds. The major aim of this study is the collection of such data.

This work was a continuation of the study of binary vapor-liquid phase behavior for selected solute gases (e.g. carbon dioxide, ethane) in a series of heavy hydrocarbon solvents. The present study focused on binary vapor-liquid equilibrium data involving ethane and the heavy paraffins; n-hexane (n-C6), n-eicosane (n-C20), n-hexatriacontane (n-C36), and n-tetratetracontane (n-C44). These data were used to determine interaction parameters for the Soave and Peng-Robinson equations of state (EOS), as well as values for Henry's constants and partial molar volumes. Also studied was the generalization of interaction parameters for ethane for a wide spectrum of n-paraffinic solvents. From this,

the effects of temperature and solvent size on interaction parameter values were determined. These studies provide a valuable addition to previously reported solubility data for ethane in heavy paraffins, and the combined studies should facilitate the further development and testing of correlations used to describe the phase behavior of multiphase, multicomponent systems.

CHAPTER II

LITERATURE REVIEW

Experimental Data

A review of pertinent vapor-liquid equilibrium literature for CO2 + benzene and ethane + n-paraffins was performed. A summary of the references obtained is given in Table I. The referenced CO2 + benzene measurements each contain an isotherm at 40 C, and they were used in the evaluation of the apparatus and procedures used in the present work. Experimental results for CO2 + benzene appear in Chapter VII.

The ethane + n-paraffin data of Table I were used to determine equation-of-state binary interaction parameters. Whenever possible, OSU data were used for a binary system; these data have been compared with other investigator's data, when available. The temperature ranges listed in Table I are those used in the analysis of the present work, not necessarily the complete range of the reported data. The minimum temperature used in the study was 310.9 K, which is above the critical value for ethane. Confining experimental work to conditions above the critical temperature of ethane eliminated problems associated with a two-phase solute; further, most of the applications of the

TABLE I

SUMMARY OF REFERENCES FOR BINARY SYSTEMS CONTAINING ETHANE

System	Reference Number	Temperature Range, K	Pressure Range, bar
CO_2 + Benzene	1	313.2	16.4 - 55.7
CO_2 + Benzene	2	313.2	12.5 - 55.2
CO_2 + Benzene	3	313.2	7.6 - 51.7
CO_2 + Benzene	4	313.2-393.2	5.0 - 59.5
CO_2 + Benzene	5	313.2-393.2	6.2 -132.9
CO_2 + Benzene	6	298.2-313.2	8.9 - 77.5
CO_2 + Benzene	7	313.2	11.8 - 30.3
C_2H_6 + n-C_3	8	322.0-366.5	17.2 - 51.7
C_2H_6 + n-C_4	9	338.7-394.3	32.4 - 55.5
C_2H_6 + n-C_5	10	310.9-444.3	3.6 - 62.1
C_2H_6 + n-C_6	11	338.7-449.8	1.7 - 75.8
C_2H_6 + n-C_7	12	338.7-449.8	31.4 - 83.8
C_2H_6 + n-C_8	13	323.2-373.2	4.1 - 52.7
C_2H_6 + n-C_{10}	2	310.9-410.9	4.2 - 82.4
C_2H_6 + n-C_{12}	14	373.2	11.1 - 53.2
	15	373.2	4.1 - 62.8
	16	373.2	6.6 - 52.7
C_2H_6 + n-C_{20}	14	323.2-423.2	4.7 - 76.9
C_2H_6 + n-C_{28}	14	348.2-423.2	5.4 - 51.8
C_2H_6 + n-C_{36}	14	373.2-423.2	2.9 - 47.6

data are at conditions above 310 K. Each system was analyzed using only solubility data (T,P,x) to achieve consistency among the different sources. During analysis of the data, no pressures above 90% of the critical pressure for that system were used. This was done to avoid entering the near-critical region where essentially all contemporary equations of state (EOS) become inherently inaccurate.

During the course of the literature survey several sources for multicomponent data containing ethane were discovered. These sources might prove useful in correlation development, and are shown in Table II.

Experimental Apparatus

A multitude of methods exist for measuring vapor-liquid equilibrium (VLE) data, and all contain the means of measuring at least three of the four variables used in solubility determination. These values are temperature, pressure, liquid composition, and vapor composition. Two of the most popular methods are (25):

1) Isothermal: A sample of known composition is confined at constant temperature and the pressure is varied.

2) Isobaric: A sample of known composition is confined at constant pressure and the temperature is varied.

After data are collected, three major methods are used to determine the bubble point of the mixture. The first is by visual sighting. When this method is used, the pressure and temperature of the system are recorded at the sighting of a phase change. This method contains the inherent problem that it is very difficult to construct a cell that allows

TABLE II

SUMMARY OF REFERENCES FOR MULTICOMPONENT ETHANE SYSTEMS

System	Reference	Temperature Range, K	Pressure Range, bar
C1 + C2 + C3	17	158.2-213.7	0.18-60.33
	18	144.2-224.2	7.16-68.50
C1 + C2 + C6	19	186.6-204.0	39.2-59.40
C1 + C2 + C7	19	167.9-210.2	21.1-61.87
	20	222.0-244.3	6.89-68.95
C2 + C3 + C4	21	304.6-306.5	6.57-49.25
	22	304.3-307.0	45.0-49.22
C2 + C4 + C6	23	321.5-403.8	23.7-67.91
C2 + C4 + C7	24	422.0-449.8	35.3-83.15

for accurate observation of phase change under all circumstances. The second method of bubble point determination is the analytical approach. Since the overall composition of the sample is known, the point at which the material becomes single-phase (the bubble point) can be determined by monitoring the liquid phase and noting when its composition first becomes equal to the overall composition of the mixture. However, this method is time consuming and requires considerably more equipment than other methods. The third method that is frequently used is a graphical analysis of the collected data. By decreasing the volume of the cell in small increments and plotting the resulting cell pressure versus the change in cell volume two straight lines are obtained; one line for the two-phase region and one line for the single-phase region. By extrapolating the lines to their point of intersection, the pressure at which the phase change occures can be accurately predicted. The graphical analysis is the method used in this study.

Several types of equilibrium cells are used to measure solubility data. One type of cell is the constant composition, variable volume piston cell (26). In this type of cell a piston is used to decrease the volume of the mixture, thereby increasing the pressure and forcing the solution toward a single-phase condition. In other types of cells, the solid piston is replaced by mercury (27), as in the present study. In fact, using mercury as the piston has the added benefit of enhanced stirring. As the material is

agitated in the cell, through rocking or internal stirring, the mercury helps to combine the components of the mixture, creating an effect similar to ball bearings in a can of spray paint. Another popular type of cell is the constant volume variable composition apparatus, in which the volume of the cell is constant and the mixture is altered by the injection of one of the components. By careful monitoring of the injections, the composition of the mixture at the point of phase change can be determined. These types of cells do not cover the entire range of cell designs; for example, one cell was designed as a bellows to allow for volume variations at low pressures (29).

CHAPTER III

REVIEW OF THEORY

Classical thermodynamics provides the mathematical framework for optimization of existing equations of state using the data obtained in this study. A review of phase equilibrium thermodynamics will develop the concepts used in current equations used for vapor-liquid equilibrium property determination.

This study involves the determination of bubble point pressures for binary mixtures which include ethane. The bubble point pressure of a mixture must exist at phase equilibrium as governed by the laws of thermodynamics. Under these laws, a system of a specified number of phases, comprised of any number of nonreactive components at equilibrium, must satisfy the three criteria of thermal, mechanical, and specie equilibrium. These three conditions can be stated as follows (30):

(1) The phases must be at the same temperature.

$$T' = T'' = \ldots = T^{M} \tag{3.1}$$

(2) The phases must be at the same pressure.

$$P' = P'' = \ldots = P^{M} \tag{3.2}$$

(3) The chemical potential for each specie must be identical in all phases.

$$u_i' = u_i'' = \ldots = u_i^{M} \quad (i = 1,N) \tag{3.3}$$

where M is the number of phases and N is the number of components.

In preference to quantifying the equilibrium condition in terms of the chemical potentials, a better behaved function, the fugacity (f), has been defined. Using fugacity, Equation (3.3) can be expressed as:

$$f_i' = f_i'' = \ldots = f_i^{M} \quad (i = 1,N) \tag{3.4}$$

where $f = f(T,P,x)$.

The relationship between fugacity and chemical potential is most easily seen for an ideal gas. The chemical potential for an ideal gas can be stated as (31):

$$\left(\partial\mu_i / \partial P\right)_{T,n} = \bar{V}_i = RT/P \tag{3.5}$$

which when integrated yields

$$\bar{\mu}_i - \mu_i^{+} = RT \ln\left(P/P^{+}\right) \tag{3.6}$$

where $(\bar{\mu}_i - \mu_i^{+})$ is the difference between the chemical potential of the pure substance and its value in some reference state. A similar relation applies to an ideal gas mixture, where the chemical potential of each component depends upon its partial pressure, Py_i.

$$\bar{\mu}_i - \mu_i^{+} = RT \ln\left(Py_i/P^{+}\right) \tag{3.7}$$

To retain the simplicity of the above equation for nonideal systems, a second function, fugacity, is defined in relationship to chemical potential as

$$d\mu = RT\, d \ln f \quad (T = \text{CONSTANT}) \tag{3.8}$$

where

$$\lim_{P \to 0} \left(f_i / P y_i \right) = 1.0 \tag{3.9}$$

Thus equation (3.7) is rewriten:

$$\bar{\mu}_i - \mu_i^+ = RT \ln \left(f_i / P^+ \right) \tag{3.10}$$

There are two standard methods used in the evaluation of fugacities, both are based on property deviations from an ideal reference. This study used an ideal gas as the reference state. This approach uses a fugacity coefficient, ϕ, which is defined as the difference of fugacity in an actual mixture and that of an ideal mixture (31).

$$\phi = \frac{\text{fugacity of component "i" in a mixture}}{\text{fugacity of component "i" in an ideal gas mixture}}$$

For an ideal gas mixture, the fugacity of a component in the mixture is given by

$$f_i = P x_i \tag{3.11}$$

and by definition

$$f_i = \phi P x_i \tag{3.12}$$

The fugacity coefficient is related to the volumetric properties of a mixture by the following equation:

$$\ln \phi = \frac{1}{RT} \int_0^P \left(\bar{V}_i - RT/P \right) dP \tag{3.13}$$

where $\bar{V}_i$ is the partial molar volume of component "i".

This study utilized two equations of state as models for the behavior of two component mixtures at vapor-liquid equilibrium. Subsequently, the fugacity coefficients were evaluated using equation (3.13).

Equations of State

This study utilized two equations of state (EOS) that are widely used by industry to model the behavior of the systems investigated. The first EOS is the Soave-Redlich-Kwong (SRK) equation (32).

$$P = \frac{RT}{V-b} - \frac{a(T)}{V(V+b)} \tag{3.14}$$

The parameter combination rules used in the present study may be written as

$$a(T) = \sum_i \sum_j y_i y_j a_{ij} \tag{3.15}$$

$$b = \sum_i \sum_j y_i y_j b_{ij} \tag{3.16}$$

$$a_{ij} = \sqrt{a_i a_j}\ (1 - C_{ij}) \tag{3.17}$$

$$b_{ij} = 0.5\,(b_i + b_j)\,(1 + D_{ij}) \tag{3.18}$$

where

$$a_i = 0.42747\,R^2 T_{ci}^{\,2}\,\alpha_i(T_{ri})/P_{ci} \tag{3.19}$$

$$\alpha_i(T_{ri}) = \left[1 + m_i\left(1 - T_{ri}^{\,0.5}\right)\right]^2 \tag{3.20}$$

$$m_i = 0.480 + 1.574\,w_i - 0.176\,w_i^{\,2} \tag{3.21}$$

$$b_i = 0.08664\,RT_{ci}/P_{ci} \tag{3.22}$$

The second EOS used in this study was the Peng-Robinson (P-R) equation (33).

$$P = RT/(v-b) - a(T)/(v(v+b)+b(v-b)) \qquad (3.23)$$

where

$$a_i = 0.45724 R^2 T_{c_i}^2 \alpha_i(T_{r_i})/P_{c_i} \qquad (3.24)$$

$$\alpha_i(T_{r_i}) = [1 + k_i(1 - T_{r_i}^{0.5})]^2 \qquad (3.25)$$

$$k_i = 0.37464 + 1.5422\omega_i - 0.26992\omega_i^2 \qquad (3.26)$$

$$b_i = 0.07780\, RT_{c_i}/P_{c_i} \qquad (3.27)$$

and a(T), b, a_{ij}, and b_{ij} are evaluated by equations (3.15) through (3.18).

In these equations, Cij and Dij are empirical "binary interaction parameters" which characterize interactions between component "i" and component "j". Most investigators use only one interaction parameter, but it has been shown in earlier studies that the use of a second interaction parameter greatly increases the accuracy of solubility predictions (34).

The optimum values of Cij and Dij (the values of these factors which result in optimized equation of state to experimental data) were determined using software developed by Gasem (3). These interaction parameters were calculated by nonlinear regression of the experimental solubility data by minimizing a deviation function. The objective function used for data reduction is:

$$S = \sum_{n=1}^{n} \frac{(P_{calc,i} - P_{ex,i})^2}{\sigma_{i,P}^{\ 2}} \tag{3.28}$$

where

$$\sigma_{i,P}^{\ 2} = e_{i,P}^{\ 2} + (\partial P/\partial x)_i^{\ 2} \sigma_{x,i}^{\ 2} \tag{3.29}$$

By minimizing the quantity S, the optimum fit to the data is obtained. Since the literature seldom contain good estimates for uncertainty of reported data, the weighting factor, σ_{ip}, was set equal to one, or all data was weighted equally.

A detailed explination of the data reduction techniques used in this study may be found in the work of Gasem (3).

CHAPTER IV

APPARATUS

The apparatus used in this study was designed for the measurement of isothermal bubble points for mixtures. Of particular interest were the measurements for solutes such as carbon dioxide and ethane in paraffinic hydrocarbons. The operation of the apparatus involves injecting known amounts of solute gas and solvent liquid in an equilibrium cell. The cell is maintained at a constant temperature while the contents are stirred and compressed by mercury injection to force the solute gas into solution in the solvent liquid. The bubble point pressure is taken as the pressure at which the vapor phase disappears.

The apparatus was originally designed and built by Gasem (3), using a rocking equilibrium cell. The system was extensively redesigned and reconstructed by Barrick (35) and Anderson (1) in later studies, in an effort to increase the rate of data collection and lessen the effects of room temperature fluctuation on measured pressures. Further modifications were made by Bufkin (2) and Ross (34), each changing the apparatus to best facilitate data acquisition on the mixtures being studied at the time.

Modifications on the apparatus during the current study include the repositioning of valves and lines to reduce dead

space and to aid in the maintenance of the system. The stirrer base was redesigned to eliminate the need for a two-part mechanism, which had previously caused excessive wear and frequent mechanical failures. A schematic drawing of the apparatus as it was used in this study is shown in Figure 1.

The apparatus has been redesigned to allow mercury to be withdrawn from the equilibrium cell (SEC) using a small high precision pump (HIP) at the same time that mercury is injected into the storage vessel (SV) utilizing a much larger displacement pump (LDP). This new procedure allows for the injection of solvent without ever placing the equilibrium cell at a pressure below atmospheric, thereby eliminating the chance of air leaking into the system.

In the previous assembly there was a problem with dead space in the injection line from the 3-way injection valve to the top of the equilibrium cell. To reduce the amount of dead space the 3-way injection valve was replaced with a manifold injection valve. The new injection setup is shown in Figure 2. By using a manifold injection valve it is possible to flood the injection line with mercury after solvent injection thereby eliminating the dead space and allowing more precise data acquisition.

Other modifications were also made to improve the handling of heavy paraffinic solvents that solidify at room temperature. To avoid solidification of these paraffins in the apparatus, all the evacuation lines were repositioned inside the central temperature bath, and an additional

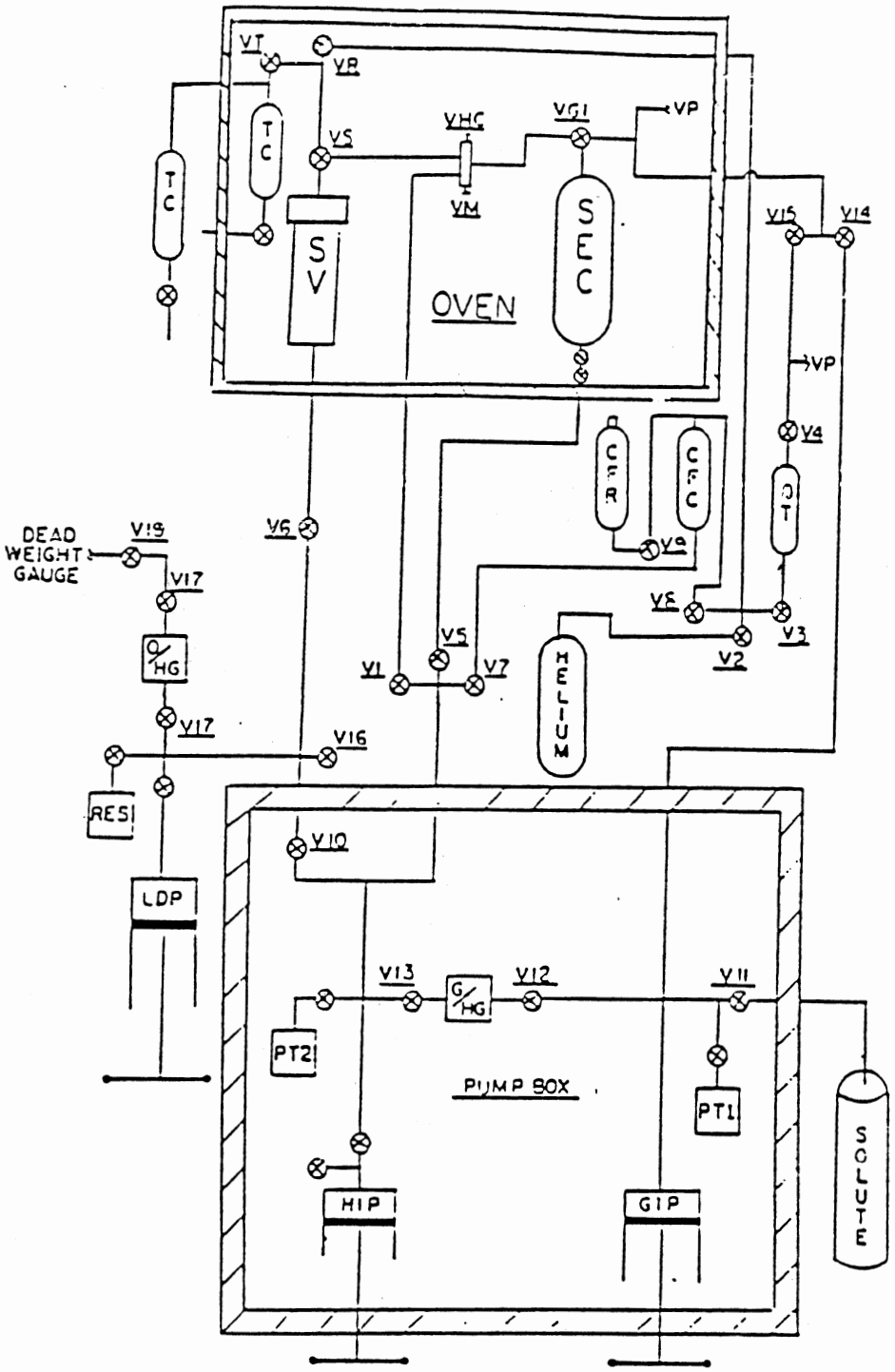

TC = Trash Cylinder
SV = Storage Cylinder
SEC = Stirred Eq. Cell
CFR = Cleaning Resivoir
CFC = Cleaning Cylinder
DT = Degasing Trap
O/HG = Oil-Mercury Interface
PT1 = Pressure Transducer
PT2 = Pressure Transducer
HIP = Hydrocarbon Pump
GIP = Gas Injection Pump
LDP = Large Displacement Pump
G/HG = Gas-Mercury Interface

Figure 1. Schematic Diagram of Solubility Apparatus.

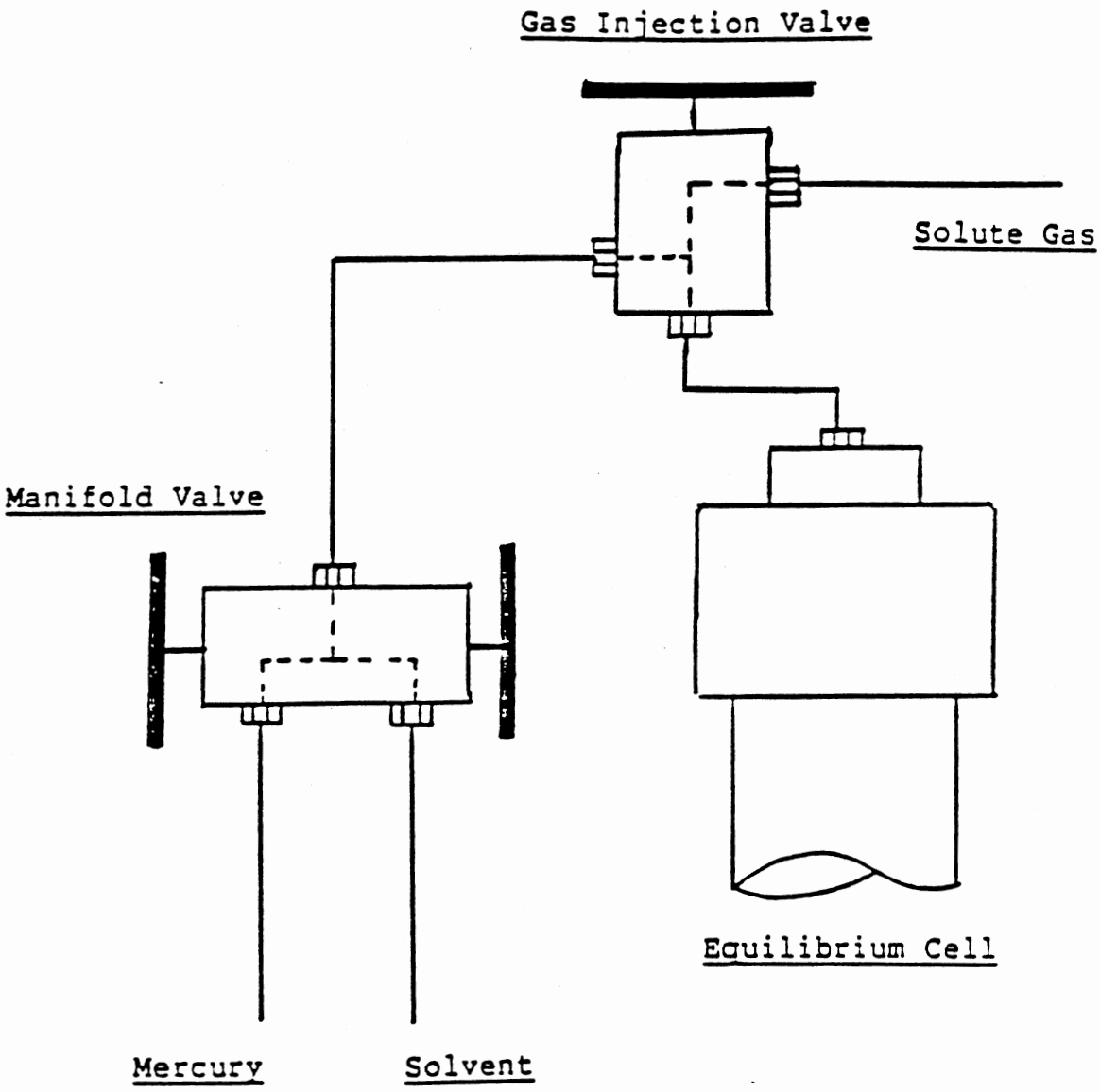

Figure 2. Modified Injection System.

vacuum line, of 1/4 inch diameter, was installed to degas the heavier solvents. This line was also wraped with heating tape.

A description of the basic components of the apparatus follow.

Equilibrium Cell & Stirring Mechanism

Figures 3 and 4 shows a side and top view, respectively, of the equilibrium cell and stirring mechanism.

An internal stirrer (ST) is fixed in the upper portion of the cell and is 1.0 inch long with an impeller blade on each side. On either side of the stirrer is a cylindrical magnet (SM) that provides the coupling necessary to rotate the stirrer. External to the cell are two horseshoe magnets (DM) used to drive the internal mechanism. These magnets are housed in a rotating magnet assembly (MS) which rests on three sets of ball bearings (BB), allowing the mechanism to rotate freely. The power is supplied by a 1/50 horsepower motor connected to a drive wheel (DW) that is in contact with the rotating magnetic assembly. A motor speed controller is used to obtain the desired rotation speed of the internal stirrer.

The equilibrium (SEC) cell is a 304 stainless steel tubular reactor (High Pressure Equipment Company Incorporated; catalog number TOC-6) that was modified for desired performance. The top 2.25 inches of the reactor was machined from an outside diameter of 1.5 inches to 1.0 inch

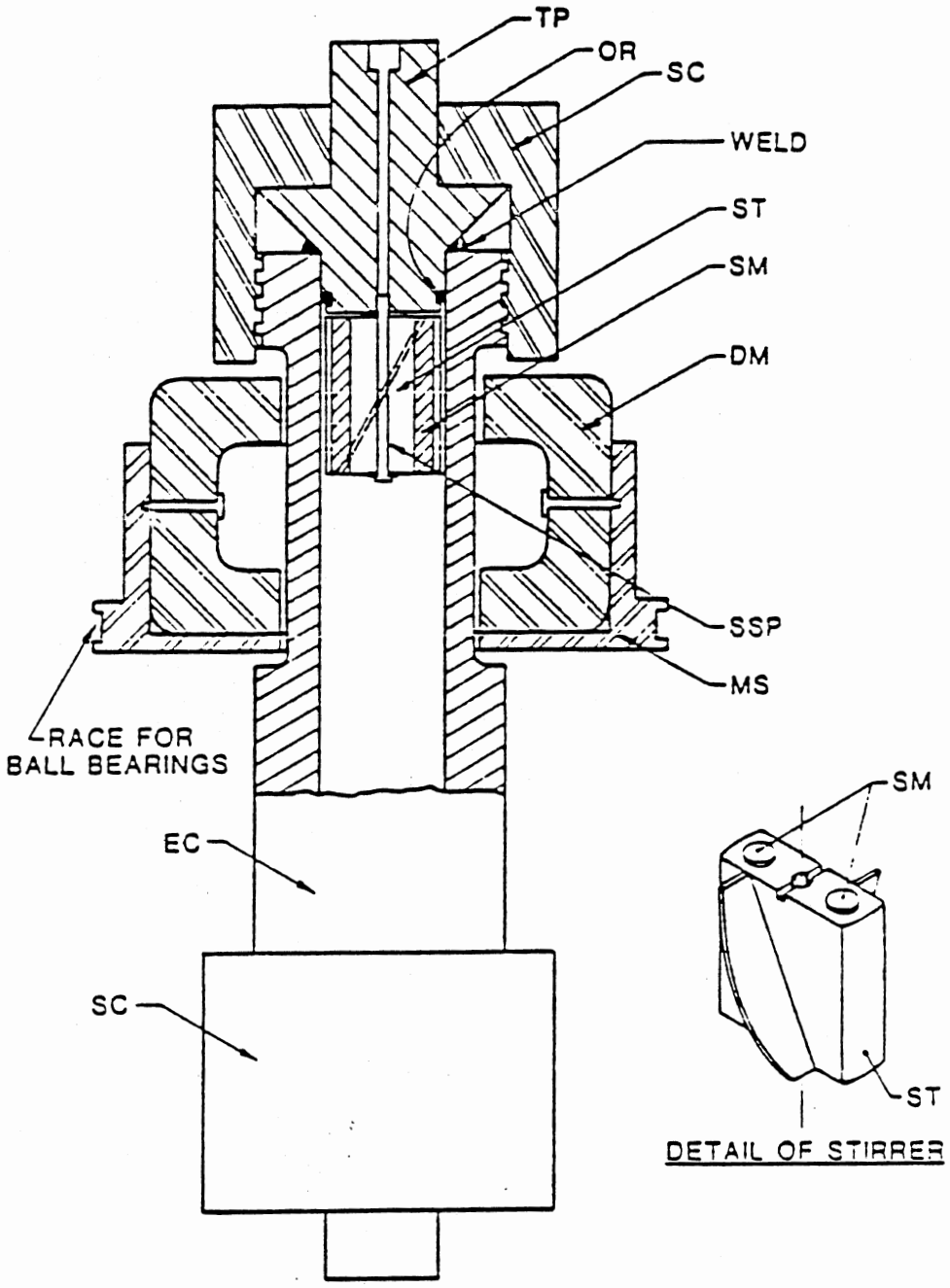

DM - DRIVE MAGNETS
EC - EQUILIBRIUM CELL (CYLINDRICAL)
MS - ROTATING MAGNET SUPPORT
OR - O RING
SC - SCREW CAP
SM - STIRRER MAGNETS
SSP - STIRRER SUPPORT PIN
ST - STIRRER
TP - TOP PLUG

Figure 3. Cross Section of Stirring Mechanism.

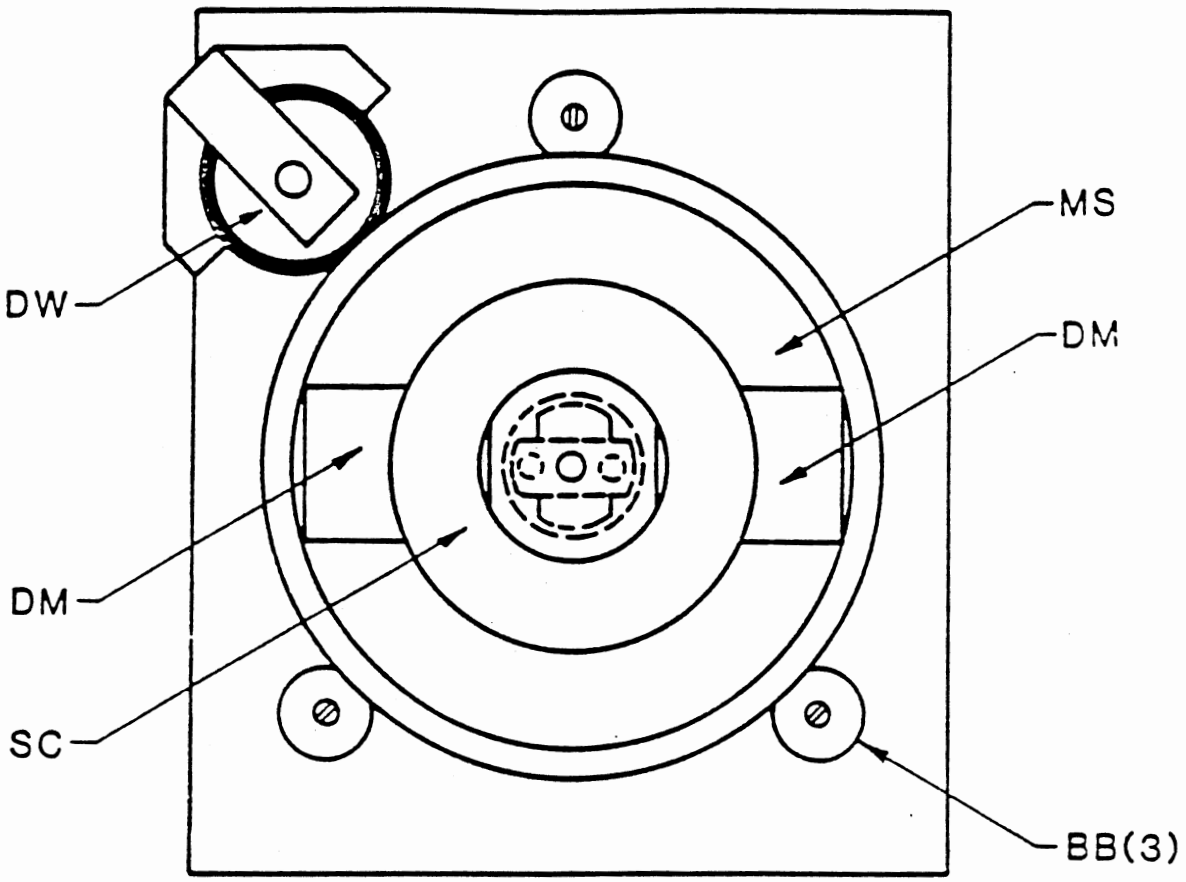

BB - BALL BEARINGS
DM - DRIVE MAGNETS
DW - DRIVE WHEEL
MS - ROTATING MAGNET SUPPORT
SC - SCREW CAP

Figure 4. Overhead View of Stirring Mechanism.

to enhance the coupling of the internal stirring magnets with the external drive magnets. The equilibrium cell has an internal volume of approximately 37 cc. The effective volume is varied by the injection or withdrawal of mercury through the bottom of the cell.

Constant Temperature Baths

Two air baths are used in the operation of the apparatus. The first temperature controlled bath is a Hotpack Oven, Model 200001, which houses the equilibrium cell, the storage cylinder, a trash cylinder, and miscellaneous lines used during cell cleanup. The original temperature controller was replaced with a Halikainen proportional integral controller, Model 1053 A, to obtain a higher precision of temperature control.

The second air bath was constructed of 1/2 inch plywood and was used to house the two injection pumps and pressure transducers. A Halikainen proportional integral controller was used to maintain the pump box at the desired temperature. For the present studies, the pump box was maintained at 50 C.

The Halikainen controllers maintained temperatures within 0.1 C of the setpoint. The temperatures were measured using platinum resistance thermometers connected to digital readouts (Fluke Incorporated, Model 2180A), which has a resolution of 0.01 C.

Pressure Measuring Equipment

The pressures within the equilibrium cell were transmitted to one of the pressure transducers (PT2), (Sensotec Incorporated, Model ST5E1890) through mercury filled lines. The second transducer (PT1) was used to measure the gas solute pressures directly from the solute pump (GIP). Each transducer has a range of 0 to 3000 psi and was calibrated at the begining of each run using a dead weight tester (Ruska Instrument Corporation, Model 2400.1). Pressure measurements were displayed on digital readouts (Sensotec Incorporated, Model 450D) with a resolution of 0.1 psi.

Injection Pumps

Three injection pumps were used during the course of each run. A 10 cc positive displacement pump (HIP), (Temco Incorporated, Model 10-1-12H) was used for measuring solvent injections as well as varying the internal volume of the equilibrium cell by injecting mercury during data acquisition. The second injection pump was a 25 cc positive displacement pump (GIP), (Temco Incorporated, Model 25-1-10HAT) used to inject solute gas into the equilibrium cell. Each pump was rated to 10,000 psi with a resolution of 0.005 cc.

The third pump was a 500 cc positive displacement pump (LDP), (Ruska Instruments Incorporated, Model 2210-801) rated to 12,000 psi with a resolution of 0.02 cc. This pump

was used only for operations where precision was not required, as in cell cleanup.

Storage Vessels

Several vessels were used during the course of operation, the most important one being the solvent storage cylinder (SV). This is a high pressure reactor (High Pressure Company Incorporated, Model OC-3) used to store the solvent at operating conditions. By doing so, enough degased solvent could be prepared for several runs, increasing the rate of data acquisition.

Other cylinders used include a 250 cc high pressure stainless steel vessel (CFC) used for cleanup, a 250 cc mercury reservoir (RES), and a 250 cc stainless steel trash cylinder (TC) used to receive spent material during cleanup.

Fittings, Tubing, and Valves

All fittings, tubing, and valves used in the apparatus are made of 316 stainless steel and were supplied by the High Pressure Equipment Company. Sizes used include 1/16, 1/8, and 1/4 inch, all were rated at 15,000 psi.

Chemicals

All chemicals used in this study were provided by commercial suppliers. No further purification of the chemicals was attempted. The suppliers and purities of the chemicals are listed in Table III.

TABLE III

CHEMICALS AND THEIR PURITIES

Chemicals	Source	Stated Purity (mole %)
Ethane	Matheson	99.9 +
Carbon Dioxide	Union Carbide	99.99
n-Pentane	Fisher Scientific	Spec. Grade
Benzene	J.T. Baker Chemical	99.8 +
n-Hexane	Aldrich	99 +
n-Eicosane	Aldrich	99 +
n-Hexatriacontane	Alfa	99 +
n-Tetratetracontane	Alfa	96 +

CHAPTER V

OPERATING PROCEDURES

This chapter contains the basic steps in the operation of the apparatus. The following is a general description of the procedure so that the fundamental workings of the system, as well as the theory behind each phase of operation, can be understood.

Filling The Storage Cell

The purpose of the storage cylinder is to hold enough solvent at operating temperature to permit several consecutive runs without refilling. Refilling the storage cylinder necessitates opening the oven door, disrupting the controlled temperature of the apparatus. To fill the storage vessel, the oven is cooled to room temperature and the top of the storage cell is removed. Care must be taken during the removal of the cap to ensure that the sealing surface is not scratched. Using a hand mirror, the mercury level is checked to ensure that it is in the lower third of the cylinder. If the mercury is above this level, the excess is withdrawn using the large displacement pump, until the level falls to a suitable position. By lowering the level of the mercury the maximum amount of solvent can be added to the cylinder, increasing the number of possible

runs before refilling is necessary.

If the solvent is a liquid, it may be added directly into the cell using a graduated cylinder. If the solvent is a solid at room temperature, it is necessary to first melt the material using a heatgun before addition into the cell. Two to three inches should be left at the top of the cell after filling to accommodate the sealing plug on the cap.

After the cap is replaced the oven is adjusted to its next operating temperature. While the oven and solvent are heating to operating conditions, the solvent should be placed under vacuum to remove as much dissolved air as possible. Even trace amounts of air will affect the experimental results of the system. The time needed for degasing will vary depending on solvent volatility and can range from fifteen minutes for solvents such as pentane or benzene to three or four hours for the heavier paraffins. After adequate degasing, the cell is pressured to approximatly 200 psi using the large displacement pump to insure that air does not leak into the system between runs.

Solvent Injection

After the storage cylinder has been charged and placed under pressure, the equilibrium cell is exposed to vacuum. After the equilibrium cell has been adequately evacuated (30 minutes), it is filled with mercury using the small displacement pump to a pressure of approximately 200 psi. The pressure and pump position, V_1, are recorded. The solvent injection valve is then opened and mercury is

withdrawn from the bottom of the equilibrium cell using the small pump. At the same time, mercury is injected into the bottom of the storage vessel with the larger pump, displacing an equal volume of solvent into the equilibrium cell. If done slowly, this procedure will transfer solvent from the storage cylinder to the equilibrium cell with little change in pressure, guaranteeing that the solvent remains single phase throughout the injection. Five to eight mililiters of solvent should be transfered before the injection valve is closed. After closing the injection valve, 2 cc of mercury are withdrawn to create a small vapor space at the top of the cell, and the solvent in the equilibrium cell is then exposed to vacuum once again. After degassing, the cell is repressurized to its original pressure, and the final pump position, V_2, is noted. By using equation (5.1) the amount of solvent injected (n_{HC}) can be determined.

$$n_{HC} = \left[\rho_{HC}(V_2 - V_1)\frac{\rho_{Hg}(T_{pump})}{\rho_{Hg}(T_{oven})}\right] \Big/ MW_{HC} \qquad (5.1)$$

Solute Injection

The solute injection pump is placed under vacuum for 30 minutes and then filled with the solute gas. After several injections it may be necessary to vacuum and refill the pump to ensure that there is enough solute for the next injection. The pressure in the pump is adjusted to

approximatly 500 psi and allowed to stabilize. Using the amount of solvent injected and the density of the solute gas at operating conditions, the volume of gas needed to achieve the desired solute mole fraction is determined. The gas pressure and solute injection pump readings are recorded, and the pump is advanced until the volume change is equal to the volume needed for the injection. Using the solvent injection pump, 2 or 3 cc of mercury are withdrawn to create a head space in the cell. The gas injection valve is opened allowing the solute gas to slowly enter the equilibrium cell; this is continued until the pressure in the pump falls to its original value. The gas injection valve is closed and the volume of the pump is adjusted until the pressure is equal to the starting pressure. By recording the final pump position, the volume of gas injected into the equilibrium cell (V_{SG}) can be determined, and by using the density of the solute gas (ρ_{SG}) at injection conditions the number of moles injected (n_{SG}) can be calculated using equation (5.2)

$$n_{SG} = \frac{V_{SG}\,\rho_{SG}}{MW_{SG}} \qquad (5.2)$$

From this value the mole fraction of solute gas (x_{SG}) can be found using equation (5.3).

$$X_{SG} = \frac{n_{SG}}{n_{SG} + n_{HC}} \qquad (5.3)$$

Data Acquisition

Following solute injection, the magnetic stirrer is engaged and the contents of the equilibrium cell are pressurized to above the bubble point pressure. The system is allowed to stabilize to ensure that the gas phase has been completly absorbed into the liquid phase. After the sample is determined to be single phase, the pressure of the mixture is readjusted to below the bubble point pressure.

Before begining data acquisition, the pressure of the equilibrium cell and the pump position are recorded. An increment of 0.01 cc of mercury is injected into the cell, and the system is allowed to stabilize. The new pressure and pump position are recorded. This injection procedure is repeated until the pressure in the cell increases sharply after an injection. This increased pressure is due to the transition from a two-phase state to a single-phase state. Increments of 0.01 cc of mercury are injected as before until three or four points are collected in the single phase region.

Due to the relatively small volume changes, both the single and two phase portions of the data can be represented by straight lines on a plot of pressure vs change in volume. Extrapolating the two lines to a point of intersection, the pressure at the intersection is the bubble point pressure. Figure 5 (3) shows results from two typical runs. After the bubble point at the initial mole fraction has been determined, more solute gas is added to the cell to increase

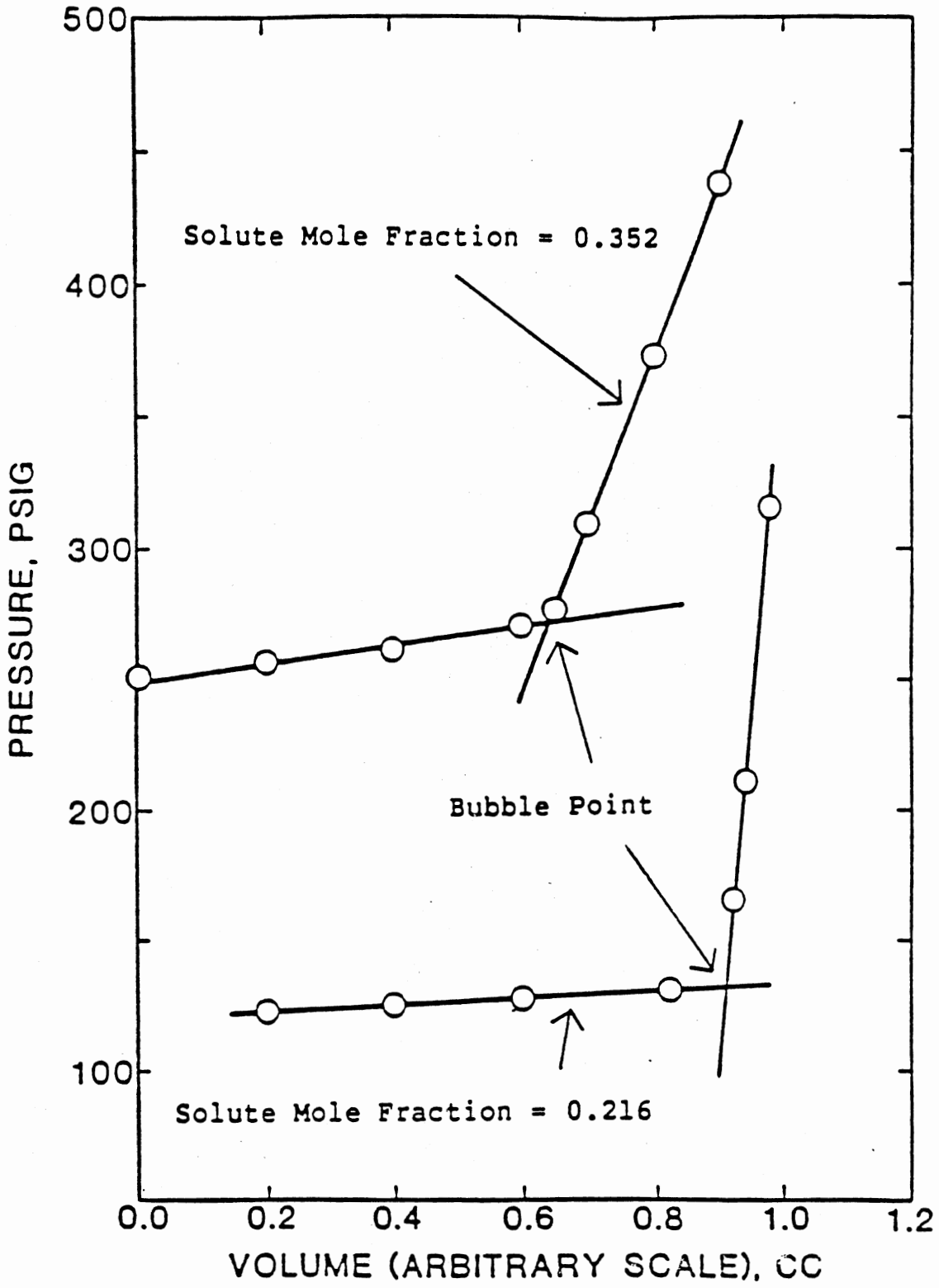

Figure 5. Typical Pressure Versus Volume Plot.

the solute mole fraction, and the entire procedure is repeated for the new composition. Typically four or five composition points are taken before the cell is cleaned. In a few of the systems it is possible to inject solute untill solute mole fractions are as high as 0.8 or 0.9. However, data up to a mole fraction of 0.5 or 0.6 is sufficient for testing the abilities of the equations of state used in this study, and more information may be gained from taking data on several systems as oppossed to concentrating so heavily on a single binary system.

To further establish the accuracy of the data, a second run is conducted at the same temperature. However, on the second run, solute mole fractions are used that lie between the mole fractions of the first run. By doing this, the consistency of the two runs can be determined.

The data from the two different runs are plotted as a "simplified Henry's plot" (P-VP/x vs x). This plot serves as a convenient way of locating erroneous data because any error in bubble point pressure is magnified by the reciprocal of the mole fraction. Errors are easily identified on the graph, and are identified as points which do not lie on the smooth curve created by the other data points. This graphing method is also helpful for locating errors in the solvent and solute injections. When two different runs are plotted on the same graph, they should form a single curve, as seen in Figure 6. If the data produce two distinguishable curves, then one set of data is in error, and a third run must be made to determine which is

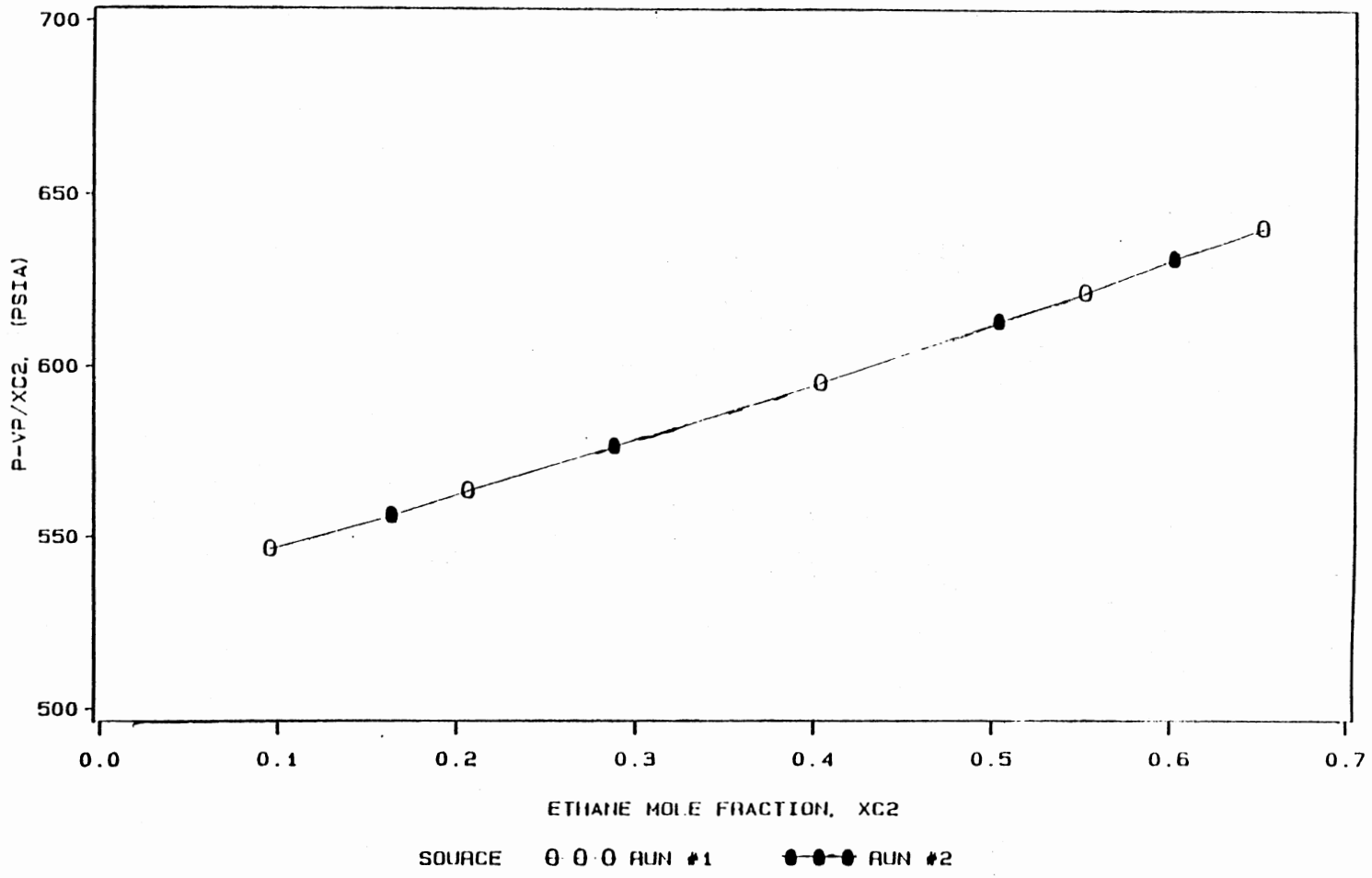

Figure 6. Typical Simplified Henry's Plot.

the erroneous data.

Cleanup

The equilibrium cell must be thoroughly cleaned after each run. This is accomplished by first opening valves between the equilibrium cell and the trash cylinder, then injecting mercury until the cell and all the lines leading to the trash cylinder are full of mercury. This displaces the contents of the cell to the trash cylinder. The contaminated mercury is then flushed from the system by blowing high pressure helium through the lines. The cell is then filled with an appropriate solvent (pentane for straight chain hydrocarbons and benzene for aromatics), and pressurized to 100 psi. The solvent is left in the cell, with the stirrer running, to dissolve the heavier hydrocarbon, and is then purged from the cell by displacement with mercury. This procedure is repeated twice more to ensure adequate cleaning of the cell. After the final cleaning, the cell is placed under vacuum at high temperature to remove any trace amounts of the cleaning solvent.

The storage vessel is cleaned in a similar way, with the main difference being a longer waiting period for the hydrocarbon to dissolve since the storage cylinder lacks a stirring mechanism.

CHAPTER VI

ANALYSIS OF EXPERIMENTAL ERROR

During the course of experimental data acquisition two types of errors are encountered. The first type are random errors, or errors which occur from random disturbances. The second type are systematic errors, which are caused by a repeated flaw in the operating procedure. Random errors can be accounted for by statistical methods, but systematic errors can only be eliminated by correcting the improper experimental procedures.

In an effort to check for systematic errors, this investigation was begun by collecting data on the system CO2 + benzene. This system has been studied by numerous investigators, so an abundance of data is available for comparison. A comparison of the results for this work with other investigators showed good agreement, indicating that there was little systematic error in the apparatus and procedures used. Detailed comparisons are given in Chapter VII.

To estimate the experimental uncertainties in the collected data, the prime errors must first be established. The second step is to determine how these prime errors propagate during the course of an experiment. Prime errors are due to imprecisions in measured quantities. In this

investigation, three quantities were routinely measured; temperature, pressure, and volume. The prime error in the temperature measurement is based on the ability of the temperature controller to hold a specified temperature, and was determined to be;

$$e_T = 0.05 \text{ K} \tag{6.1}$$

The error in the pressure measurement was established to be 0.05 psi, which is equal to the resolution of the digital readout. The error is expressed as:

$$e_P = 0.05 \text{ psi} \tag{6.2}$$

The prime error for the volume measurement was based on the ability of the operator to read the scale on the injection pump. The volume error is stated as:

$$e_V = 0.0025 \text{ cc} \tag{6.3}$$

To determine how the errors propagate in a typical experiment, equation (6,4) is used to find the error in liquid mole fractions (2):

$$e_{xi} = X_1 X_2 \left[\left(e_{\rho 1}/\rho_1 \right)^2 + \left(e_{v1}/\sum_1 V_i \right)^2 + \left(e_{\rho 2}/\rho_2 \right)^2 + \left(e_{v2}/\sum V_2 \right)^2 \right]^{1/2} \tag{6.4}$$

where 1 and 2 refer to the solute and solvent, respectively.

The uncertainty in the solute density has been previously determined by Bufkin (2) as 0.28%. The error associated with the solvent density has been experimentally determined by Anderson (1) and Barrick (35) as 0.003 g/cc.

A typical run involving ethane consists of a hydrocarbon injection of 5 cc, and five separate 6 cc injections of ethane. Substituting these values into equation (6,4) yields:

$$e_{xc_2} = 0.005\, x_1 x_2 \tag{6.5}$$

with the maximum error of 0.00125 occurring at the point $X_1 = X_2 = 0.5$.

Experimental uncertainty in the bubble point pressures can be estimated by:

$$e_{bp}^2 = e_p^2 + (\partial P/\partial X_i)^2 e_{x_1}^2 + (\partial P/\partial T)\, e_T^2 \tag{6.6}$$

By assuming that the error due to the temperature is negligible this expression becomes:

$$e_{bp}^2 = (0.05)^2 + (\partial P/\partial x_1)^2 (0.00125)^2 \tag{6.7}$$

where e_{xi} is given by equation (6,4).

The value of $(\partial P/\partial x_i)$ was estimated by calculating the pressure difference between the two data points at the highest pressures for each binary system divided by the difference in the corresponding mole fractions. Since the greatest errors occur at the highest pressures, this method generates the maximum expected error for each system. Table IV lists the results of these calculations.

TABLE IV

MAXIMUM EXPECTED ERRORS FOR
INDIVIDUAL BINARY SYSTEMS

System	Maximum Error in Bubble Point Pressure (psi)
CO2 + Benzene	1.4
Ethane + n-Hexane	2.0
Ethane + n-Eicosane	1.6
Ethane + n-Hexatriacontane	1.9
Ethane + n-Tetratetracontane	1.9

CHAPTER VII

EXPERIMENTAL RESULTS AND DISCUSSION

This chapter presents information on the data taken during this study. These data are compared with those of other investigators, where available, and the experimental results and analysis of the data are discussed. A comparison of these data with a wide range of other ethane binary systems is given in Chapter VIII.

Carbon Dioxide + Benzene

Due to the fact that the experimental apparatus has undergone several modifications, the system was tested to demonstrate the reliability of data acquisition procedures. The CO2 + benzene system at 40 C was chosen because it has been the test system used at OSU in several different studies, so there is a multitude of data available for comparison. This system has also been studied by several other investigators, which allows for further comparisons. Table V lists the different studies that have been conducted on CO2 + benzene at 40 C.

The data obtained for this test system are listed in Table VI. The data can be compared with previous investigators by using a "simplified Henry's law plot" on which $(P-VP)/X_{CO_2}$, where VP is the vapor pressure of pure

TABLE V

PREVIOUS INVESTIGATIONS OF
CO2 + BENZENE AT 40 C

Investigator	Ref #	Year	Cell Type
Ross	34	1987	Internal Stirrer
Bufkin	2	1986	Internal Stirrer
Anderson	1	1985	Internal Stirrer
Gasem	3	1985	Rocking
Gupta	5	1982	Rocking
Donohue	4	1986	Circulation
Ohgaki	6	1976	Rocking
Orbey	7	1983	Rocking

TABLE VI

SOLUBILITY OF CARBON DIOXIDE IN BENZENE

Mole Fraction Carbon Dioxide	Pressure MPa	Pressure psia
313.2 K (40.0 C, 104 F)		
0.099	1.217	176.5
0.205	2.362	342.6
0.300	3.307	479.6
0.301	3.372	489.0
0.399	4.222	612.3
0.400	4.220	612.0
0.503	5.004	725.7

benzene at 40 C, is plotted against the CO2 liquid mole fraction. By plotting the data in this fashion,the errors are magnified by the reciprocal of the CO2 mole fraction; thus, differences in data sets becomes easily discernable. Figure 7 is a "simplified Henry's plot" where data from this study are compared to the work of previous investigators at OSU. Upon examination, the plot reveals that there is substantial agreement between the different data sets, with scatter occurring only at CO2 liquid mole fractions below 0.2. However, this scatter is explained by the magnifying effect of the CO2 mole fraction at low values; the maximum difference between runs is approximatly 15 psi, occurring at a mole fraction of 0.15. The data from this work appear to be in best agreement with those of Ross and of Bufkin, with a maximum difference of approximately 7 psi.

The data from this work were regressed to obtain the optimum binary interaction parameters, Cij and Dij, for the Soave-Redlich-Kwong (SRK) and Peng-Robinson (P-R) equations of state. For both equations of state (EOS) the data were used to generate a single binary interaction parameter, Cij (Dij=0), as well as two interaction parameters. In both cases the errors for the SRK and P-R were nearly identical. This consistency between the two equations of state is expected due to the similarities of these equations with respect to solubility determination. The results are listed in Table VII. These results clearly show the improvement in the predictive power of the EOS when two interaction parameters are used instead of one. A single interaction

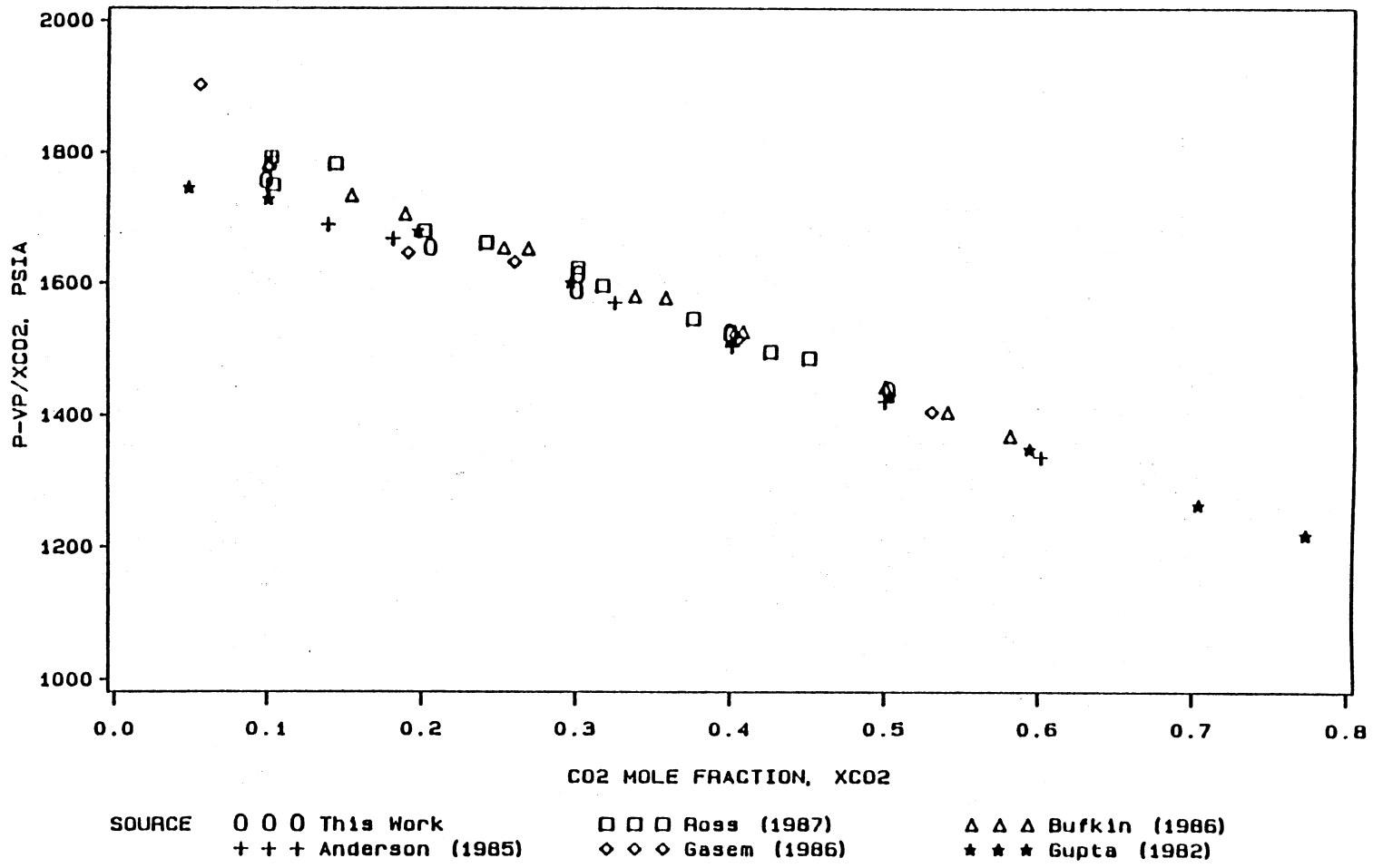

Figure 7. Comparison of Bubble-Point Data for CO2 + Benzene at 40 C.

TABLE VII

SOAVE AND PENG-ROBINSON EQUATION OF STATE
REPRESENTATIONS OF SOLUBILITY DATA
FOR CARBON DIOXIDE IN BENZENE

Temperature K(F)	Soave parameters (P-R Parameters) Cij	Dij	Error in Solute Mole Fraction * RMS	Max.
CO2 + Benzene				
313.2 (104)	0.075 (0.074)	0.030 (0.030)	0.002	0.004
	0.097 (0.097)	--- ---	0.010	0.020

*Errors are essentially identical for the Soave and the Peng-Robinson equations of state.

parameter allows prediction of CO2 solubility in benzene to within a maximum error 0.020, but this value was reduced to 0.004 with the addition of a second interaction parameter. Table VIII shows SRK interaction parameters from several different studies of CO2 in benzene at 40 C. A comparison reveals the reasonable agreement among the studies.

Figure 8 presents comparisons of the solubility data for several OSU investigators in terms of deviations from SRK predictions based on parameters optimized to fit the present data (Cij=0.075, Dij=0.030). The data agree well below 700 psi with deviations less than 0.005. However, Figure 9 shows that the data obtained by investigators outside OSU are in greater disagreement.

Figures 8, 9, and Table VIII show that there is a general consistency between this work and the work of other investigators. Based on these results, the current apparatus was considered to function properly.

Ethane + n-Hexane

The system ethane + n-hexane was studied at 100 F, 150 F, 200 F, and 250 F. The primary reason for studying this binary system was to resolve an inconsistency that had surfaced during a study performed by Ross (34) on ethane + n-paraffins. In the study, Ross found that the data for ethane + n-hexane by Zais (11) were in serious disagreement with systems on either side (n-pentane and n-heptane), to the extent that he did not use the hexane data in his generalized study of ethane + n-paraffins. Therefore, in

TABLE VIII

COMPARISONS OF BINARY INTERACTION PARAMETERS
FOR CARBON DIOXIDE IN BENZENE

Investigator	SRK Single parameter Cij (Dij=0)	SRK Two Parameters Cij	Dij
This Work	0.0974	0.075	0.030
Ross	0.1010	0.073	0.034
Bufkin	0.0967	0.071	0.036
Anderson	0.0915	0.067	0.036
Gasem	0.0959	0.071	0.033
Gupta	0.0882	0.067	0.038
Donohue	0.0872	0.071	0.026
Ohgaki	0.0740	0.057	0.031
Orbey	0.0947	0.073	0.020

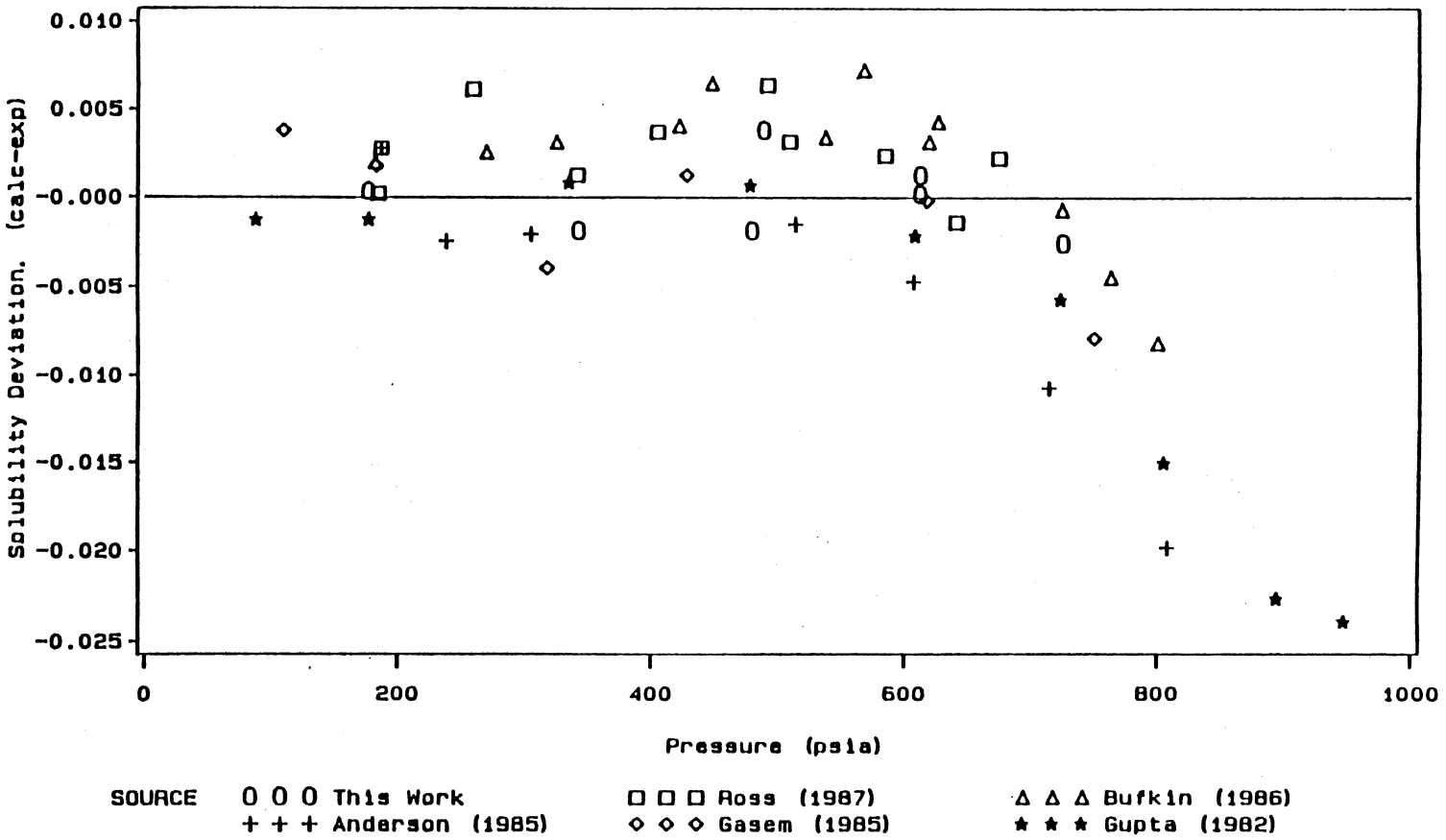

Figure 8. Comparison of Solubility Data for CO2 + Benzene at 40 C.

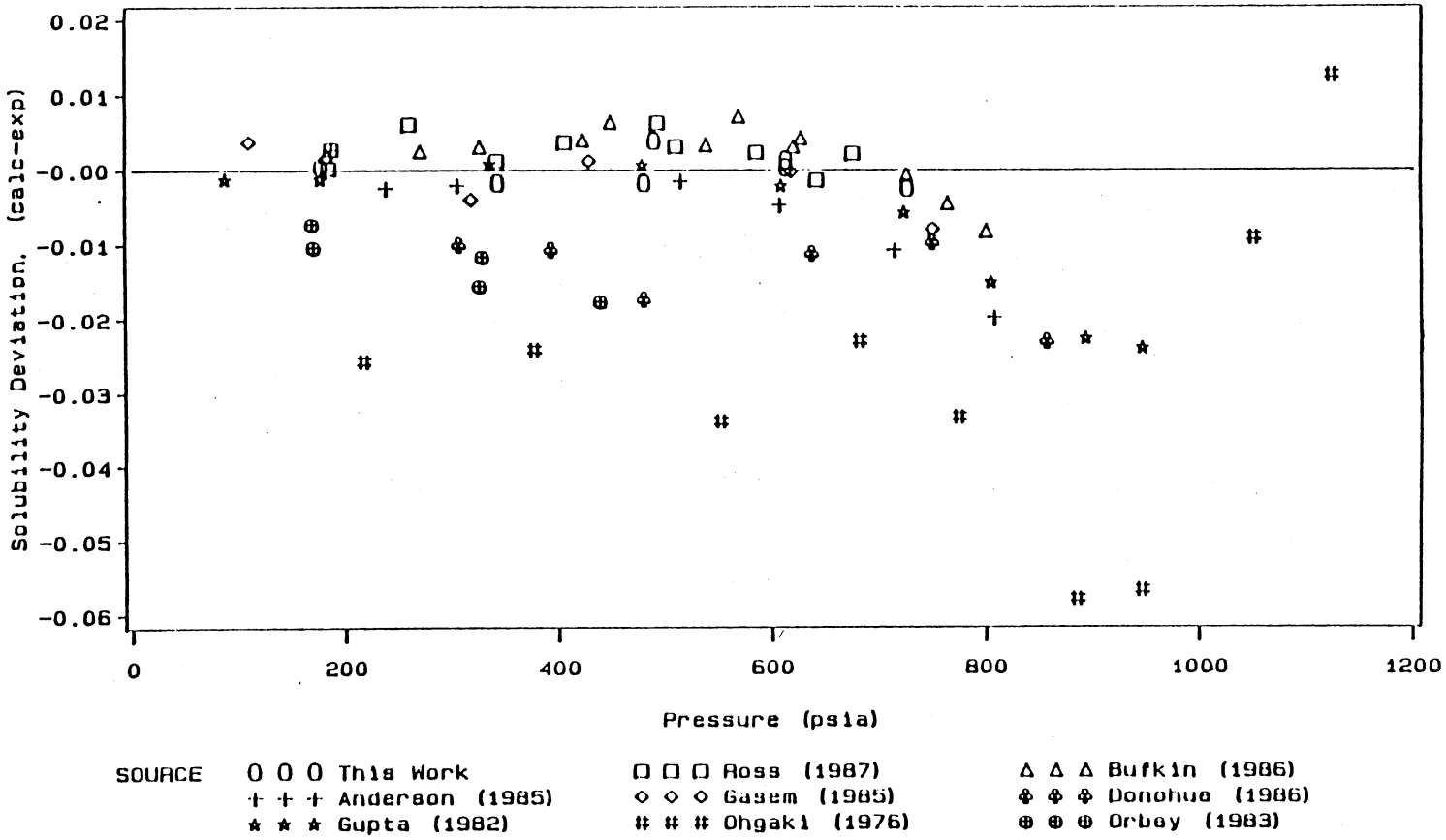

Figure 9. Comparison of Solubility Data for CO2 + Benzene at 40 C with all Available Sources.

order to complement this ethane + n-paraffin study, new ethane + n-hexane data were needed. The data gathered on four isotherms appear in Table IX. Figure 10 shows a "simplified Henry's plot" for these data.

Table X contains the interaction parameters generated for the SRK and P-R equations of state. These values reveal some of the behaviors of binary interaction parameters. The first behavior is the obvious dependence of Cij on temperature. A second noticable trend is that the root mean squared error (RMSE) is essentially the same whether one or two interaction parameters are used. (The definitions of RMSE and other statistical values are defined in Appendix A.) This was not the case in the CO2 + benzene study. Chapter VIII of this study contains a detailed investigation into temperature and carbon number effects on Cij and Dij.

Figure 11 shows the solubility deviations of the data, with a maximum deviation of 0.002. Figures 12 and 13 show a comparison between these data and the data of Zais (11) at 150 F and 250 F, respectively. The differences between these data and Zais' are obvious not only in the large deviations, but in the noticable pattern for each isotherm of Zais' data.

Ethane + n-Eicosane

Another system studied was ethane + n-eicosane at 50 C. This binary system was run later than the others, when during the ethane + n-paraffin study the isotherm of ethane + n-eicosane at 50 C taken by Bufkin appeared to be in

TABLE IX

SOLUBILITY OF ETHANE IN n-HEXANE

Mole Fraction Ethane	Pressure MPa	Pressure psia
310.9 K (37.8 C, 100 F)		
0.095	0.393	57.0
0.136	0.552	80.1
0.163	0.660	95.7
0.206	0.834	121.0
0.259	1.057	153.3
0.288	1.178	170.8
0.347	1.429	207.3
0.373	1.560	226.3
0.403	1.689	245.0
0.503	2.164	313.8
0.522	2.257	327.3
0.552	2.401	348.3
0.602	2.657	385.4
0.610	2.699	391.4
0.652	2.914	422.7
338.7 K (65.6 C, 150 F)		
0.072	0.463	67.1
0.107	0.642	93.1
0.201	1.180	171.1
0.204	1.200	174.0
0.301	1.787	259.2
0.352	2.116	306.9
0.392	2.372	344.0
0.442	2.717	394.0
0.499	3.119	452.4
0.520	3.268	474.0
0.564	3.590	520.7

TABLE IX (Continued)

Mole Fraction Ethane	Pressure MPa	Pressure psia
366.5 K (93.3 C, 200 F)		
0.109	0.958	138.9
0.111	0.964	139.8
0.112	0.982	142.4
0.202	1.659	240.6
0.203	1.643	238.3
0.208	1.690	245.1
0.300	2.428	352.1
0.306	2.471	358.4
0.310	2.507	363.6
0.382	3.121	452.6
0.397	3.254	471.9
394.3 K (121.1 C, 250 F)		
0.076	1.051	152.5
0.108	1.333	193.3
0.162	1.819	263.8
0.199	2.157	312.9
0.251	2.672	387.6
0.307	3.236	469.3
0.309	3.256	472.3
0.358	3.772	547.1
0.401	4.223	612.5
0.407	4.309	625.0
0.504	5.399	783.0

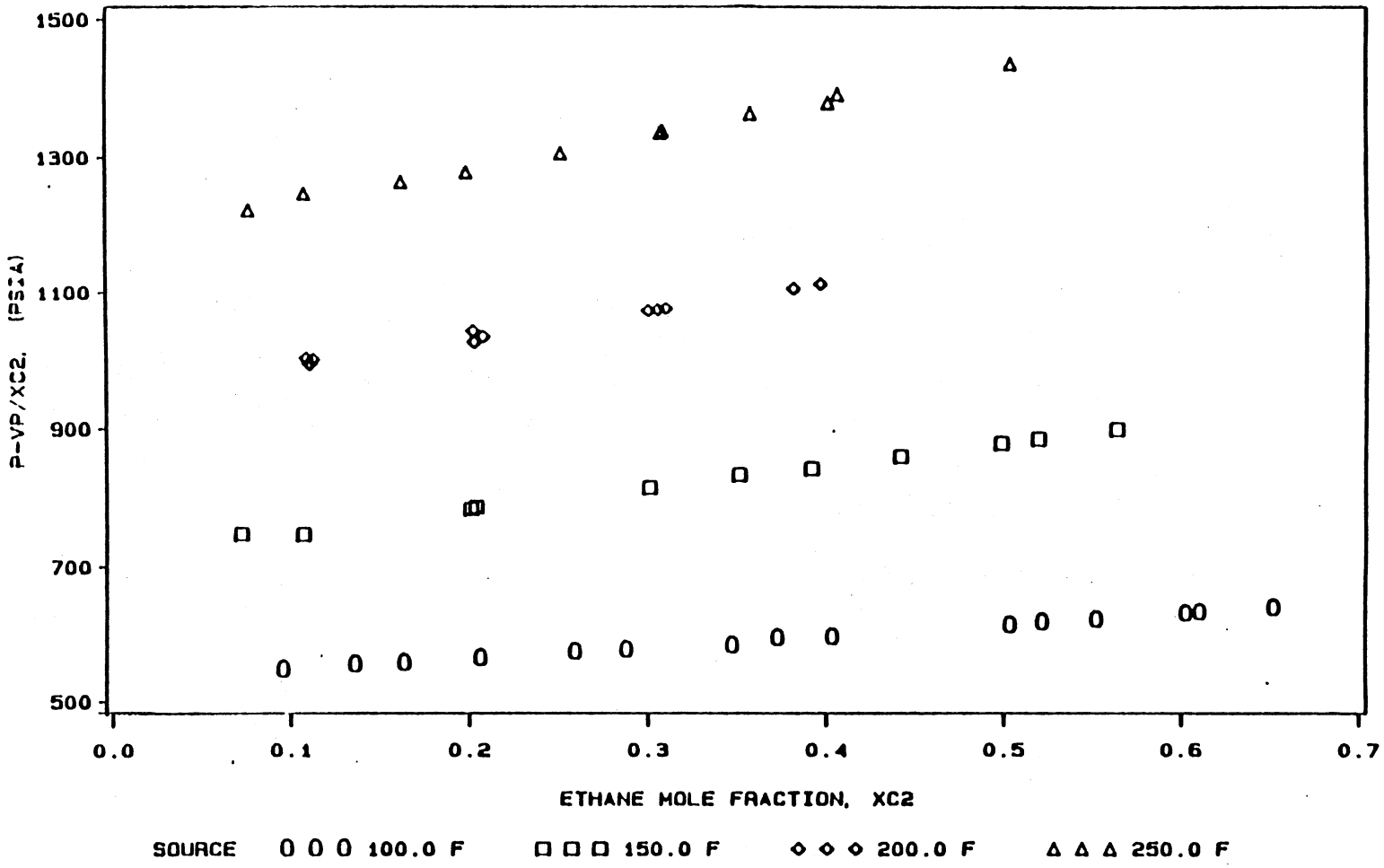

Figure 10. Simplified Henry's Plot for Ethane + n-Hexane.

TABLE X

SOAVE AND PENG-ROBINSON EQUATION OF STATE
REPRESENTATIONS OF SOLUBILITY DATA
FOR ETHANE IN n-HEXANE

Temperature K(F)	Soave parameters (P-R Parameters) Cij	Dij	Error in Solute Mole Fraction * RMS	Max.
---------- C2 + Hexane ----------				
310.9 (100)	0.000 (0.005)	0.002 (0.000)	0.001	0.002
	0.001 (0.005)	----- -----	0.001	0.002
338.7 (150)	0.003 (0.005)	-0.004 (-0.004)	0.001	0.002
	0.000 (0.002)	----- -----	0.001	0.003
366.5 (200)	0.006 (0.005)	-0.007 (-0.005)	0.001	0.002
	0.000 (0.001)	----- -----	0.001	0.002
394.3 (250)	0.025 (0.021)	-0.021 (-0.018)	0.001	0.002
	0.011 (0.009)	----- -----	0.003	0.007
310.9, 338.7 366.5, 394.3	0.008 (0.010)	-0.008 (-0.008)	0.004	0.010
	0.003 (0.005)	----- -----	0.004	0.013

*Errors are essentially identical for the Soave and the Peng-Robinson equations of state.

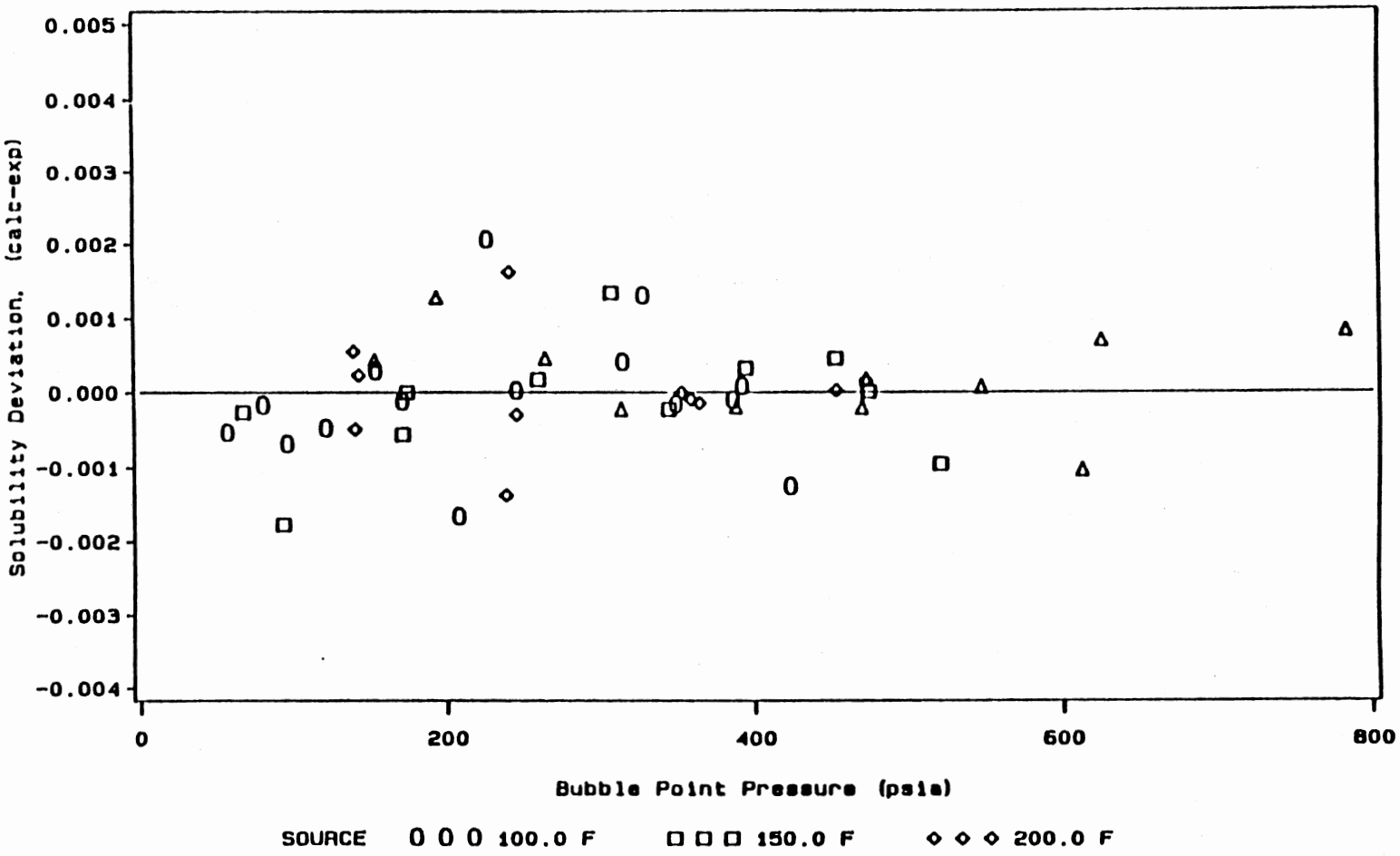

Figure 11. Solubility Data for Ethane + n-Hexane.

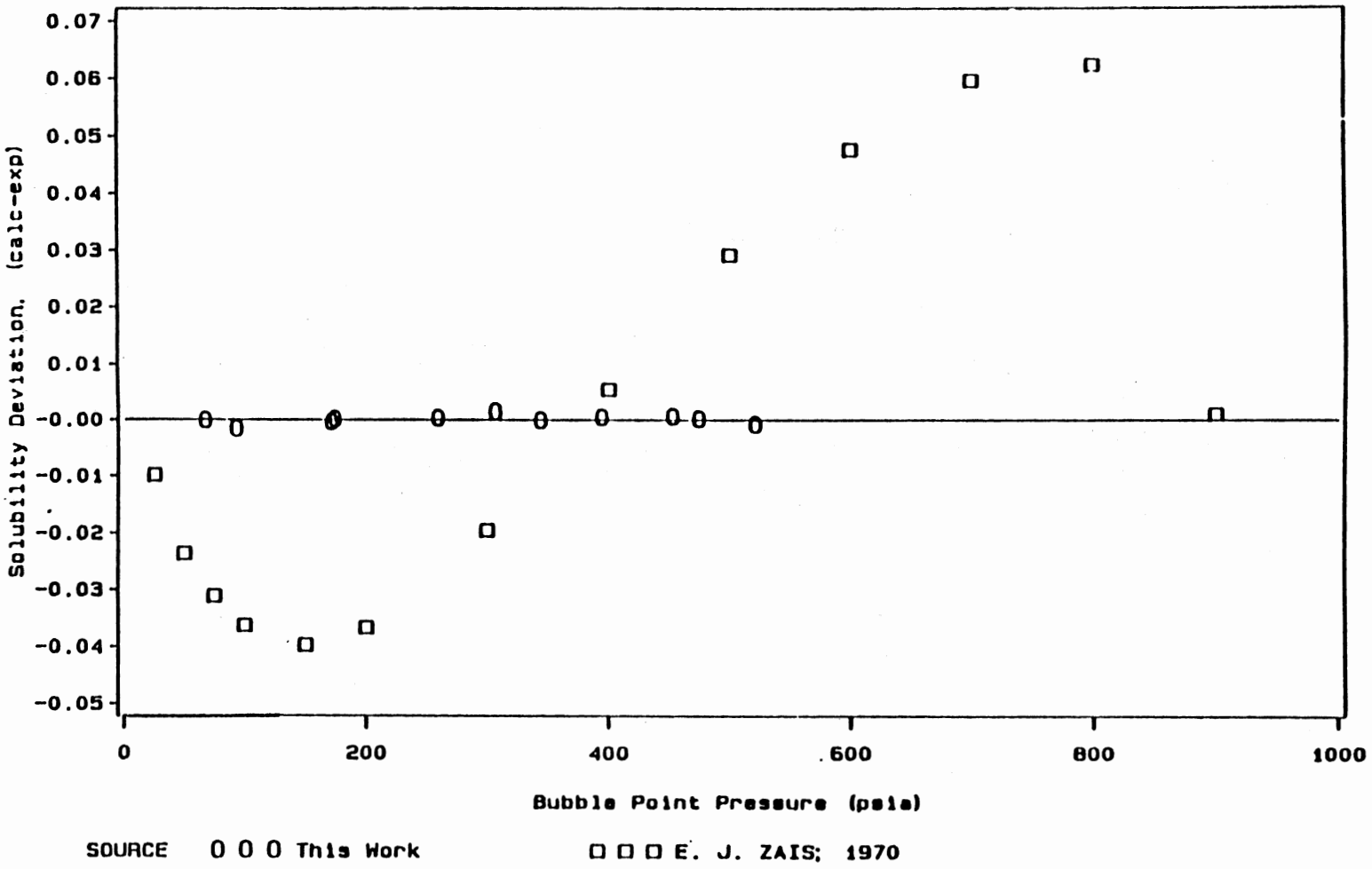

Figure 12. Comparison of Solubility Data for Ethane + n-Hexane at 150 F.

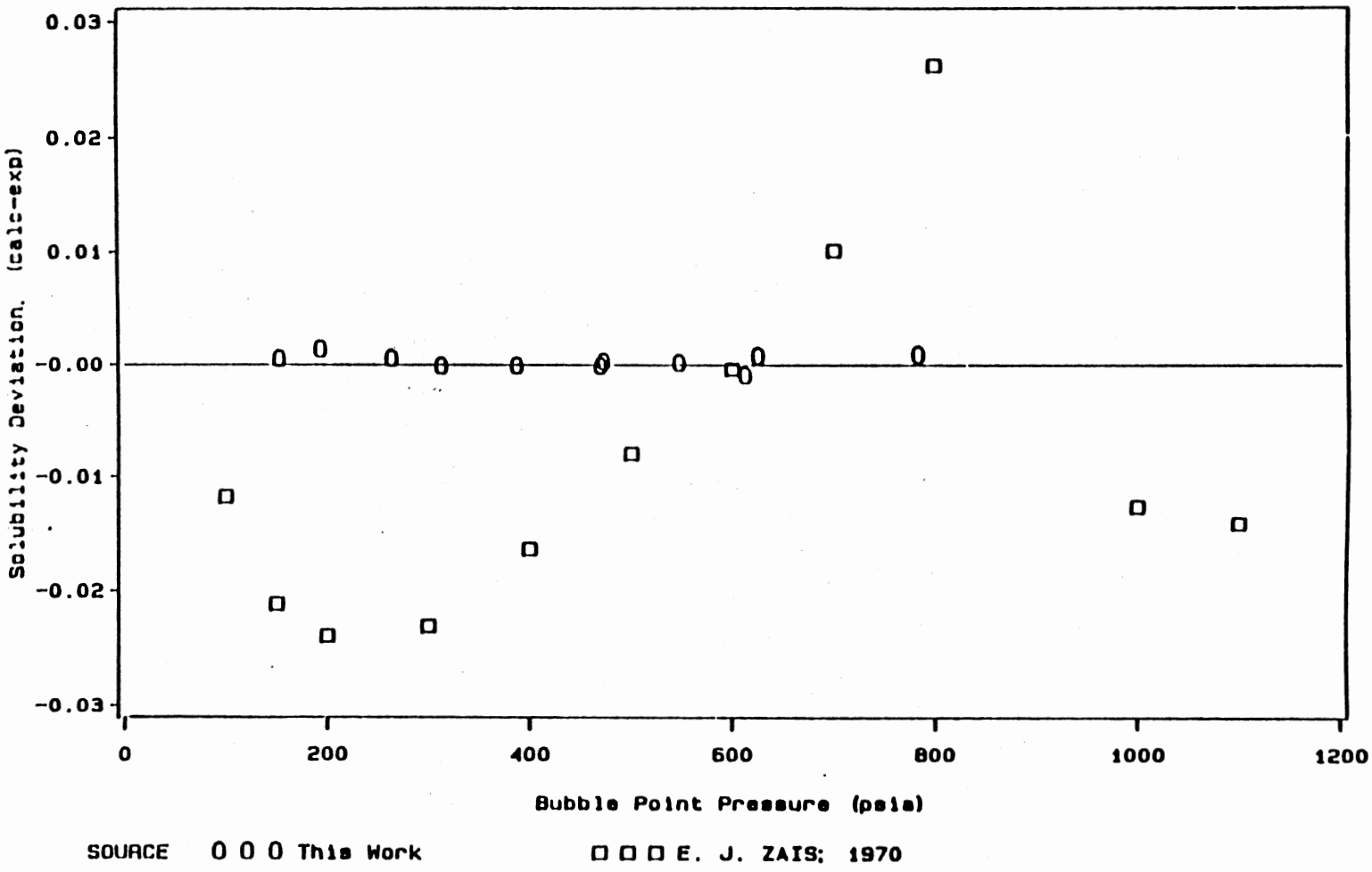

Figure 13. Comparison of Solubility Data for Ethane + n-Hexane at 250 F.

disagreement with other data. Data for the new run appear in Table XI. Figure 14 shows the differences in the data of the two investigations. Although both runs are smooth, they do not lie on the same curve, indicating a difference ineither the solute or solvent injections. By regressing the data (values listed in Table XII) and plotting the results on Figure 15, the results clearly show that Bufkin's data consistently gave deviations higher than the data of this study. Bufkin's data were replaced for the detailed investigation in Chapter VIII.

Ethane + n-Hexatriacontane

Another system investigated was ethane + n-hexatriacontane at 100 C. Although two isotherms of ethane + n-hexatriacontane had been measured by Bufkin at 100 C and 150 C (2), the isotherm at 100 C did not fit well with other data. The data acquired in this study appear in Table XIII. These data were compared to the data taken by Bufkin on a "simplified Henry's plot" shown in Figure 16.

The SRK and P-R regressed parameters for the ethane + n-hexatriacontane system are shown in Table XIV. Once again, the enhanced performance of the EOS using two interaction parameters is easily seen when comparing the overall error of 0.0192, using only Cij, as compared to 0.0009 when two parameters are utilized. Figure 17 shows graphically the SRK representation of these data compared to Bufkin's data using parameters optimized from the data of this study. Figure 17 demonstrates even more clearly than

TABLE XI

SOLUBILITY OF ETHANE IN n-EICOSANE

Mole Fraction Ethane	Pressure MPa	Pressure psia
323.2 K (50.0 C, 122 F)		
0.149	0.505	73.2
0.249	0.938	136.1
0.320	1.274	184.8
0.411	1.793	260.1
0.553	2.801	406.3
0.649	3.666	531.7

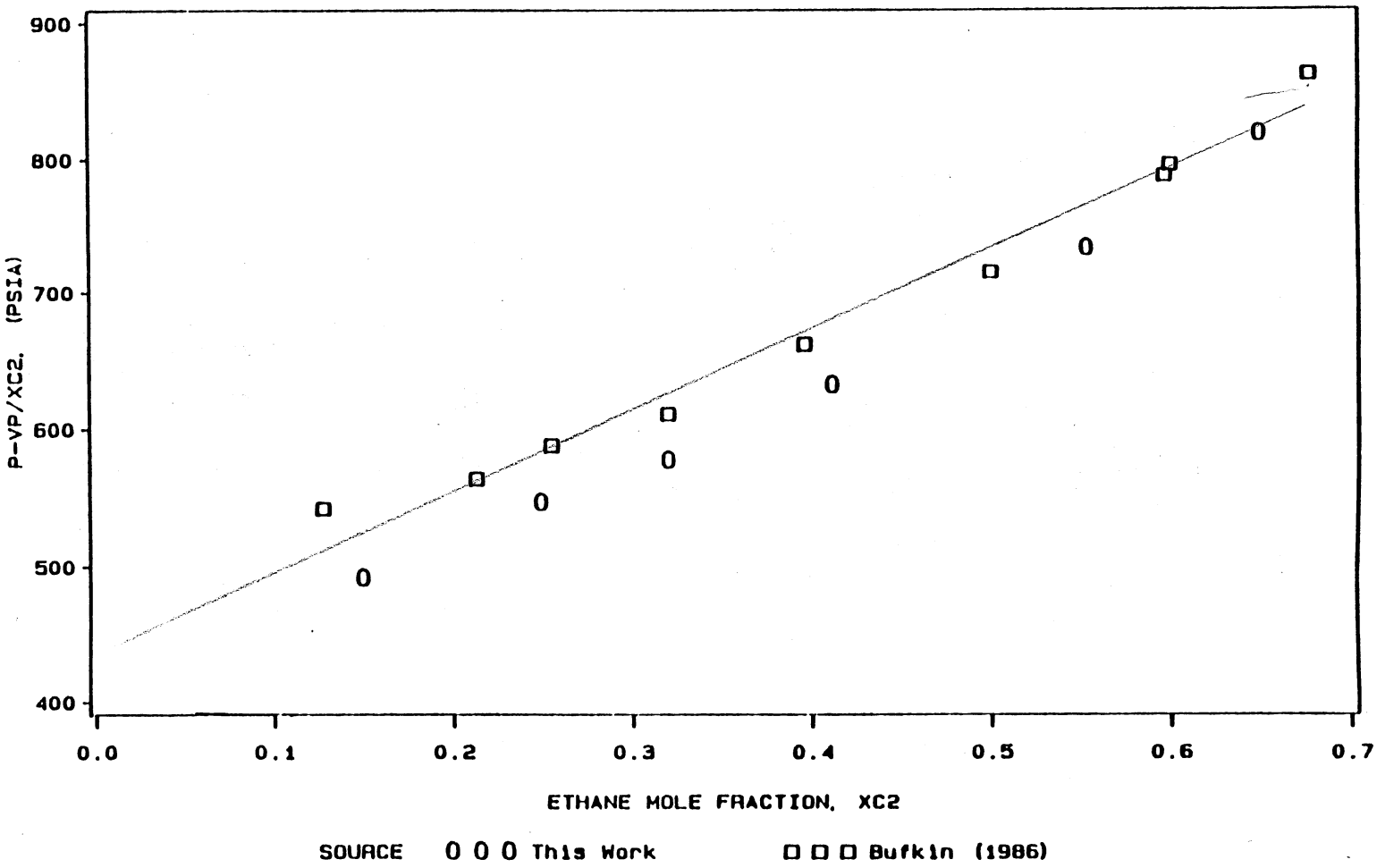

Figure 14. Comparison of Bubble-Point Data for Ethane + n-Eicosane at 50 C.

TABLE XII

SOAVE AND PENG-ROBINSON EQUATION OF STATE
REPRESENTATIONS OF SOLUBILITY DATA
FOR ETHANE IN n-EICOSANE

Temperature K(F)	Soave parameters (P-R Parameters) Cij	Dij	Error in Solute Mole Fraction * RMS	Max.
---------- C2 + Eicosane ----------				
323.2 (122)	0.028	-0.023	0.002	0.004
	(0.025)	(-0.023)		
	0.001	-----	0.025	0.031
	(-0.003)	-----		

*Errors are essentially identical for the Soave and the Peng-Robinson equations of state.

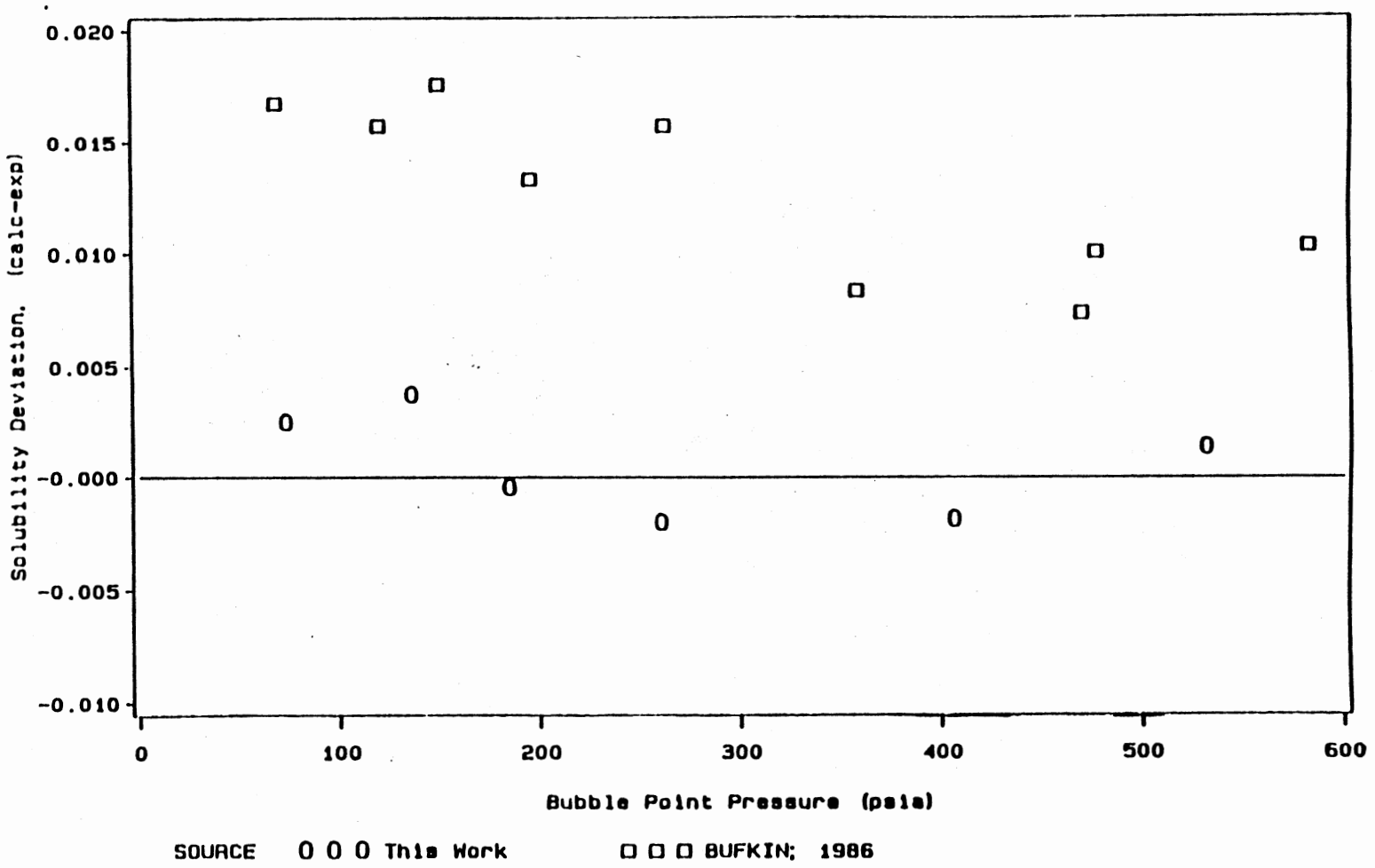

Figure 15. Comparison of Solubility Data for Ethane + n-Eicosane at 50 C.

TABLE XIII

SOLUBILITY OF ETHANE IN n-HEXATRIACONTANE

Mole Fraction Ethane	Pressure MPa	Pressure psia
373.2 K (100.0 C, 212 F)		
0.087	0.368	53.4
0.166	0.752	109.1
0.251	1.238	179.5
0.307	1.627	236.0
0.354	1.979	287.0
0.427	2.605	377.8
0.531	3.671	532.5

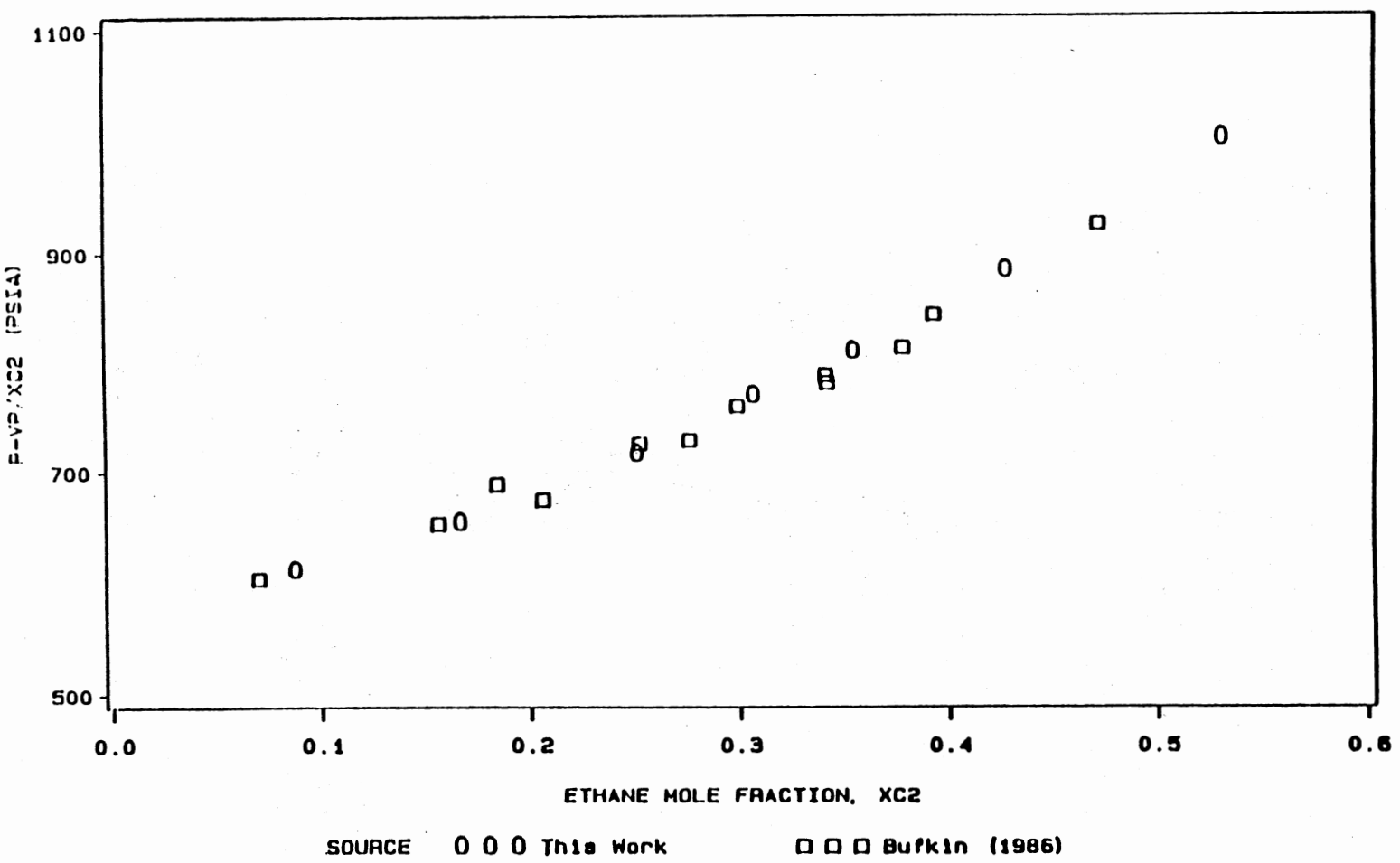

Figure 16. Comparison of Bubble-Point Data for Ethane + n-Hexatriacontane at 100 C.

TABLE XIV

SOAVE AND PENG-ROBINSON EQUATION OF STATE
REPRESENTATIONS OF SOLUBILITY DATA
FOR ETHANE IN n-HEXATRIACONTANE

Temperature K(F)	Soave parameters (P-R Parameters) Cij	Dij	Error in Solute Mole Fraction * RMS	Max.
C2 + Hexatriacontane				
373.2 (212)	0.043	-0.019	0.001	0.002
	(0.027)	(-0.012)		
	-0.018	-----	0.019	0.025
	(-0.034)	-----		

*Errors are essentially identical for the Soave and the Peng-Robinson equations of state.

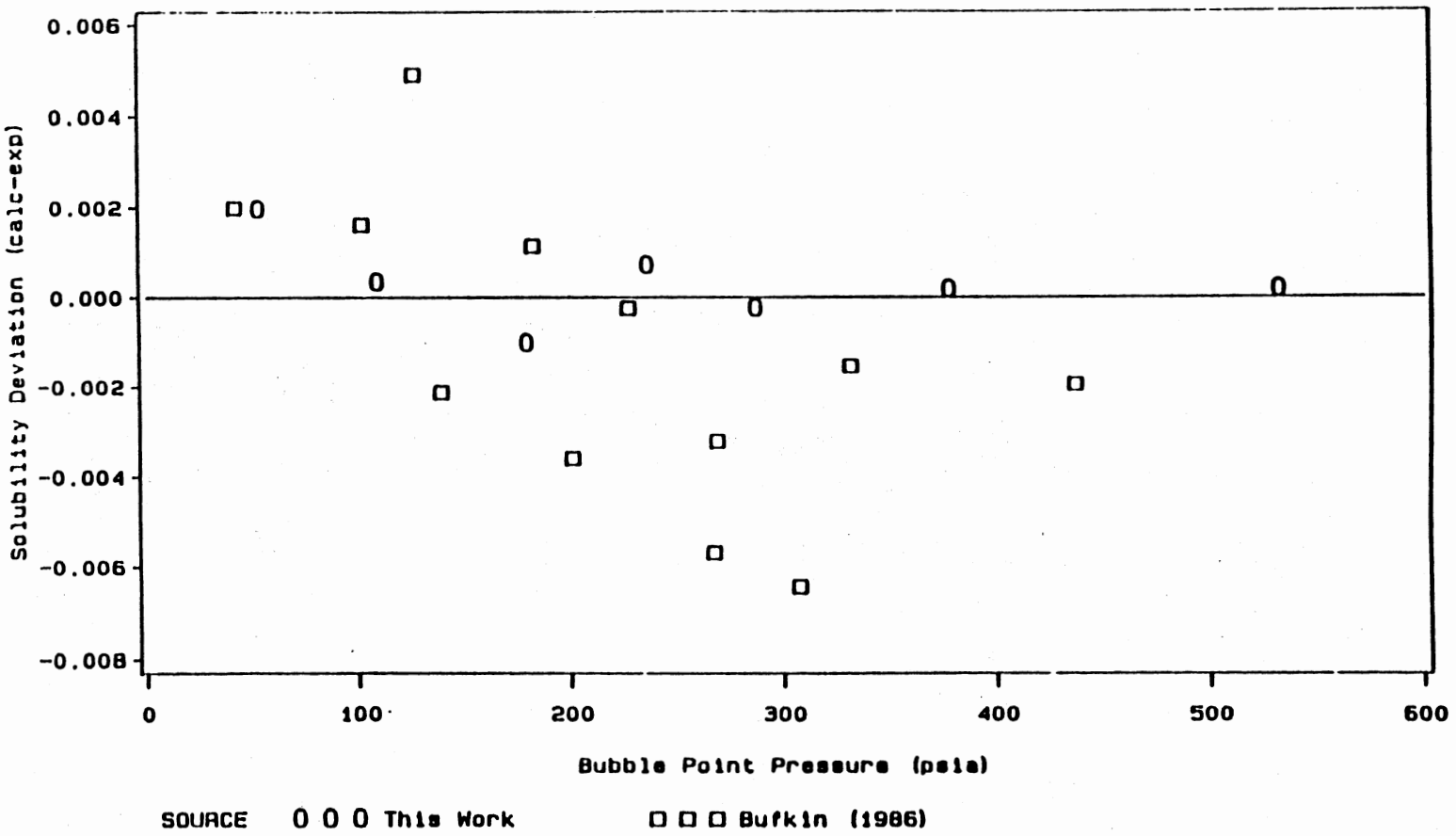

Figure 17. Comparison of Solubility Data for Ethane + n-Hexatriacontane at 100 C.

Figure 16 the disagreement between the two studies.

Ethane + n-Tetratetracontane

Another system investigated was ethane + n-tetratetracontane at 100 C and 150 C. This is the largest hydrocarbon chain studied with ethane to date, although CO2 + n-tetratetracontane has been investigated by Gasem (3). The data from the two isotherms are presented in Table XV, and are examined graphically in Figure 18 using a "simplified Henry's plot".

As with previous systems, the data were regressed using the SRK and P-R equations of state. The interaction parameters are shown in Table XVI. Since data of this binary system were taken at different temperatures, the effect of temperature on interaction parameters can be examined. For this binary system, Cij and Dij were regressed for each isotherm as well as the whole set of data. An interesting point emerged when the regression was held to a single parameter, Cij. The error remained roughly the same whether the data were grouped or not, implying that Cij may not be temperature dependent. Figure 19 shows the deviation of the data from the EOS prediction.

TABLE XV

SOLUBILITY OF ETHANE IN n-TETRATETRACONTANE

Mole Fraction Ethane	Pressure MPa	Pressure psia
373.2 K (100.0 C, 212 F)		
0.110	0.387	56.1
0.167	0.620	89.9
0.245	0.994	144.2
0.304	1.373	199.1
0.360	1.724	250.1
0.361	1.762	255.5
0.448	2.476	359.1
0.501	3.004	435.7
0.516	3.107	450.7
423.2 K (150.0 C, 302 F)		
0.099	0.527	76.5
0.122	0.656	95.1
0.209	1.234	179.0
0.303	1.937	281.0
0.340	2.266	328.6
0.409	2.981	432.3

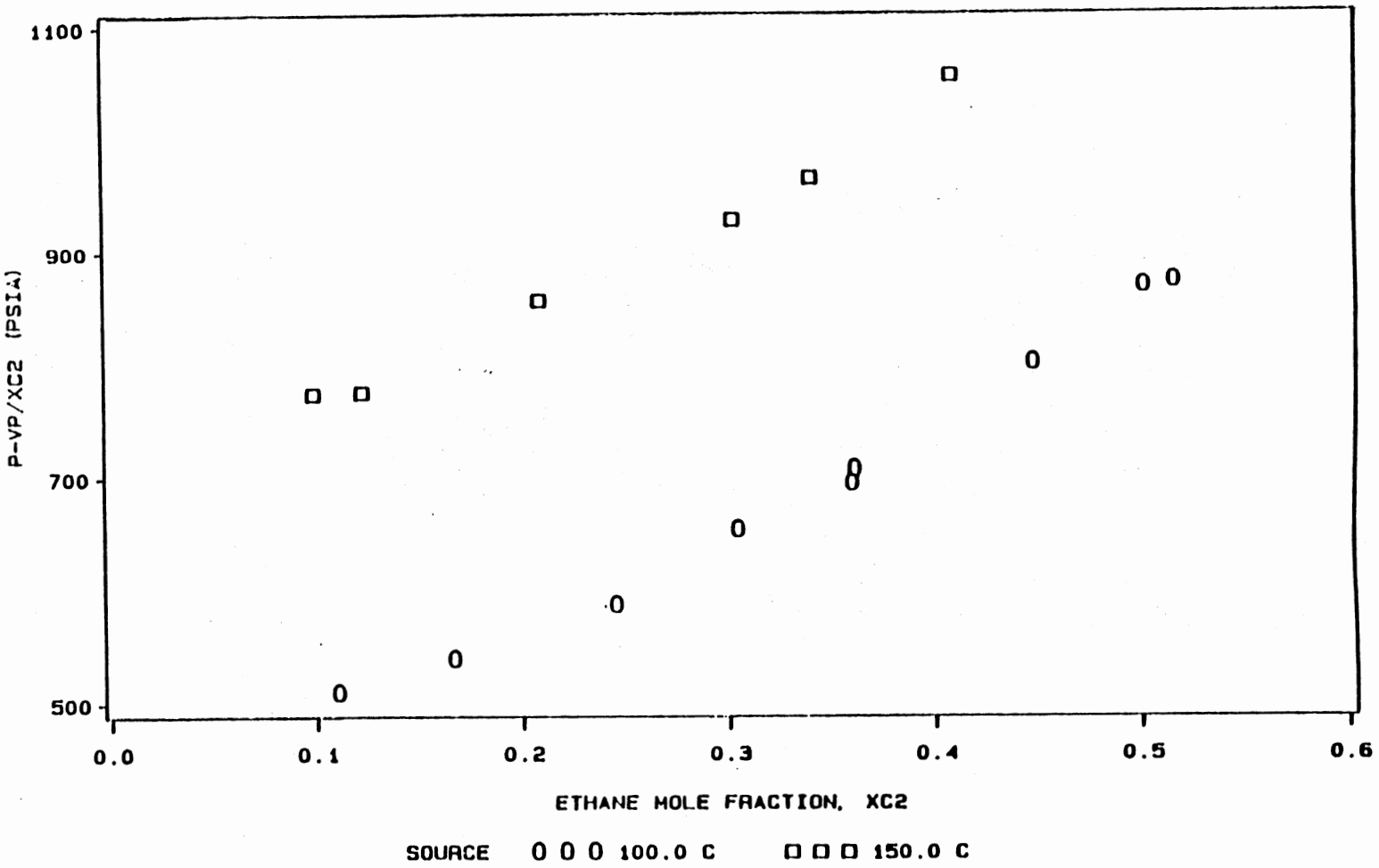

Figure 18. Simplified Henry's Plot for Ethane + n-Tetratetracontane.

TABLE XVI

SOAVE AND PENG-ROBINSON EQUATION OF STATE
REPRESENTATIONS OF SOLUBILITY DATA
FOR ETHANE IN n-TETRATETRACONTANE

Temperature K(F)	Soave parameters (P-R Parameters) Cij	Dij	Error in Solute Mole Fraction * RMS	Max.
---------- C2 + Tetratetracontane ----------				
373.2 (212)	0.069 (0.048)	-0.023 (-0.025)	0.002	0.003
	-0.028 (-0.050)	----- -----	0.026	0.039
423.2 (302)	0.059 (0.038)	-0.016 (-0.018)	0.002	0.002
	-0.030 (-0.053)	----- -----	0.010	0.013
373.2, 423.2	0.052 (0.031)	-0.018 (-0.020)	0.007	0.013
	-0.028 (-0.051)	----- -----	0.021	0.039

*Errors are essentially identical for the Soave and the Peng-Robinson equations of state.

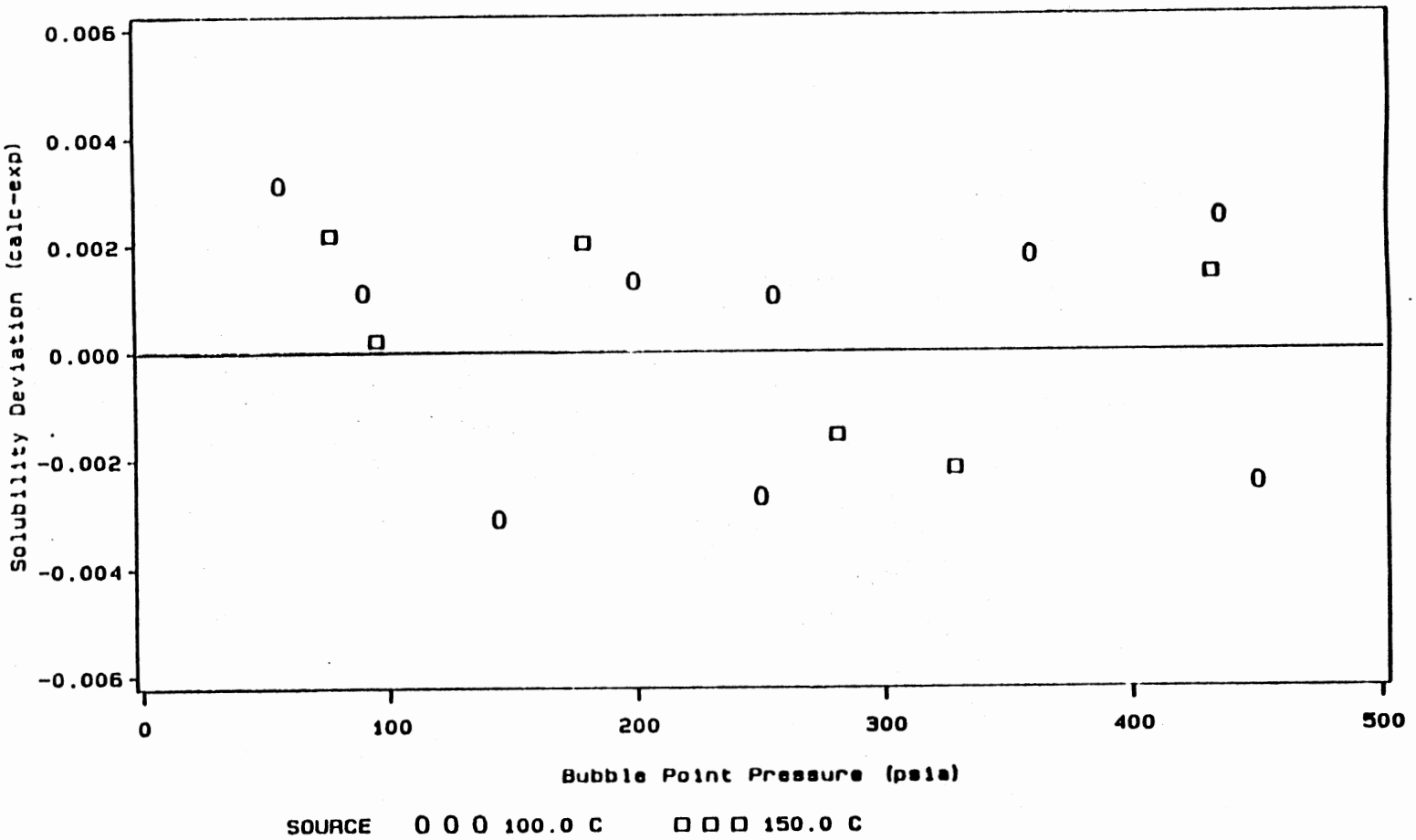

Figure 19. Solubility Data for Ethane + n-Tetratetracontane.

CHAPTER VIII

CORRELATIONS OF ETHANE SOLUBILITIES IN n-PARAFFINS

To fully represent a binary vapor-liquid system at its bubble point, the measured properties of temperature, pressure, and liquid mole fraction are needed. Using these values the data can be regressed to optimize Cij and Dij using equations (3.28) and (3.29). From these regressions the validity of the EOS predictions can be determined.

By using a large data base the EOS may be evaluated under several conditions. The data and their sources used in this investigation appear in Table XVII. All data chosen were taken at constant temperature and are reported as liquid mole fraction as a function of pressure. The data were analyzed using the SRK and P-R equations of state, utilizing a program developed by Gasem (3). During the course of the investigation, several cases were studied to gain further insight into the behavior of binary interaction parameters. Special cases studied are listed in Table XVIII. The critical properties used in this study are presented in Table XIX. For carbon numbers below 17, values for the critical properties can be determined experimentally. However, experimental determination is not possible for the higher carbon numbers since these compounds

TABLE XVII

DATA EMPLOYED IN ETHANE + n-PARAFFIN STUDIES

Temperature (F)	Pressure (psia)	Mole Fraction Ethane	Ref
	C3, Propane		
100.0	200.0	0.031	(8)
100.0	250.0	0.149	
100.0	300.0	0.255	
100.0	350.0	0.353	
100.0	400.0	0.447	
100.0	450.0	0.535	
100.0	500.0	0.622	
100.0	550.0	0.705	
100.0	600.0	0.781	
100.0	700.0	0.895	
100.0	725.0	0.919	
140.0	400.0	0.152	(8)
140.0	450.0	0.230	
140.0	500.0	0.305	
140.0	550.0	0.378	
140.0	600.0	0.448	
140.0	700.0	0.581	
140.0	725.0	0.613	
140.0	750.0	0.652	
180.0	525.0	0.069	(8)
180.0	550.0	0.102	
180.0	575.0	0.135	
180.0	600.0	0.168	
180.0	625.0	0.201	
180.0	675.0	0.270	
180.0	700.0	0.309	

TABLE XVII (Continued)

Temperature (F)	Pressure (psia)	Mole Fraction Ethane	Ref
	C4, Butane		
150.0	514.0	0.482	(9)
150.0	558.0	0.524	
150.0	637.0	0.596	
150.0	765.0	0.714	
150.0	805.0	0.753	
200.0	547.0	0.322	(9)
200.0	594.0	0.364	
200.0	613.0	0.381	
200.0	666.0	0.424	
200.0	691.0	0.437	
200.0	769.0	0.506	
200.0	795.0	0.529	

TABLE XVII (Continued)

Temperature (F)	Pressure (psia)	Mole Fraction Ethane	Ref
	C5, Pentane		
40.0	50.0	0.143	(10)
40.0	100.0	0.289	
40.0	150.0	0.432	
40.0	200.0	0.566	
40.0	250.0	0.695	
40.0	300.0	0.814	
100.0	50.0	0.062	(10)
100.0	100.0	0.152	
100.0	150.0	0.237	
100.0	200.0	0.320	
100.0	250.0	0.400	
100.0	300.0	0.477	
100.0	350.0	0.551	
100.0	400.0	0.622	
100.0	450.0	0.688	
100.0	500.0	0.747	
220.0	100.0	0.005	(10)
220.0	150.0	0.051	
220.0	200.0	0.095	
220.0	250.0	0.137	
220.0	300.0	0.180	
220.0	350.0	0.221	
220.0	400.0	0.263	
220.0	450.0	0.303	
220.0	500.0	0.343	
220.0	700.0	0.489	
220.0	800.0	0.557	

TABLE XVII (Continued)

Temperature (F)	Pressure (psia)	Mole Fraction Ethane	Ref
	C6, Hexane		
100.0	57.0	0.095	This Work
100.0	80.1	0.136	
100.0	95.7	0.163	
100.0	121.0	0.206	
100.0	153.3	0.259	
100.0	170.8	0.288	
100.0	207.3	0.347	
100.0	226.3	0.373	
100.0	245.0	0.403	
100.0	313.8	0.503	
100.0	327.3	0.522	
100.0	348.3	0.552	
100.0	385.4	0.602	
100.0	391.4	0.610	
100.0	422.7	0.652	
150.0	67.1	0.072	This Work
150.0	93.1	0.107	
150.0	171.1	0.201	
150.0	174.0	0.204	
150.0	259.2	0.301	
150.0	306.9	0.352	
150.0	344.0	0.392	
150.0	394.0	0.442	
150.0	452.4	0.499	
150.0	474.0	0.520	
150.0	520.7	0.564	

TABLE XVII (Continued)

Temperature (F)	Pressure (psia)	Mole Fraction Ethane	Ref
	C6, Hexane		
200.0	138.9	0.109	This Work
200.0	139.8	0.111	
200.0	142.4	0.112	
200.0	240.6	0.202	
200.0	238.3	0.203	
200.0	245.1	0.208	
200.0	352.1	0.300	
200.0	358.4	0.306	
200.0	363.6	0.310	
200.0	452.6	0.382	
200.0	471.9	0.397	
250.0	152.5	0.076	This Work
250.0	193.3	0.108	
250.0	263.8	0.162	
250.0	312.9	0.199	
250.0	387.6	0.251	
250.0	469.3	0.307	
250.0	472.3	0.309	
250.0	547.1	0.358	
250.0	612.5	0.401	
250.0	625.0	0.407	
250.0	783.0	0.504	

TABLE XVII (Continued)

Temperature (F)	Pressure (psia)	Mole Fraction Ethane	Ref
	C7, Heptane		
150.0	455.0	0.517	(12)
150.0	569.0	0.616	
150.0	669.0	0.699	
150.0	783.0	0.776	
150.0	887.0	0.848	
150.0	947.0	0.887	
150.0	968.0	0.903	
250.0	718.0	0.476	(12)
250.0	874.0	0.563	
250.0	1020.0	0.631	
250.0	1142.0	0.700	
250.0	1215.0	0.738	
350.0	717.0	0.333	(12)
350.0	855.0	0.407	
350.0	993.0	0.473	
350.0	1102.0	0.536	
350.0	1156.0	0.569	

TABLE XVII (Continued)

Temperature (F)	Pressure (psia)	Mole Fraction Ethane	Ref
	C8, Octane		
122.0	176.4	0.248	(13)
122.0	235.1	0.322	
122.0	293.9	0.392	
122.0	352.7	0.458	
122.0	411.5	0.517	
122.0	470.3	0.577	
122.0	529.1	0.636	
122.0	587.8	0.693	
122.0	646.6	0.749	
122.0	705.4	0.807	
122.0	764.2	0.863	
167.0	58.8	0.057	(13)
167.0	117.6	0.126	
167.0	176.4	0.173	
167.0	235.1	0.231	
167.0	293.9	0.288	
167.0	352.7	0.346	
167.0	411.5	0.399	
167.0	470.3	0.449	
167.0	529.1	0.493	
167.0	587.8	0.537	
167.0	646.6	0.578	
167.0	705.4	0.622	
167.0	764.2	0.663	
212.0	58.8	0.047	(13)
212.0	117.6	0.093	
212.0	176.4	0.139	
212.0	235.1	0.186	
212.0	293.9	0.232	
212.0	352.7	0.278	
212.0	411.5	0.324	
212.0	470.3	0.367	
212.0	529.1	0.405	

TABLE XVII (Continued)

Temperature (F)	Pressure (psia)	Mole Fraction Ethane	Ref
	C10, Decane		
100.0	61.4	0.108	(2)
100.0	71.3	0.127	
100.0	120.9	0.211	
100.0	158.6	0.271	
100.0	177.8	0.300	
100.0	185.3	0.308	
100.0	256.5	0.413	
100.0	301.3	0.470	
100.0	325.8	0.501	
100.0	408.0	0.601	
160.0	86.7	0.105	(2)
160.0	171.5	0.203	
160.0	275.4	0.305	
160.0	401.0	0.422	
160.0	514.4	0.510	
160.0	604.4	0.579	
160.0	680.3	0.631	
220.0	117.0	0.106	(2)
220.0	232.1	0.202	
220.0	404.3	0.328	
220.0	524.8	0.408	
220.0	694.8	0.505	
220.0	875.1	0.600	
280.0	145.8	0.105	(2)
280.0	309.1	0.215	
280.0	495.3	0.323	
280.0	650.9	0.404	
280.0	859.4	0.500	
280.0	1052.1	0.582	
280.0	1194.6	0.638	

TABLE XVII (Continued)

Temperature (F)	Pressure (psia)	Mole Fraction Ethane	Ref
	C12, Dodecane		
212.0	161.2	0.155	(14)
212.0	231.9	0.211	
212.0	300.0	0.267	
212.0	341.5	0.297	
212.0	497.9	0.401	
212.0	771.5	0.554	
212.0	112.5	0.111	(3)
212.0	195.5	0.179	
212.0	226.0	0.204	
212.0	279.5	0.244	
212.0	353.5	0.297	
212.0	361.0	0.300	
212.0	515.0	0.399	
212.0	518.0	0.403	
212.0	671.0	0.487	
212.0	759.0	0.534	
212.0	58.8	0.050	(15)
212.0	293.9	0.247	
212.0	352.7	0.292	
212.0	411.5	0.334	
212.0	470.3	0.373	
212.0	529.1	0.409	
212.0	587.8	0.444	
212.0	646.6	0.475	
212.0	705.4	0.506	
212.0	764.2	0.536	
212.0	823.0	0.565	
212.0	881.8	0.594	
212.0	911.2	0.608	
212.0	95.7	0.087	(16)
212.0	269.8	0.237	
212.0	423.5	0.348	
212.0	487.3	0.392	
212.0	639.6	0.475	
212.0	764.4	0.547	

TABLE XVII (Continued)

Temperature (F)	Pressure (psia)	Mole Fraction Ethane	Ref
	C20, Eicosane		
122.0	73.2	0.149	This Work
122.0	136.1	0.249	
122.0	184.8	0.320	
122.0	260.1	0.411	
122.0	406.3	0.553	
122.0	531.7	0.649	
212.0	155.7	0.175	(14)
212.0	293.2	0.298	
212.0	508.3	0.445	
212.0	708.8	0.551	
212.0	834.6	0.604	
212.0	963.8	0.653	
302.0	135.1	0.118	(14)
302.0	339.6	0.257	
302.0	455.2	0.324	
302.0	611.8	0.400	
302.0	768.5	0.466	
302.0	930.0	0.525	
302.0	1115.1	0.582	

TABLE XVII (Continued)

Temperature (F)	Pressure (psia)	Mole Fraction Ethane	Ref
	C28, Octacosane		
167.0	85.5	0.149	(14)
167.0	128.1	0.207	
167.0	161.3	0.256	
167.0	200.3	0.299	
167.0	252.4	0.350	
167.0	268.7	0.373	
167.0	314.8	0.413	
167.0	336.3	0.434	
167.0	423.1	0.503	
167.0	451.5	0.520	
212.0	81.6	0.111	(14)
212.0	113.7	0.150	
212.0	174.7	0.221	
212.0	254.5	0.300	
212.0	454.6	0.450	
212.0	516.5	0.487	
212.0	549.5	0.508	
302.0	100.3	0.102	(14)
302.0	187.6	0.179	
302.0	286.1	0.253	
302.0	353.5	0.300	
302.0	466.4	0.366	
302.0	637.3	0.451	
302.0	751.6	0.500	

TABLE XVII (Continued)

Temperature (F)	Pressure (psia)	Mole Fraction Ethane	Ref
	C36, Hexatriacontane		
212.0	53.4	0.087	This Work
212.0	109.1	0.166	
212.0	179.5	0.251	
212.0	236.0	0.307	
212.0	287.0	0.354	
212.0	377.8	0.427	
212.0	532.5	0.531	
302.0	139.9	0.153	(14)
302.0	196.8	0.207	
302.0	335.4	0.315	
302.0	492.1	0.408	
302.0	617.4	0.468	
302.0	690.4	0.500	

TABLE XVII (Continued)

Temperature (F)	Pressure (psia)	Mole Fraction Ethane	Ref
	C44, Tetratetracontane		
212.0	56.1	0.110	This Work
212.0	89.9	0.167	
212.0	144.2	0.245	
212.0	199.1	0.304	
212.0	250.1	0.360	
212.0	255.5	0.361	
212.0	359.1	0.448	
212.0	435.7	0.501	
212.0	450.7	0.516	
302.0	76.5	0.099	This Work
302.0	95.1	0.122	
302.0	179.0	0.209	
302.0	281.0	0.303	
302.0	328.6	0.340	
302.0	432.3	0.409	

TABLE XVIII

CASES FOR INTERACTION PARAMETER INVESTIGATIONS

Case	Description
1. Cij = 0, Dij = 0	This shows the "raw ability" of the EOS. This case permits predictions from pure component data only.
2. Cij (all), Dij = 0	A single parameter is used for ethane with all solvents. This is the most basic use of an interaction parameter.
3. Cij (CN), Dij = 0	A single parameter is determined for ethane with each solvent. This is the most commonly employed option in use.
4. Cij (CN,T) Dij = 0	A separate parameter is used at each temperature in each system. This case permits Cij to be both solvent and temperature dependent.
5. Cij (all), Dij (all)	All data are represented by a single pair of interaction parameters.
6. Cij (CN), Dij (CN)	A pair of interaction parameters is determined for ethane with each solvent, independent of temperature.
7. Cij (CN,T) Dij (CN,T)	A separate pair of parameters is determined for each binary system at each temperature. This is the most detailed use of parameters, reflecting both solvent and temperature effects.

TABLE XIX

PURE FLUID PROPERTIES USED IN EQUATIONS OF STATE PREDICTIONS

Components	Reference	Tc, F	Pc, psi	Omega (ω)
Benzene	36	487.42	701.11	0.2120
CO2	36	87.91	1056.75	0.2251
C2	36	89.92	706.54	0.1004
n-C3	36	206.01	615.98	0.1542
n-C4	36	305.62	550.56	0.2004
n-C5	36	385.88	489.65	0.2511
n-C6	36	454.53	433.43	0.2978
n-C7	36	512.58	396.68	0.3499
n-C8	36	564.21	362.30	0.3995
n-C10	36	651.92	304.14	0.4885
n-C12	36	725.18	261.94	0.5708
n-C20	34	920.14	155.05	0.8791
n-C28	34	1029.7	95.87	1.1617
n-C36	34	1095.5	62.08	1.4228
n-C44	34	1136.3	42.10	1.6664

decompose before thier critical values can be reached. Critical values for C20 and higher are taken from the work of Ross (34). In this work Ross used a software package developed by Gasem (3) in order to regress these parameters using the SRK equation of state. Acceptance of the estimates obtained for a given property were based on a reasonable agreement with established relationships among a set of properties, when available, or by the quality of fit attained using the SRK equation of state.

Case 1: Cij=0, Dij=0

The first case studied used no interaction parameters, and therefore tested the raw ability of the cubic EOS to predict bubble point pressures and solubilities. By doing this, a base case was developed by which further cases could be judged. Results of Case 1 appear in Table XX. Case 1 produces a reasonable representation of the data with a RMSE of less than 1.5 bar, and a maximum deviation from experimental values of 5.3 bar. Table XX shows that although the EOS, using no interaction parameters, predicts the lower carbon number systems fairly well, the lack of fit increases with the size of the solvent molecule.

Case 2: Cij(all), Dij=0

Case 2 employs the use of an interaction parameter on its most basic level, using a single parameter to represent the entire range of temperatures and solvents. Results are shown in Table XXI. The use of a single interaction

TABLE XX

BUBBLE-POINT CALCULATIONS USING THE SRK EQUATION OF STATE CASE 1

ISO	CN	T(K)	C(I,J)	D(I,J)	RMSE BAR	BIAS BAR	AAD BAR	%AAD	NO PT
1	3	310.9	0.0000	0.0000	0.33	0.26	0.28	1.2	11
2	3	333.1	0.0000	0.0000	0.19	-0.12	0.14	0.4	8
3	3	355.4	0.0000	0.0000	0.12	-0.03	0.10	0.2	7
4	4	338.7	0.0000	0.0000	1.39	-1.23	1.23	2.9	5
5	4	366.5	0.0000	0.0000	2.19	-1.90	1.90	4.4	7
6	5	277.6	0.0000	0.0000	0.21	-0.20	0.20	1.9	6
7	5	310.9	0.0000	0.0000	0.11	0.00	0.10	0.8	10
8	5	377.6	0.0000	0.0000	0.74	-0.51	0.52	1.6	11
9	6	310.9	0.0000	0.0000	0.07	-0.06	0.06	0.5	15
10	6	338.7	0.0000	0.0000	0.08	0.03	0.06	0.6	11
11	6	366.5	0.0000	0.0000	0.08	0.01	0.06	0.4	11
12	6	394.3	0.0000	0.0000	0.77	-0.59	0.59	1.6	11
13	7	338.7	0.0000	0.0000	0.90	0.35	0.79	1.8	7
14	7	394.3	0.0000	0.0000	2.34	-2.07	2.07	2.8	5
15	7	449.8	0.0000	0.0000	4.77	-4.72	4.72	7.1	5
16	8	323.1	0.0000	0.0000	1.21	-1.12	1.12	3.6	11
17	8	348.1	0.0000	0.0000	1.78	-1.65	1.65	6.7	13
18	8	373.1	0.0000	0.0000	1.32	-1.23	1.23	6.4	9
19	10	310.9	0.0000	0.0000	0.45	-0.36	0.36	2.3	10
20	10	344.3	0.0000	0.0000	0.45	-0.23	0.33	1.3	6
21	10	377.6	0.0000	0.0000	0.40	0.07	0.35	1.7	5
22	10	410.9	0.0000	0.0000	1.01	-0.21	0.80	2.4	6
23	12	373.1	0.0000	0.0000	1.72	-1.07	1.27	3.6	35
24	20	323.1	0.0000	0.0000	1.38	0.49	1.27	10.5	6
25	20	373.1	0.0000	0.0000	2.18	-0.16	1.90	6.7	6
26	20	423.1	0.0000	0.0000	2.35	1.31	2.13	8.0	7
27	28	348.1	0.0000	0.0000	1.82	1.73	1.73	12.9	10
28	28	373.1	0.0000	0.0000	1.65	1.53	1.53	11.8	7
29	28	423.1	0.0000	0.0000	2.37	2.21	2.21	12.0	7
30	36	373.1	0.0000	0.0000	1.74	1.55	1.58	14.5	7
31	36	423.1	0.0000	0.0000	1.76	0.69	1.66	8.7	6
32	44	373.1	0.0000	0.0000	2.18	2.00	2.00	18.9	9
33	44	423.1	0.0000	0.0000	1.41	1.36	1.36	11.5	6

MODEL OVERALL STATISTICS

RMSE	= 1.4889 BAR	NO PT	= 296
AAD	= 1.0362 BAR	%AAD	= 4.768
MIN DEV=	-5.2979 BAR	MIN %DEV	= -12.415
MAX DEV=	3.2278 BAR	MAX %DEV	= 40.822
BIAS	= -0.1870 BAR	C-VAR	= 0.093
RESTRICTIONS	: P LE 0.90 PC	R-SQR	=0.918535
AUX. MODELS	: 000 000 000/ 000 000		

TABLE XXI

BUBBLE-POINT CALCULATIONS USING THE SRK EQUATION OF STATE CASE 2

ISO	CN	T(K)	C(I,J)	D(I,J)	RMSE BAR	BIAS BAR	AAD BAR	%AAD	NO PT
1	3	310.9	0.0049	0.0000	0.48	0.41	0.43	1.8	11
2	3	333.1	0.0049	0.0000	0.27	-0.04	0.19	0.5	8
3	3	355.4	0.0049	0.0000	0.16	0.03	0.13	0.3	7
4	4	338.7	0.0049	0.0000	1.57	-1.35	1.35	3.0	5
5	4	366.5	0.0049	0.0000	1.96	-1.73	1.73	3.9	7
6	5	277.6	0.0049	0.0000	0.09	-0.06	0.07	0.6	6
7	5	310.9	0.0049	0.0000	0.26	0.21	0.21	1.0	10
8	5	377.6	0.0049	0.0000	0.54	-0.29	0.32	1.0	11
9	6	310.9	0.0049	0.0000	0.21	0.19	0.19	1.3	15
10	6	338.7	0.0049	0.0000	0.33	0.33	0.33	2.1	11
11	6	366.5	0.0049	0.0000	0.29	0.28	0.28	1.6	11
12	6	394.3	0.0049	0.0000	0.49	-0.29	0.34	0.9	11
13	7	338.7	0.0049	0.0000	1.17	0.62	0.99	2.3	7
14	7	394.3	0.0049	0.0000	1.95	-1.60	1.60	2.1	5
15	7	449.8	0.0049	0.0000	4.39	-4.34	4.34	6.6	5
16	8	323.1	0.0049	0.0000	0.85	-0.75	0.75	2.3	11
17	8	348.1	0.0049	0.0000	1.36	-1.25	1.25	5.1	13
18	8	373.1	0.0049	0.0000	1.00	-0.93	0.93	4.9	9
19	10	310.9	0.0049	0.0000	0.19	-0.05	0.14	0.9	10
20	10	344.3	0.0049	0.0000	0.31	0.19	0.28	1.9	6
21	10	377.6	0.0049	0.0000	0.57	0.51	0.51	2.8	5
22	10	410.9	0.0049	0.0000	0.86	0.31	0.80	2.9	6
23	12	373.1	0.0049	0.0000	1.28	-0.54	0.97	3.1	35
24	20	323.1	0.0049	0.0000	1.43	0.91	1.35	11.9	6
25	20	373.1	0.0049	0.0000	1.96	0.58	1.80	7.2	6
26	20	423.1	0.0049	0.0000	2.60	1.96	2.42	9.1	7
27	28	348.1	0.0049	0.0000	2.16	2.11	2.11	15.0	10
28	28	373.1	0.0049	0.0000	1.99	1.91	1.91	13.6	7
29	28	423.1	0.0049	0.0000	2.72	2.61	2.61	13.4	7
30	36	373.1	0.0049	0.0000	1.97	1.84	1.84	16.1	7
31	36	423.1	0.0049	0.0000	1.80	1.05	1.65	9.1	6
32	44	373.1	0.0049	0.0000	2.40	2.26	2.26	20.4	9
33	44	423.1	0.0049	0.0000	1.59	1.54	1.54	12.7	6

MODEL OVERALL STATISTICS

PAR(1).. PAR(N)= 0.489936D-02 0.0000000D+00

RMSE = 1.4290 BAR
AAD = 1.0137 BAR
MIN DEV= -4.9325 BAR
MAX DEV= 3.6631 BAR
BIAS = 0.1436 BAR
RESTRICTIONS : P LE 0.90 PC
AUX. MODELS : 000 000 000/ 000 000
SQUARE ERROR IN PRESSURE MINIMIZED

NO PT = 296
%AAD = 4.948
MIN %DEV = -10.649
MAX %DEV = 42.521
C-VAR = 0.050
R-SQR =0.919618

parameter (Cij=0.005) had little effect on the RMSE, lowering it from 1.49 bar to 1.43 bar. However, the use of an interaction parameter has a "leveling" effect on the data, meaning that the fit of each binary system is closer to the average, although an enhanced fit still exists for the lighter solvents.

Case 3: Cij(CN), Dij=0

Case 3 utilizes a single interaction parameter for each binary system; results are listed on Table XXII. This case produces a definite improvement over Case 2, dropping the RMSE by nearly 25% to 1.1 bar. The lighter hydrocarbons still experience a better fit than the heavier solvents, but surprisingly, the largest error occurs for the ethane + n-heptane binary system. This was also true for Case 1 and Case 2. This binary system contains data collected at a temperature higher than that of the other isotherms, 449.8 K, and what is being observed is the inability to properly fit this isotherm because of its high temperature. When an interaction parameter is used to fit data over a wide range, the data that exist outside the norm often experiences an inaccurate fit. In order to obtain a more accurate fit for the ethane + n-heptane binary, an interaction parameter that is temperature dependent must be used.

Case 4: Cij(CN,T), Dij=0

This case is the most specific use of a single interaction parameter. By fitting an individual parameter

TABLE XXII

BUBBLE-POINT CALCULATIONS USING THE SRK EQUATION OF STATE CASE 3

ISO	CN	C(I,J)	D(I,J)	RMSE BAR	BIAS BAR	AAD BAR	%AAD	NO PT
1	3	-0.0019	0.0000	0.24	0.01	0.18	0.6	26
2	4	0.0143	0.0000	1.49	-1.31	1.31	2.9	12
3	5	0.0072	0.0000	0.37	0.04	0.22	1.0	27
4	6	0.0032	0.0000	0.32	0.04	0.22	1.0	48
5	7	0.0222	0.0000	2.30	-0.15	1.98	3.7	17
6	8	0.0177	0.0000	0.35	-0.02	0.29	1.7	33
7	10	0.0039	0.0000	0.50	0.10	0.39	1.8	27
8	12	0.0120	0.0000	0.94	0.26	0.79	3.3	35
9	20	0.0013	0.0000	2.03	0.75	1.78	8.6	19
10	28	-0.0176	0.0000	1.27	0.48	1.17	7.8	24
11	36	-0.0079	0.0000	1.65	0.65	1.53	10.5	13
12	44	-0.0284	0.0000	1.28	0.49	1.15	10.5	15

MODEL OVERALL STATISTICS

RMSE =	1.0798 BAR	NO PT =	296
AAD =	0.7336 BAR	%AAD =	3.575
MIN DEV=	-3.5633 BAR	MIN %DEV =	-6.191
MAX DEV=	3.4029 BAR	MAX %DEV =	31.402
BIAS =	0.1272 BAR	C-VAR =	0.065
RESTRICTIONS :	P LE 0.90 PC	R-SQR =	0.927078
AUX. MODELS :	000 000 000/ 000 000		
	SQUARE ERROR IN PRESSURE MINIMIZED		

to each binary system at each isotherm, no set of data can be influenced by another. The results for this case are shown in Table XXIII. The overall error was lowered by only 0.17 bar, and the maximum deviation stayed relatively constant. Since a single parameter was not forced to fit data over a wide range of temperatures, the RMSE values for each system are brought closer to a central value. This "dampening" or "leveling" effect of RMSE is best seen in the ethane + n-heptane binary system. In Case 2 the RMSE of the ethane + n-heptane binary system were 1.17, 1.95, and 4.39, for the three isotherms, but by using a temperature dependent interaction parameter the large range of temperatures is more easily handled, and the errors dropped to 0.54, 1.27, and 0.52, which do not show the abnormal spread of the previous cases.

Figure 20 shows the dependence of Cij on temperature and carbon number of the solvent. Although it is difficult to see a pattern in the data, a few trends are obvious. The first trend shows that each binary system definitely has some temperature dependence, although the dependence differs for each system. Another pattern is the general trend to more negative values of Cij as the carbon number of the solvent increases.

Case 5: Cij(all), Dij(all)

Case 5 is the first case in which a second interaction parameter is regressed. By applying two parameters to the entire set of data, the overall improvement gained from the

TABLE XXIII

BUBBLE-POINT CALCULATIONS USING THE SRK EQUATION OF STATE CASE 4

ISO	CN	T(K)	C(I,J)	D(I,J)	RMSE BAR	BIAS BAR	AAD BAR	%AAD	NO PT
1	3	310.9	-0.0075	0.0000	0.18	0.03	0.15	0.7	11
2	3	333.1	0.0023	0.0000	0.15	-0.06	0.13	0.3	8
3	3	355.4	0.0009	0.0000	0.11	-0.02	0.10	0.2	7
4	4	338.7	0.0020	0.0000	1.35	-1.21	1.21	2.8	5
5	4	366.5	0.0207	0.0000	1.64	-1.53	1.53	3.2	7
6	5	277.6	0.0068	0.0000	0.07	-0.01	0.05	0.6	6
7	5	310.9	-0.0003	0.0000	0.11	-0.01	0.10	0.8	10
8	5	377.6	0.0126	0.0000	0.37	0.06	0.29	1.1	11
9	6	310.9	0.0011	0.0000	0.05	0.00	0.04	0.2	15
10	6	338.7	-0.0002	0.0000	0.08	0.02	0.07	0.6	11
11	6	366.5	0.0001	0.0000	0.08	0.02	0.06	0.4	11
12	6	394.3	0.0108	0.0000	0.30	0.07	0.24	1.0	11
13	7	338.7	-0.0112	0.0000	0.54	-0.26	0.48	0.9	7
14	7	394.3	0.0196	0.0000	1.27	-0.12	1.20	1.8	5
15	7	449.8	0.0568	0.0000	0.52	0.01	0.49	0.8	5
16	8	323.1	0.0148	0.0000	0.32	0.01	0.29	1.2	11
17	8	348.1	0.0193	0.0000	0.31	-0.03	0.29	1.8	13
18	8	373.1	0.0184	0.0000	0.28	-0.07	0.26	1.7	9
19	10	310.9	0.0063	0.0000	0.16	0.04	0.14	1.1	10
20	10	344.3	0.0037	0.0000	0.29	0.09	0.28	1.7	6
21	10	377.6	0.0007	0.0000	0.40	0.13	0.37	1.9	5
22	10	410.9	0.0046	0.0000	0.86	0.28	0.80	2.9	6
23	12	373.1	0.0120	0.0000	0.94	0.26	0.79	3.3	35
24	20	323.1	0.0008	0.0000	1.38	0.55	1.26	10.6	6
25	20	373.1	0.0059	0.0000	1.95	0.73	1.80	7.3	6
26	20	423.1	-0.0036	0.0000	2.29	0.84	2.09	7.5	7
27	28	348.1	-0.0188	0.0000	1.06	0.36	0.94	7.1	10
28	28	373.1	-0.0136	0.0000	1.14	0.49	1.02	8.2	7
29	28	423.1	-0.0202	0.0000	1.57	0.64	1.49	7.9	7
30	36	373.1	-0.0177	0.0000	1.31	0.56	1.16	10.2	7
31	36	423.1	-0.0001	0.0000	1.76	0.68	1.66	8.7	6
32	44	373.1	-0.0277	0.0000	1.53	0.60	1.46	13.3	9
33	44	423.1	-0.0303	0.0000	0.73	0.29	0.67	6.2	6

MODEL OVERALL STATISTICS

RMSE	= 0.9124 BAR	NO PT	= 296
AAD	= 0.6177 BAR	%AAD	= 3.237
MIN DEV	= -3.5389 BAR	MIN %DEV	= -5.950
MAX DEV	= 2.8115 BAR	MAX %DEV	= 31.619
BIAS	= 0.1143 BAR	C-VAR	= 0.057
RESTRICTIONS	: P LE 0.90 PC	R-SQR	=0.922901
AUX. MODELS	: 000 000 000/ 000 000		
	SQUARE ERROR IN PRESSURE MINIMIZED		

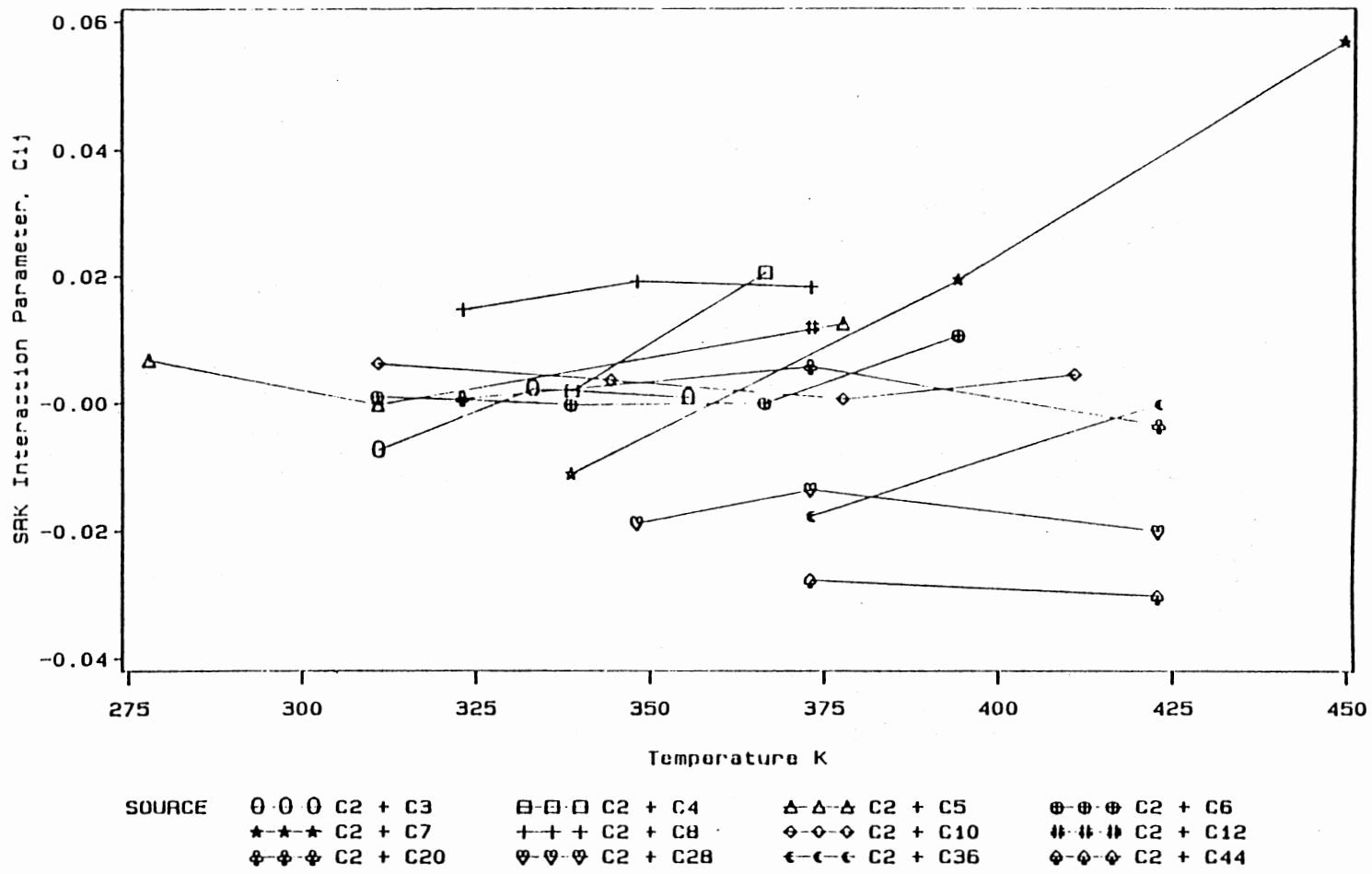

Figure 20. Temperature and Molecular Size Effects on Cij (Dij=0) for Ethane + n-Paraffins.

addition of a second parameter may be ascertained without the interference of temperature and carbon number dependence. Results are shown in Table XXIV. By comparing Case 5 to Case 2, where only Cij was used, a substantial improvement is evident. The RMSE has been reduced by more than one-third, and the maximum deviation has been lowered by more than 1.0 bar to 3.8 bar. In fact, the performance using a second interaction parameter is comparable to Case 4, where Cij is optimized for each isotherm. Another interesting note is that by using Dij the errors are much more uniform over the range of solvent sizes. From these results, the use of a second interaction parameter seems justified.

Case 6: Cij(CN), Dij(CN)

Case 6 is an investigation of the Cij, Dij dependence on solvent size. The results, shown in Table XXV, reveal that the use of a second parameter has enhanced the fit of the solubility data. The RMSE has been lowered from 1.08 bar, in case 3, to 0.66 bar. Also present is the "leveling" of errors over the entire range of data that was seen in Case 5.

Even though utilizing a second parameter for each binary system improves the quality of fit, there is some evidence that Dij is not dependent on carbon number. Figure 21 shows Dij as a function of carbon number, and although there is scatter in the data below a carbon number of ten, values beyond that point are fairly constant at -0.02.

TABLE XXIV

BUBBLE-POINT CALCULATIONS USING THE SRK EQUATION OF STATE CASE 5

ISO	CN	T(K)	C(I,J)	D(I,J)	RMSE BAR	BIAS BAR	AAD BAR	%AAD	NO PT
1	3	310.9	0.0209	-0.0140	0.73	0.64	0.66	2.6	11
2	3	333.1	0.0209	-0.0140	0.36	0.16	0.34	0.9	8
3	3	355.4	0.0209	-0.0140	0.23	0.20	0.21	0.5	7
4	4	338.7	0.0209	-0.0140	1.19	-1.02	1.02	2.2	5
5	4	366.5	0.0209	-0.0140	1.91	-1.82	1.82	3.9	7
6	5	277.6	0.0209	-0.0140	0.17	0.14	0.14	1.2	6
7	5	310.9	0.0209	-0.0140	0.66	0.55	0.56	2.6	10
8	5	377.6	0.0209	-0.0140	0.22	0.02	0.15	0.6	11
9	6	310.9	0.0209	-0.0140	0.63	0.52	0.52	2.7	15
10	6	338.7	0.0209	-0.0140	0.79	0.70	0.70	3.3	11
11	6	366.5	0.0209	-0.0140	0.55	0.49	0.49	2.3	11
12	6	394.3	0.0209	-0.0140	0.14	0.08	0.12	0.4	11
13	7	338.7	0.0209	-0.0140	1.97	1.59	1.61	3.8	7
14	7	394.3	0.0209	-0.0140	0.84	-0.05	0.80	1.2	5
15	7	449.8	0.0209	-0.0140	3.34	-3.32	3.32	5.1	5
16	8	323.1	0.0209	-0.0140	0.18	-0.02	0.14	0.5	11
17	8	348.1	0.0209	-0.0140	0.78	-0.71	0.71	4.2	13
18	8	373.1	0.0209	-0.0140	0.91	-0.85	0.85	5.2	9
19	10	310.9	0.0209	-0.0140	0.23	0.02	0.20	2.0	10
20	10	344.3	0.0209	-0.0140	0.64	0.49	0.52	1.9	6
21	10	377.6	0.0209	-0.0140	0.78	0.68	0.68	2.4	5
22	10	410.9	0.0209	-0.0140	0.87	0.83	0.83	2.6	6
23	12	373.1	0.0209	-0.0140	0.70	-0.35	0.59	2.2	35
24	20	323.1	0.0209	-0.0140	0.60	0.46	0.57	4.7	6
25	20	373.1	0.0209	-0.0140	0.91	0.54	0.81	3.1	6
26	20	423.1	0.0209	-0.0140	1.61	1.32	1.51	5.4	7
27	28	348.1	0.0209	-0.0140	0.54	0.48	0.49	3.5	10
28	28	373.1	0.0209	-0.0140	0.41	0.31	0.31	2.1	7
29	28	423.1	0.0209	-0.0140	0.89	0.77	0.79	4.3	7
30	36	373.1	0.0209	-0.0140	0.59	-0.28	0.37	1.7	7
31	36	423.1	0.0209	-0.0140	2.01	-1.33	1.37	3.4	6
32	44	373.1	0.0209	-0.0140	0.83	-0.26	0.63	4.0	9
33	44	423.1	0.0209	-0.0140	1.00	-0.83	0.83	5.0	6

MODEL OVERALL STATISTICS

PAR(1).. PAR(N)= 0.209222D-01 -0.139737D-01

RMSE = 0.9463 BAR
AAD = 0.6652 BAR
MIN DEV= -3.7985 BAR
MAX DEV= 2.9395 BAR
BIAS = 0.0229 BAR
RESTRICTIONS : P LE 0.90 PC
AUX. MODELS : 000 000 000/ 000 000
SQUARE ERROR IN PRESSURE MINIMIZED

NO PT = 296
%AAD = 2.667
MIN %DEV = -14.121
MAX %DEV = 12.072
C-VAR = 0.033
R-SQR = 0.974553

TABLE XXV

BUBBLE-POINT CALCULATIONS USING THE SRK EQUATION OF STATE CASE 6

ISO	CN	C(I,J)	D(I,J)	RMSE BAR	BIAS BAR	AAD BAR	%AAD	NO PT
1	3	0.0046	-0.0104	0.23	0.00	0.18	0.6	26
2	4	-0.0069	0.0876	0.73	-0.23	0.56	1.3	12
3	5	0.0128	-0.0094	0.35	0.03	0.23	1.0	27
4	6	0.0084	-0.0076	0.30	0.01	0.22	0.9	48
5	7	0.0249	-0.0188	2.23	-0.05	1.85	3.5	17
6	8	0.0187	-0.0016	0.35	-0.02	0.28	1.7	33
7	10	0.0141	-0.0128	0.30	-0.05	0.26	1.9	27
8	12	0.0272	-0.0172	0.52	-0.01	0.41	1.9	35
9	20	0.0325	-0.0277	0.37	-0.05	0.30	1.8	19
10	28	0.0344	-0.0217	0.23	-0.03	0.18	1.4	24
11	36	0.0621	-0.0216	0.63	0.00	0.44	1.8	13
12	44	0.0517	-0.0176	0.52	0.00	0.47	3.7	15

MODEL OVERALL STATISTICS

RMSE = 0.6613 BAR		NO PT =	296
AAD = 0.3825 BAR		%AAD =	1.621
MIN DEV= -3.5681 BAR		MIN %DEV =	-14.605
MAX DEV= 3.2574 BAR		MAX %DEV =	8.672
BIAS = -0.0218 BAR		C-VAR =	0.040
RESTRICTIONS : P LE 0.90 PC		R-SQR =	0.987038
AUX. MODELS : 000 000 000/ 000 000			

SQUARE ERROR IN PRESSURE MINIMIZED

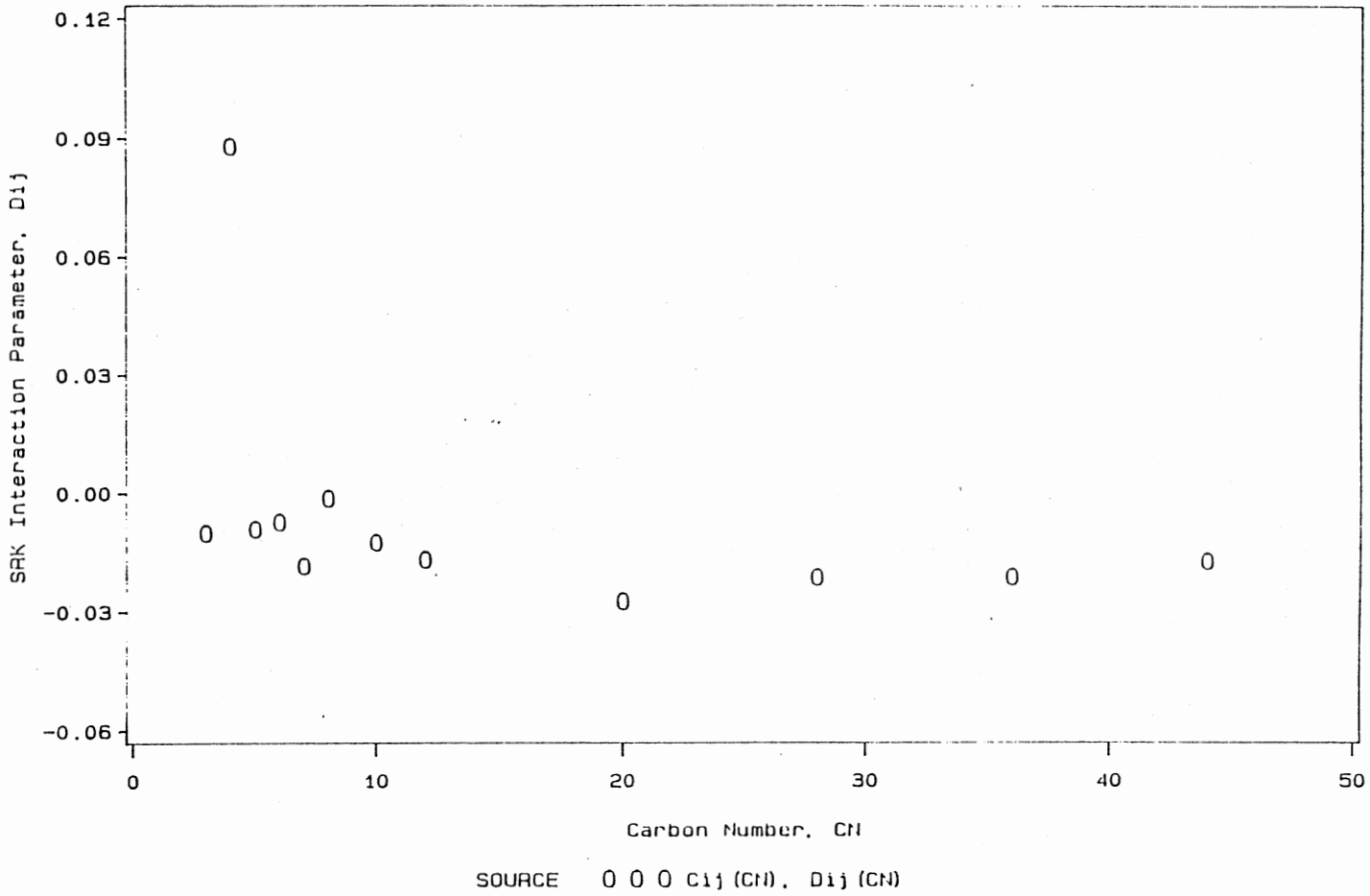

Figure 21. Molecular Size Effects on Dij for Ethane + n-Paraffins.

However, this does not hold true for Cij. As seen in Figure 22, Cij is dependent on carbon number. When only one parameter is used, Cij becomes increasingly more negative as carbon number increases, but if a second interaction parameter is used the value becomes increasingly more positive. In either case, a generalized formula might be developed for determining Cij as a function of carbon number.

Case 7: Cij(CN,T), Dij(CN,T)

This is the most specific use of interaction parameters. By applying two parameters to each isotherm of each binary, the best possible fit (subject to the chosen mixing rules for the EOS) is established. This enhanced fit is seen in Table XXVI, with a RMSE of 0.27 bar and a maximum deviation of 1.65 bar. The use of two interaction parameters for each isotherm appears to support the added complexity of application by the amount of improvement gained over the other six cases. Case 7 displays the "leveling" effect more than the other cases; there is no discernable difference between the light and heavy solvents, all being fitted equally well.

Figures 23 and 24 show the dependence on temperature of Dij and Cij respectively. Once again it appears that Dij is not greatly dependent on temperature. There might be a slight downward trend toward heavier hydrocarbons, although not enough to justify any function of temperature. The parameter Cij shows a much greater dependence on

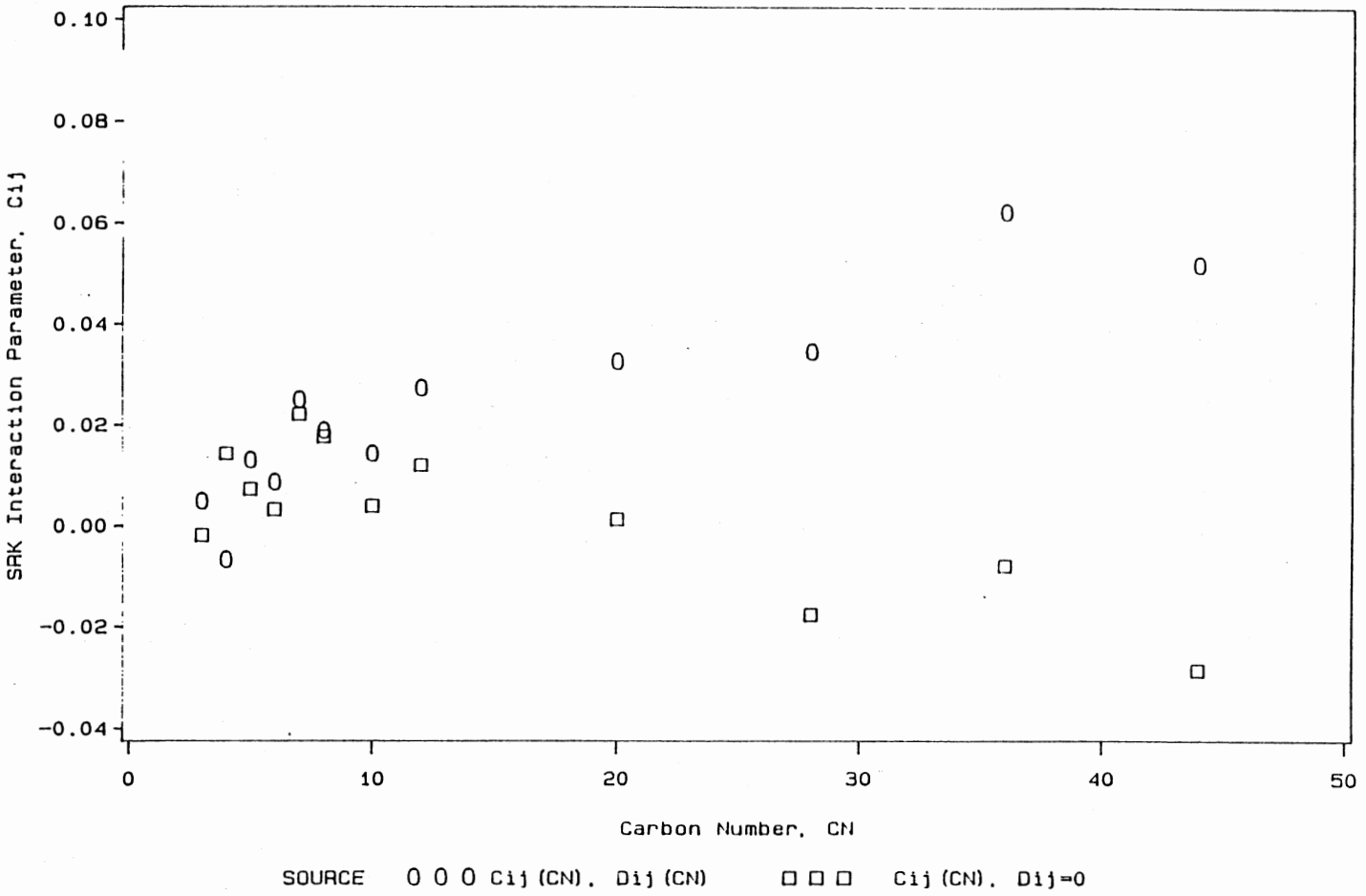

Figure 22. Molecular Size Effects on Cij for Ethane + n-Paraffins.

TABLE XXVI

BUBBLE-POINT CALCULATIONS USING THE SRK EQUATION OF STATE CASE 7

ISO	CN	T(K)	C(I,J)	D(I,J)	RMSE BAR	BIAS BAR	AAD BAR	%AAD	NO PT
1	3	310.9	0.0268	-0.0540	0.10	0.02	0.08	0.4	11
2	3	333.1	0.0005	0.0041	0.14	-0.03	0.12	0.3	8
3	3	355.4	-0.0022	0.0049	0.11	-0.01	0.10	0.2	7
4	4	338.7	0.0045	0.0510	0.55	-0.16	0.45	1.0	5
5	4	366.5	-0.0115	0.1020	0.79	-0.30	0.64	1.4	7
6	5	277.6	0.0114	-0.0072	0.04	-0.01	0.04	0.3	6
7	5	310.9	-0.0049	0.0083	0.06	0.00	0.04	0.2	10
8	5	377.6	0.0278	-0.0254	0.16	-0.01	0.13	0.6	11
9	6	310.9	-0.0002	0.0020	0.04	0.00	0.03	0.2	15
10	6	338.7	0.0026	-0.0043	0.05	0.01	0.03	0.3	11
11	6	366.5	0.0055	-0.0065	0.05	0.00	0.03	0.2	11
12	6	394.3	0.0246	-0.0210	0.08	-0.01	0.06	0.2	11
13	7	338.7	-0.0080	-0.0183	0.25	-0.05	0.20	0.4	7
14	7	394.3	0.0226	-0.0375	0.32	0.00	0.27	0.4	5
15	7	449.8	0.0607	-0.0184	0.24	-0.01	0.19	0.3	5
16	8	323.1	0.0195	-0.0099	0.12	0.02	0.11	0.3	11
17	8	348.1	0.0200	-0.0013	0.31	-0.04	0.28	1.8	13
18	8	373.1	0.0034	0.0155	0.15	0.02	0.13	1.2	9
19	10	310.9	0.0119	-0.0059	0.07	-0.01	0.06	0.7	10
20	10	344.3	0.0105	-0.0086	0.12	-0.01	0.11	0.7	6
21	10	377.6	0.0127	-0.0135	0.10	-0.01	0.08	0.4	5
22	10	410.9	0.0194	-0.0219	0.08	-0.01	0.06	0.3	6
23	12	373.1	0.0272	-0.0172	0.52	-0.01	0.41	1.9	35
24	20	323.1	0.0283	-0.0227	0.13	-0.02	0.12	0.9	6
25	20	373.1	0.0301	-0.0252	0.25	-0.04	0.21	0.9	6
26	20	423.1	0.0389	-0.0331	0.21	-0.03	0.19	0.7	7
27	28	348.1	0.0302	-0.0200	0.17	-0.01	0.15	1.0	10
28	28	373.1	0.0296	-0.0191	0.17	-0.03	0.14	1.3	7
29	28	423.1	0.0418	-0.0252	0.13	-0.02	0.11	0.8	7
30	36	373.1	0.0434	-0.0185	0.05	-0.01	0.04	0.5	7
31	36	423.1	0.0818	-0.0257	0.22	-0.03	0.20	1.2	6
32	44	373.1	0.0685	-0.0229	0.17	-0.01	0.15	1.1	9
33	44	423.1	0.0586	-0.0160	0.14	-0.02	0.13	1.0	6

MODEL OVERALL STATISTICS

RMSE	= 0.2697 BAR	NO PT	= 296
AAD	= 0.1678 BAR	%AAD	= 0.803
MIN DEV	= -1.6482 BAR	MIN %DEV	= -14.605
MAX DEV	= 1.5375 BAR	MAX %DEV	= 6.711
BIAS	= -0.0196 BAR	C-VAR	= 0.017
RESTRICTIONS	: P LE 0.90 PC	R-SQR	=0.998960
AUX. MODELS	: 000 000 000/ 000 000		
	SQUARE ERROR IN PRESSURE MINIMIZED		

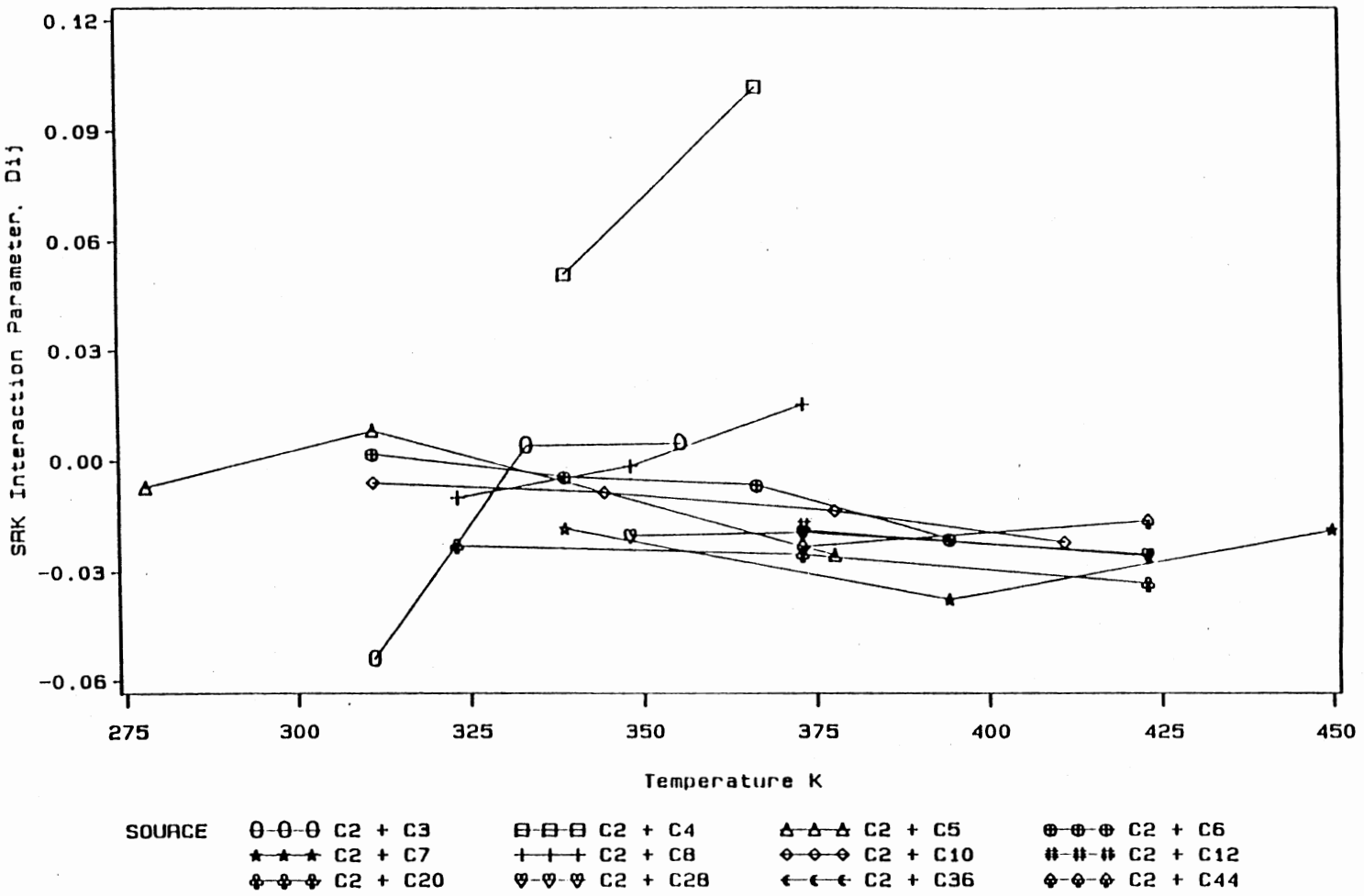

Figure 23. Temperature and Molecular Size Effects on Dij for Ethane + n-Paraffins.

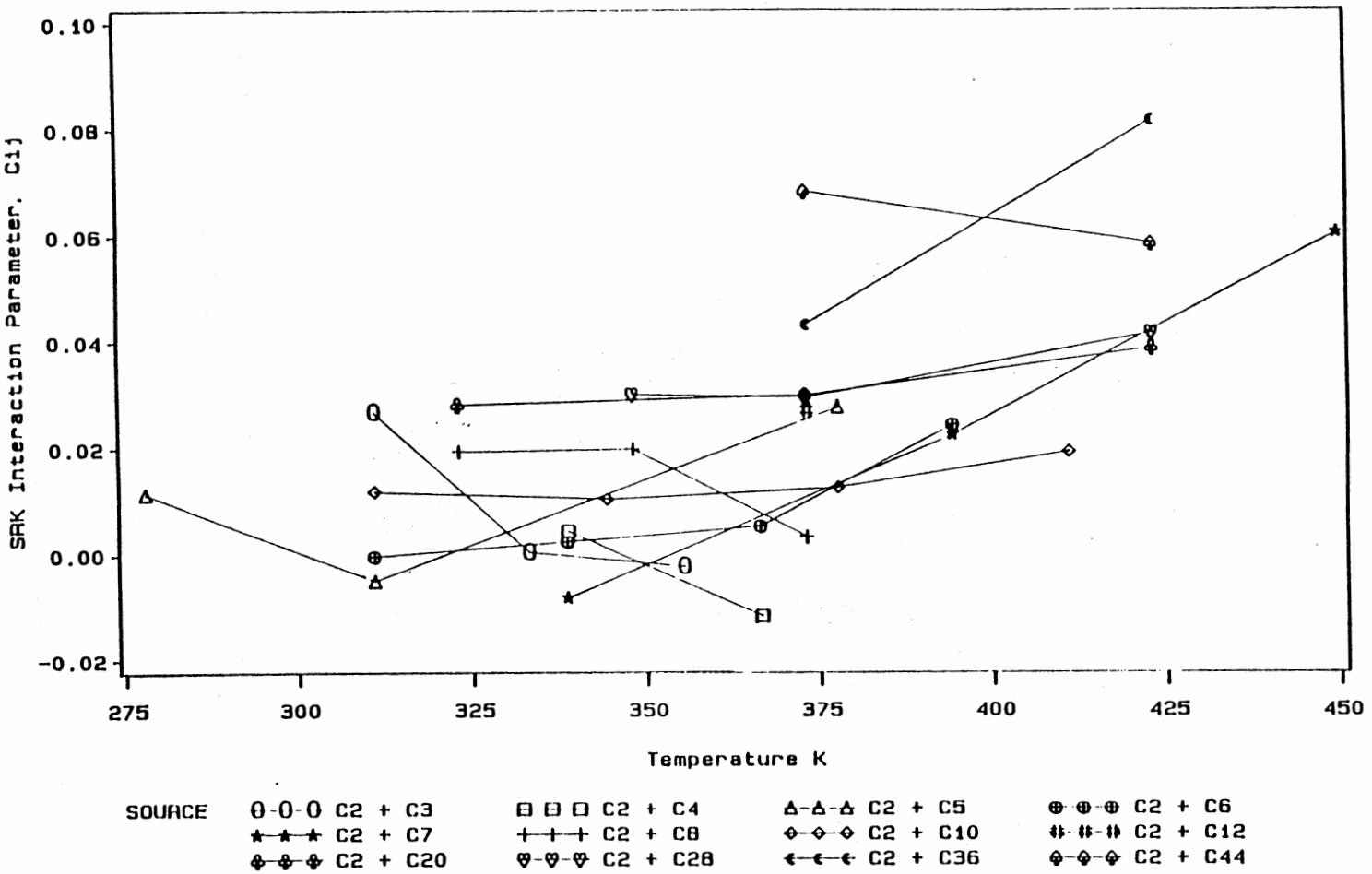

Figure 24. Temperature and Molecular Size Effects on Cij (Dij(T)) for Ethane + n-Paraffins.

temperature. When a second interaction parameter is used (shown in Figure 24) the dependence on temperature for Cij translates into an increasing value as solvent molecular weight increases, which is the opposite of that displayed in Figure 20, when only one parameter was used.

Summary

Table XXVII contains a summary of results obtained for Cases 1 through 7. The table also compares the SRK results with P-R results, showing that they are essentially identical. As stated earlier, the advantage of using specific interaction parameters is obvious in the decrease in RMSE from 1.49 in Case 1 to 0.27 in Case 7.

Although the use of a second interaction parameter clearly improves the quality of fit, as seen in the reduction of the RMSE, there is some uncertainty as to whether it is necessary to regress an individual Dij for each isotherm (Case 7) or even for each binary system (Case 6). As seen in Figure 21 and 23, Dij appears to be a consistent -0.02 at all conditions. In order to verify this suspicion Case 6 and 7 were rerun holding the value of Dij constant. Results, presented as RMSE, appear in Tables XXVIII and XXIX.

Tables XXVIII and XXIX show that varying Dij gives a better fit of experimental data than holding Dij constant. However, there appears to be a difference in the quality of fit depending on the molecular size of the solvent; the lighter the solvent the less the need for a specific Dij.

TABLE XXVII

SUMMARY OF RESULTS FOR CUBIC EOS REPRESENTATIONS FOR ETHANE + N-PARAFFINS

	Bars (P-R Results)				
Case	RMSE	BIAS	AAD	%AAD	MAX
1	1.49 (1.72)	-0.19 (-0.01)	1.04 (1.22)	4.77 (5.87)	5.30 (5.44)
2	1.43 (1.71)	0.14 (0.14)	1.01 (1.19)	4.95 (5.79)	4.93 (5.23)
3	1.08 (1.06)	0.13 (0.10)	0.73 (0.71)	3.58 (3.48)	3.56 (3.73)
4	0.91 (0.91)	0.11 (0.11)	0.62 (0.61)	3.24 (3.21)	3.54 (3.61)
5	0.95 (0.90)	0.02 (-0.09)	0.67 (0.63)	2.67 (2.53)	3.80 (3.43)
6	0.66 (0.63)	-0.02 (-0.03)	0.38 (0.37)	1.62 (1.62)	3.57 (3.32)
7	0.27 (0.31)	-0.02 (-0.04)	0.17 (0.17)	0.80 (0.82)	1.65 (2.33)

TABLE XXVIII

EFFECTS OF Dij ON THE OVERALL ERROR WHEN Cij(CN)

CN	Cij(CN) Dij(CN)	Cij(CN) Dij=0.00	Cij(CN) Dij=-0.01	Cij(CN) Dij=-0.02	Cij(CN) Dij=-0.03
		Root Mean Squared Error			
3	0.23	0.24	0.23	0.24	0.28
4	0.73	1.49	2.14	2.53	2.56
5	0.35	0.37	0.35	0.37	0.42
6	0.30	0.32	0.31	0.35	0.43
7	2.23	2.30	2.25	2.23	2.26
8	0.35	0.35	0.43	0.67	0.95
10	0.30	0.50	0.31	0.37	0.61
12	0.52	0.94	0.62	0.54	0.78
20	0.37	2.03	1.31	0.65	0.40
28	0.23	1.27	0.70	0.25	0.51
36	0.63	1.66	1.02	0.64	0.84
44	0.52	1.28	0.72	0.55	0.94
Overall	0.66	1.08	0.90	0.86	0.96

TABLE XXIX

EFFECTS OF Dij ON THE OVERALL ERROR WHEN Cij(CN,T)

	Root Mean Squared Error				
CN	Cij(CN,T) Dij(CN,T)	Cij(CN,T) Dij=0.00	Cij(CN,T) Dij=-0.01	Cij(CN,T) Dij=-0.02	Cij(CN,T) Dij=-0.03
3	0.10	0.18	0.16	0.14	0.12
3	0.14	0.15	0.22	0.20	0.46
3	0.11	0.11	0.13	0.12	0.11
4	0.55	1.35	1.64	1.96	1.52
4	0.79	1.64	1.80	2.03	2.66
5	0.04	0.07	0.05	0.10	0.17
5	0.06	0.11	0.21	0.32	0.43
5	0.16	0.37	0.26	0.17	0.17
6	0.04	0.05	0.17	0.30	0.44
6	0.05	0.08	0.09	0.22	0.36
6	0.05	0.08	0.06	0.14	0.22
6	0.08	0.30	0.17	0.08	0.15
7	0.25	0.54	0.34	0.26	0.41
7	0.32	1.27	0.96	0.66	0.41
7	0.24	0.52	0.32	0.25	0.38
8	0.12	0.32	0.12	0.33	0.63
8	0.31	0.31	0.41	0.64	0.91
8	0.15	0.28	0.41	0.56	0.70
10	0.07	0.16	0.12	0.34	0.58
10	0.12	0.29	0.13	0.37	0.66
10	0.10	0.40	0.14	0.21	0.47
10	0.08	0.86	0.47	0.11	0.32
12	0.52	0.94	0.62	0.54	0.78
20	0.13	1.38	0.77	0.20	0.43
20	0.25	1.95	1.17	0.46	0.43
20	0.21	2.29	1.59	0.91	0.30
28	0.17	1.06	0.55	0.17	0.53
28	0.17	1.14	0.55	0.18	0.61
28	0.13	1.57	0.94	0.34	0.31
36	0.05	1.31	0.59	0.11	0.77
36	0.22	1.76	1.06	0.43	0.35
44	0.17	1.53	0.85	0.25	0.47
44	0.14	0.73	0.30	0.22	0.60
Overall	0.27	0.91	0.64	0.54	0.69

This behavior is seen in both Table XXVIII (Cij(CN)) and XXIX (Cij(CN,T)). Figure 25 shows graphically the lack of sensitivity to Dij at low carbon numbers.

Figure 25 gives a clear indication of the effect Dij has on Cij; the more negative Dij, the more positive the slope of the Cij vs. solvent molecular size relationship. Also, this figure shows that if Dij is to be held constant, a value of about -0.02 gives results very similar to the case where both Cij and Dij are regressed as functions of solvent carbon number. Another point of interest is that when Dij=-0.01, Cij becomes relatively constant at a value of about 0.015 (These values are close to those for Case 5, where a single Cij and Dij are regressed for the entire data set). Further, if Dij is to be held constant, holding Cij constant as well, only decreases the quality of fit by 0.09 bar (from 0.86 bar when Cij(CN) and Dij=-0.02, to 0.95 bar for Case 5).

Table XXX provides some insight regarding the effects of solvent molecular size on the EOS predictions. This table reveals that two of the binary systems are not fit as well as the rest of the data sets. In the case of the ethane + n-heptane system, the abnormally large RMSE maybe the result of the larger temperature range of the data. This explanation is supported by the fact that the errors are more uniform in Cases 4 and 7, where an interaction parameter was used that was dependent on temperature. For the case of the ethane + n-butane system, the error seems to be more the result of data that is simply inconsistent with

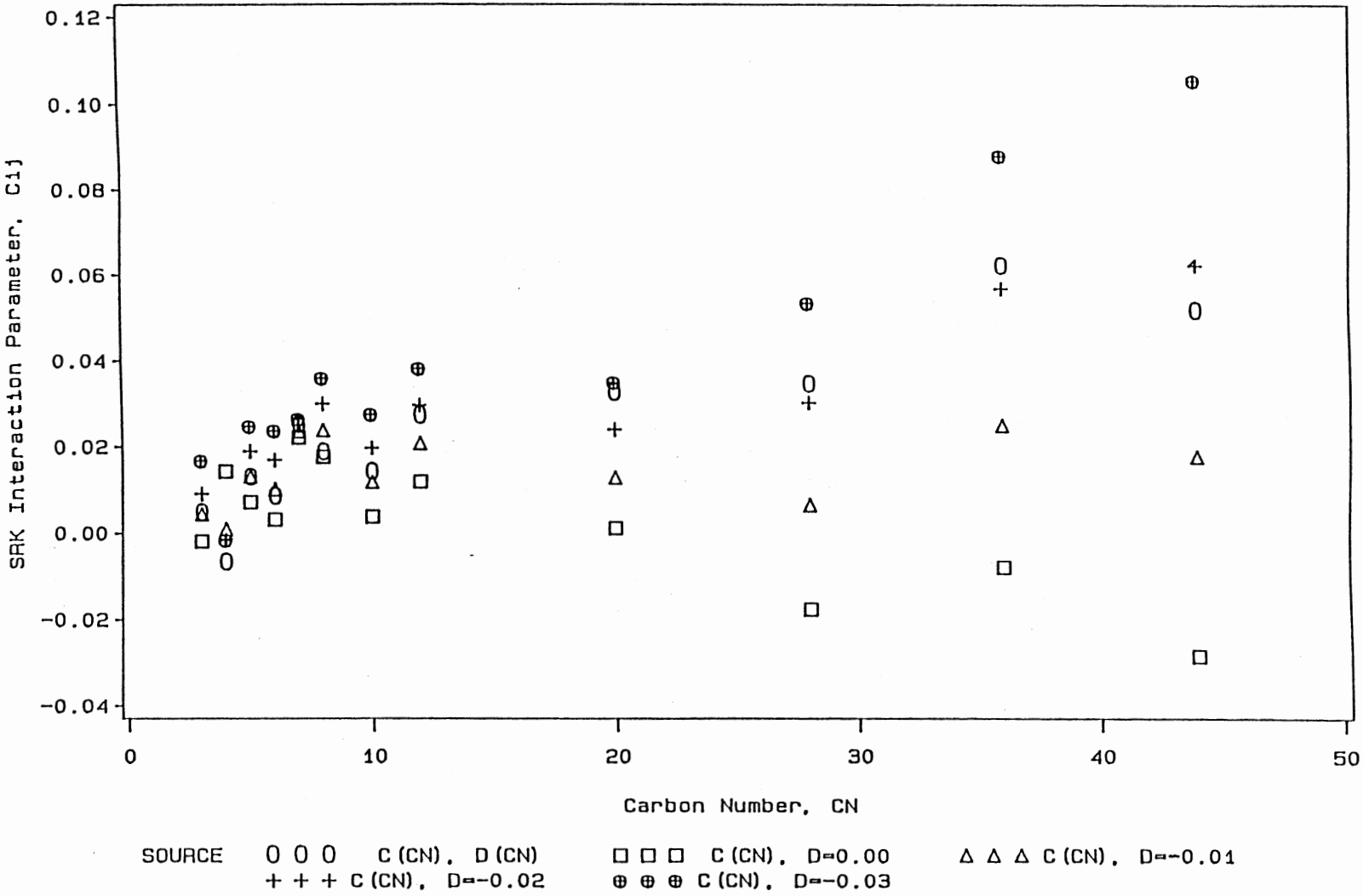

Figure 25. Effects of Dij on Values of Cij

TABLE XXX

EFFECTS OF PARAFFIN MOLECULAR SIZE ON SRK PREDICTIONS

	Root Mean Squared Error in Bubble Point (Bars)				
CN	Case: 1	3	4	6	7
3	0.25	0.24	0.15	0.23	0.12
4	1.90	1.49	1.50	0.73	0.67
5	0.49	0.37	0.18	0.35	0.07
6	0.37	0.32	0.13	0.30	0.06
7	2.94	2.30	0.78	2.23	0.27
8	1.49	0.35	0.30	0.35	0.19
10	0.61	0.50	0.42	0.30	0.09
12	1.72	0.94	0.94	0.52	0.52
20	2.03	2.03	1.87	0.37	0.20
28	1.95	1.27	1.26	0.23	0.16
36	1.75	1.65	1.54	0.63	0.14
44	1.91	1.28	1.13	0.52	0.16

the other data sets. This inconsistency is easily seen in Figures 21 and 23. The cause of the problem is not known. Figure 26 shows the results of Table XXX graphically. Even though the results are scattered for solvents lighter than C10, Figure 26 shows that there is a need for specific interaction parameters at the higher carbon numbers.

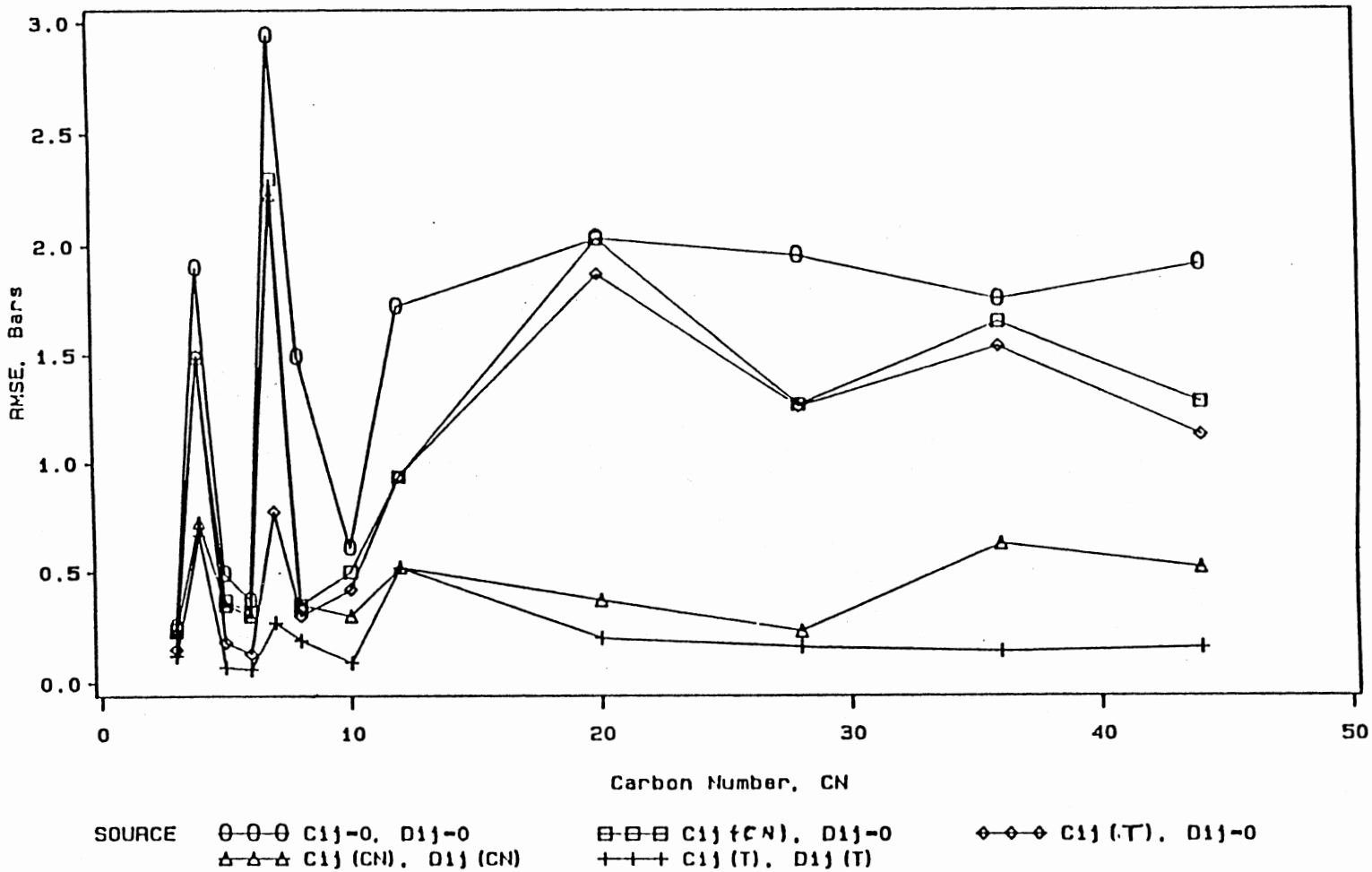

Figure 26. Effects of Interaction Parameter Usage and Molecular Size on SRK Predictions for Ethane + n-Paraffins.

CHAPTER IX

HENRY'S CONSTANTS

In addition to using the SRK and P-R equations of state to generate binary interaction parameters for ethane + paraffins, the Krichevsky-Kasarnovsky (K-K) equation (37) was used to determine Henry's constants and partial molar volumes of selected ethane mixtures. The purpose of finding the Henry's constants is to verify the consistance of the collected data. The K-K method is applicable to systems where the solubility of the solute in the solvent is small, and the solvent has a low vapor pressure. Because of these limitations the study of Henry's constants was restricted to the hydrocarbon solvent n-eicosane and heavier.

For a system at constant temperature and pressure, Henry's law can be used to find Henry's constants if the fugacity of the system is known. Unfortunately the data acquired in this study were not at constant temperature and pressure so adjustments had to be made. The effect of pressure on fugacity can be stated as

$$d\ln(f_i) = \bar{V}_i \, dP/RT \qquad (9.1)$$

where $\bar{V}_i$ is the partial molar volume of component "i". By integrating this equation from P1 to P2, and taking the partial molar volume as a constant, yields

$$\ln(f_{i,P2}/f_{i,P1}) = \bar{V}_i (P_2 - P_1)/RT \qquad (9.2)$$

By setting P1 in the above equation equal to the vapor pressure of the solvent (P^o), and then combining equation (9.2) with Henry's law results in

$$\ln(f_{i,P}/x_i) = \ln(H_i) + \bar{V}_i (P - P^o)/RT \qquad (9.3)$$

Since the systems under investigation contain solvents with very low vapor pressures, the fugacity of the vapor phase may be replaced with the fugacity of the pure solute at the same pressure, resulting in the final expression of

$$\ln(f_{c2}/x_{c2}) = \ln(H_{c2}) + \bar{V}_{c2}(P - P^o)/RT \qquad (9.4)$$

By plotting equation (9.4) as a straight line (ln(f/x) vs ($P-P^o$)), the y-intercept and slope yield the Henry's constant and partial molar volume, respectively. Figure 27 shows an example of this plot. Due to the low values of P^o, the value ($P-P^o$) has been replaced with just the bubble point pressure of the solvent. The higher pressures were ignored since Henry's law applys only to infinite dilution, and the higher the pressures the higher the deviations.

To use this method of determination the fugacity at different temperatures and pressures must be known. The most obvious source for fugacity is published literature, and although complete tables of fugacity could not be found, enough data is contained in the NBS Technical Note 684 'Thermophysical Properties of Ethane' (38) to determine the

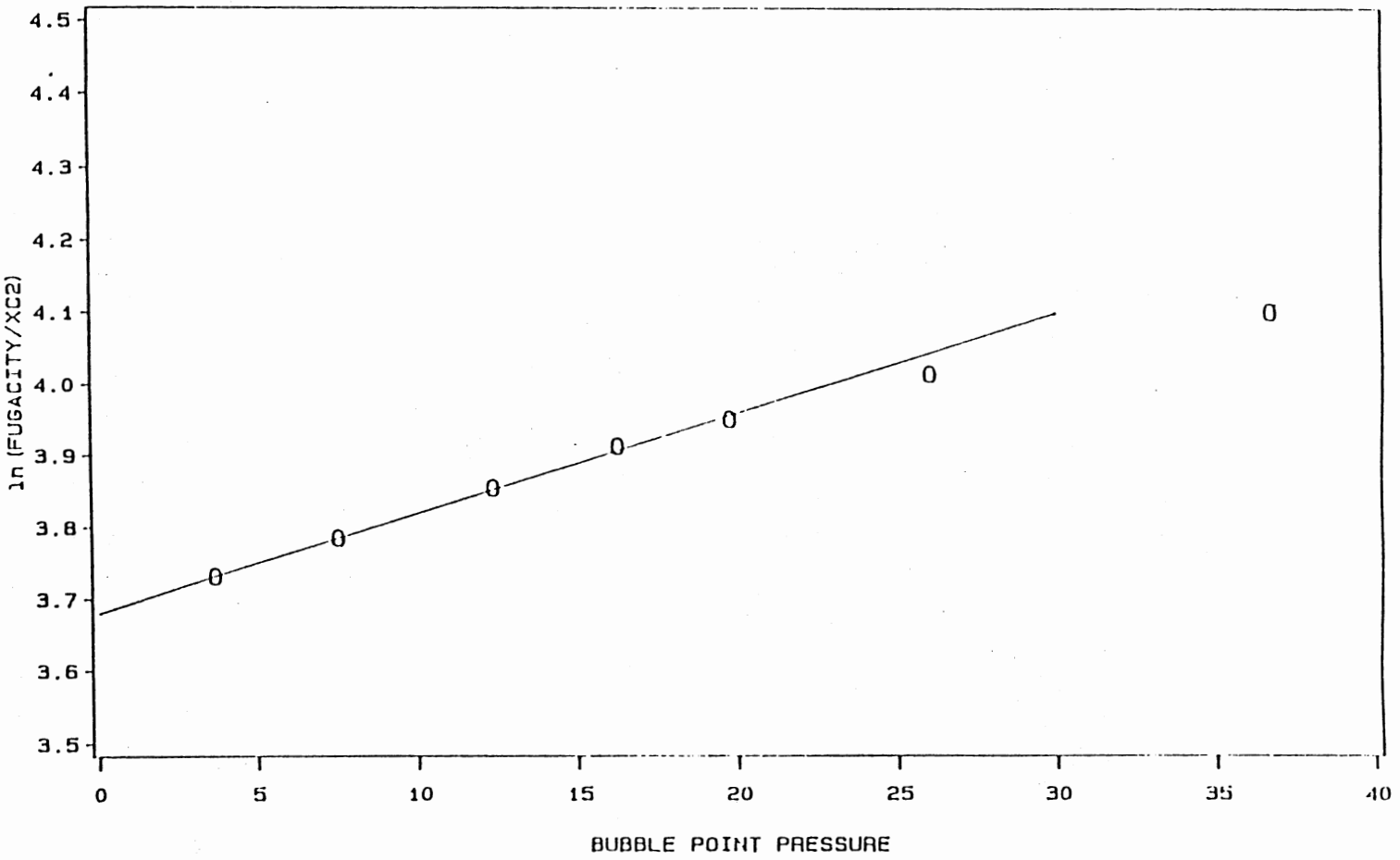

Figure 27. Krichevsky-Kasarnovsky (K-K) Method for Determination of Henry's Constants.

necessary fugacities. By using the following equation (39)

$$\ln(\phi) = \Delta S'/R - \Delta H'/RT \tag{9.5}$$

where $\Delta S'$ and $\Delta H'$ are residual entropy and enthalpy, respectively, the fugacity can be found at any listed temperature and pressure. However, this method is time consuming and not easily programable.

An alternate method is to use a virial equation to solve for the fugacity. Starting with equation (4) in the NBS note

$$Z = 1 + B(T)d/d_c + C(T)(d/d_c)^2 \tag{9.6}$$

or

$$Z = 1 + \bar{B}(T)/v + \bar{C}(T)/v^2 \tag{9.7}$$

where

$$\bar{B}(T) = B(T)/d_c \tag{9.8}$$

and

$$\bar{C}(T) = C(T)/d_c^2 \tag{9.9}$$

Since data are measured as a function of pressure (not volume) an expression in terms of pressure is needed

$$Z = 1 + B'P + C'P^2 \tag{9.10}$$

However, since

$$B' = \bar{B}/RT \qquad \text{and} \qquad C' = (\bar{C}-\bar{B}^2)/(RT)^2 \tag{9.11}$$

equation (9.10) becomes

$$Z = 1 + (\bar{B}(T)/RT)P + \left[(\bar{C}(T) - \bar{B}(T)^2)/(RT)^2\right] P^2 \qquad (9.12)$$

When equations (9.12), (9.8), and (9,9) are combined with

$$\ln(f) = \ln(P) + B'P + C'^2 P^2/2 \qquad (9.13)$$

the following equation is the result

$$\ln(f) = \ln(P) + (B(T)/d_c)P/RT + \frac{P^2}{2}\left[(C(T)/d_c^2 - B(T)/d_c)^2/(RT)^2\right] \qquad (9.14)$$

where B(T) and C(T) are given by equations (4-a) and (4-b) of the NBS technical notes

$$B(T) = B1 + B2(TC/T) + B3(TC/T)^2 + B4(TC/T)^{4.5} \qquad (9.15)$$

where

B1 = 0.522671 B3 = -0.592947

B2 = -1.106244 B4 = -0.041944

and

$$C(T) = (1-(TO/T))(C1(TC/T) + C2(TC/T)^3 + C3(TC/T)^5) \qquad (9.16)$$

where

C1 = 0.24423 C3 = 0.53488

C2 = 0.83253 TO = 217.8 K

As can be seen from Table XXXI the truncated virial equation does an excellent job of predicting fugacities at low pressures, and only slightly less accurate at higher

TABLE XXXI

PUBLISHED DATA VERSUS THE VIRIAL EQUATION FOR FUGACITY DETERMINATION

TEMP(K)	PRES (BARS)	VIRIAL EQUATION	NBS	DEV (VIR-NBS)
270.0	4.0	3.873	3.735	0.101
270.0	12.0	10.546	10.266	0.280
270.0	20.0	16.018	15.542	0.476
300.0	4.0	3.881	3.781	0.100
300.0	12.0	10.940	10.654	0.286
300.0	20.0	17.088	16.652	0.436
300.0	28.0	22.365	21.749	0.616
300.0	36.0	26.814	25.934	0.879
350.0	4.0	3.926	3.826	0.100
350.0	12.0	11.340	11.051	0.289
350.0	20.0	18.182	17.741	0.442
350.0	28.0	24.472	23.894	0.578
350.0	36.0	30.226	29.543	0.683
350.0	44.0	35.463	34.691	0.772
350.0	52.0	40.203	39.354	0.849

pressures, with the largest error in the neighborhood of 3.0% of actual values. This method contains the added benefit of being easily coded directly into a program using the K-K equation.

A still simpler alternative is to use the SRK equation of state program used in the C2 + paraffin study. This program, coded by Gasem (3), provides values for the fugacity-mole fraction ratio which, are easily used in the K-K program. Table XXXII shows a comparison of fugacities determined from the virial equation and the SRK for selected points of interest in this study.

The data were regressed, using both the virial and the SRK generated fugacities, with equation (9.4) to generate Henry's constants and partial molar volumes. The resulting values are given in Table XXXIII. Figures 28 to 31 show K-K plots for each isotherm.

Table XXXIV shows a comparison of Henry's constants from other investigators with data of this work. Figure 32 shows that all investigators are in general agreement.

TABLE XXXII

COMPARISON OF THE VIRIAL EQUATION VERSUS THE SRK EQUATION FOR FUGACITY DETERMINATION

CN	TEMP(K)	MOLE FRACTION	VIRIAL EQUATION	SRK
20	323.2	0.1489	4.893	4.897
		0.3199	11.788	11.801
		0.5534	23.496	23.531
20	423.2	0.1180	9.100	9.118
		0.3240	29.004	29.196
		0.5820	63.254	64.736
28	348.2	0.1490	5.731	5.736
		0.3500	15.997	16.054
		0.5200	26.710	26.853
28	423.2	0.1020	6.797	6.808
		0.2530	18.773	18.851
		0.5000	45.466	46.070
36	373.2	0.0872	3.632	3.634
		0.2506	11.802	11.821
		0.5309	31.805	32.019
36	423.2	0.1530	9.415	9.440
		0.3150	21.821	21.911
		0.4680	38.239	38.629
44	373.2	0.1101	3.813	3.817
		0.3598	16.138	16.169
		0.5161	27.532	27.653
44	423.2	0.0986	5.202	5.208
		0.2088	11.963	11.996
		0.3404	21.402	21.493

TABLE XXXIII

HENRY'S CONSTANTS AND MOLAR VOLUMES
FOR ETHANE IN N-PARAFFINS USING
THE K-K MODEL

CN	TEMP(K)	VIRIAL H (BAR)	VIRIAL V (CC/MOL)	SRK H (BAR)	SRK V (CC/MOL)
20	323.2	32.3 (0.6)	250 (23)	32.4 (0.6)	252 (23)
20	373.2	56.5 (0.7)	156 (9)	56.5 (0.6)	164 (8)
20	423.2	75.7 (1.2)	173 (11)	75.6 (1.1)	184 (11)
28	348.2	36.8 (0.4)	319 (17)	36.8 (0.4)	324 (17)
28	373.2	47.4 (0.2)	254 (4)	47.4 (0.2)	260 (5)
28	423.2	64.2 (0.5)	243 (8)	64.2 (0.4)	252 (8)
36	373.2	40.8 (0.6)	343 (22)	40.8 (0.6)	350 (22)
36	423.2	56.7 (0.3)	299 (7)	56.7 (0.3)	308 (6)
44	373.2	33.4 (0.6)	494 (27)	33.4 (0.6)	500 (27)
44	423.2	49.9 (0.4)	362 (14)	49.9 (0.4)	370 (15)

* Standard deveation listed in ( )

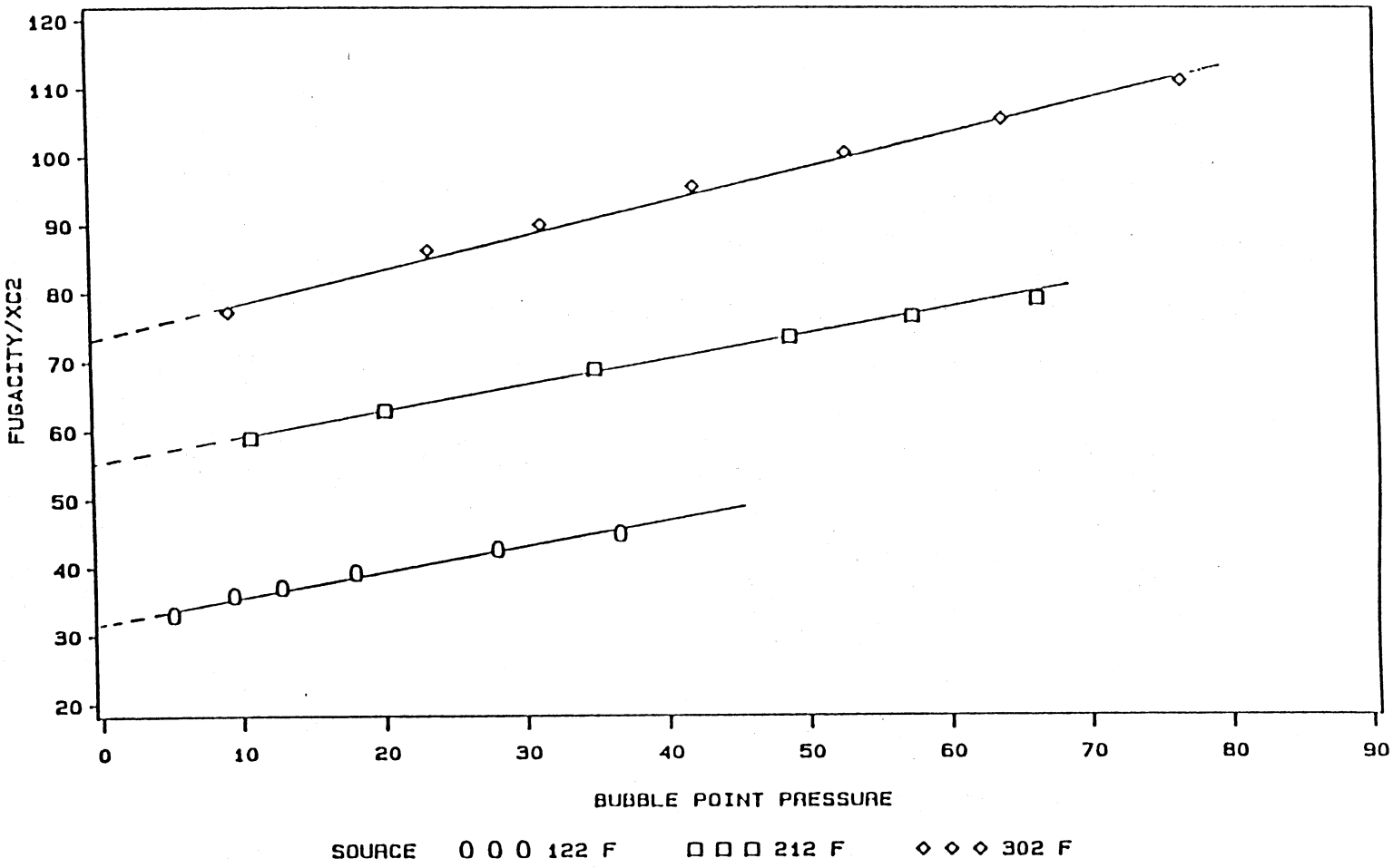

Figure 28. K-K Plots for Ethane + n-Eicosane.

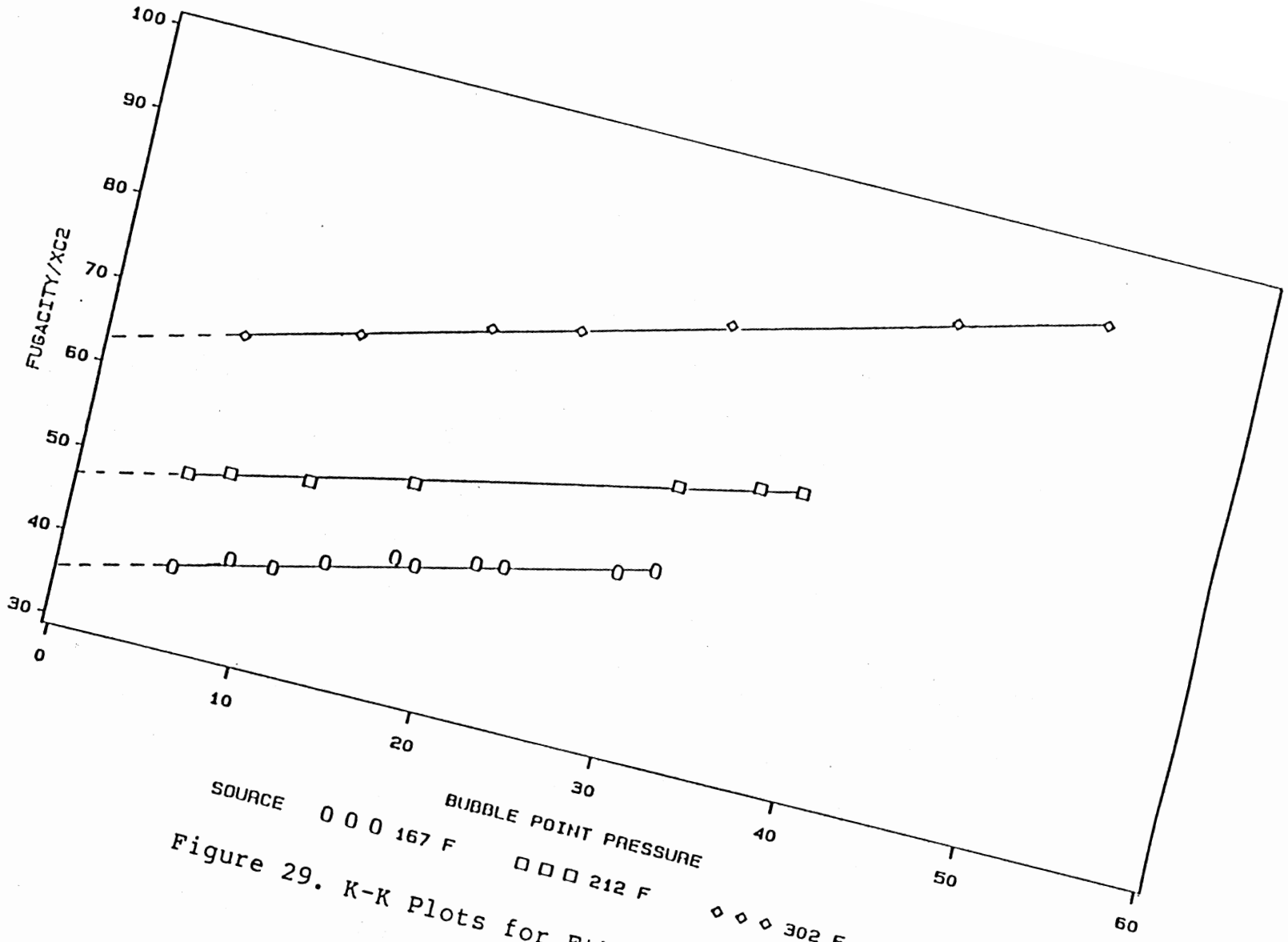

Figure 29. K-K Plots for Ethane + n-Octacosane.

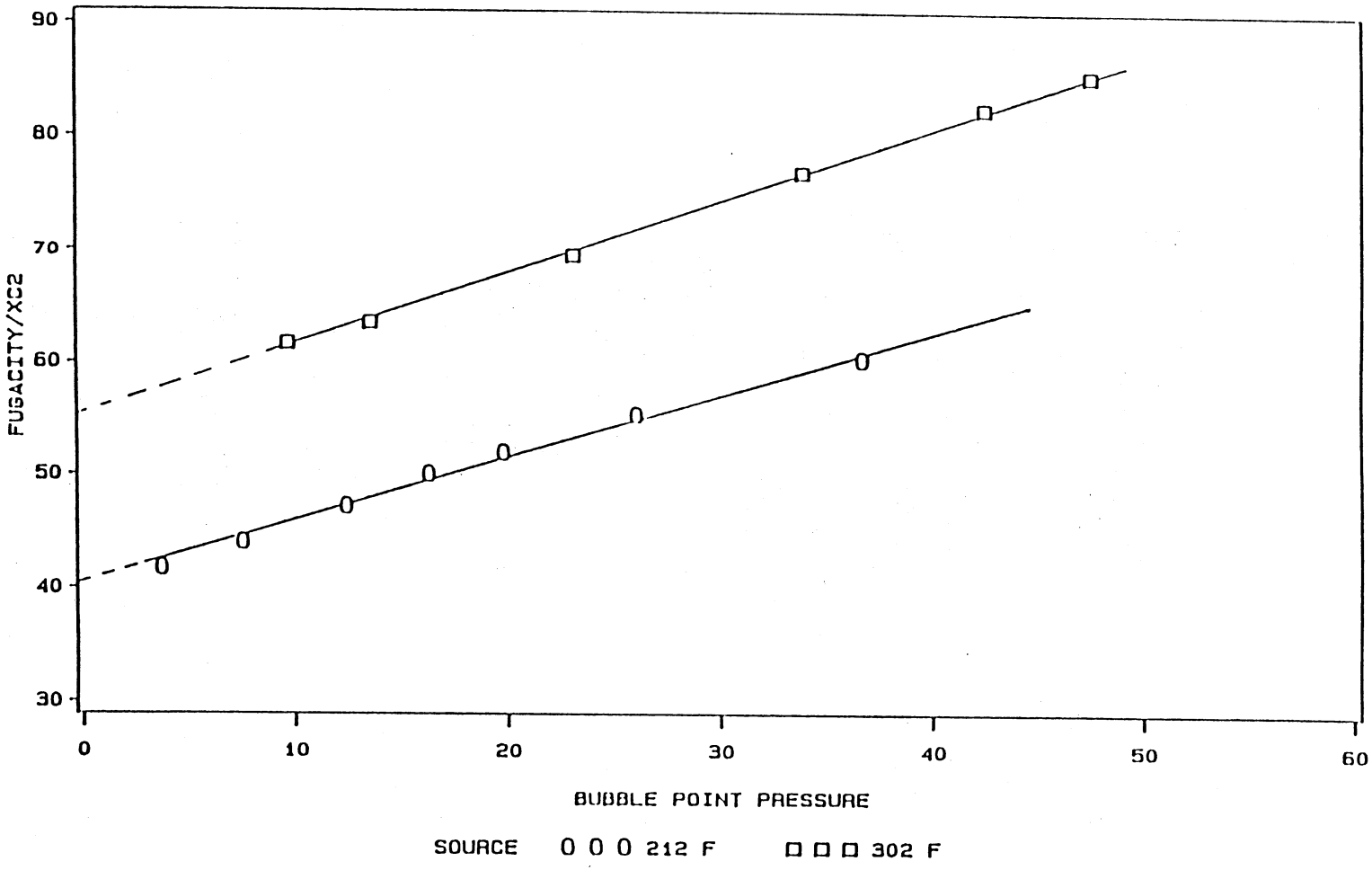

Figure 30. K-K Plots for Ethane + n-Hexatriacontane.

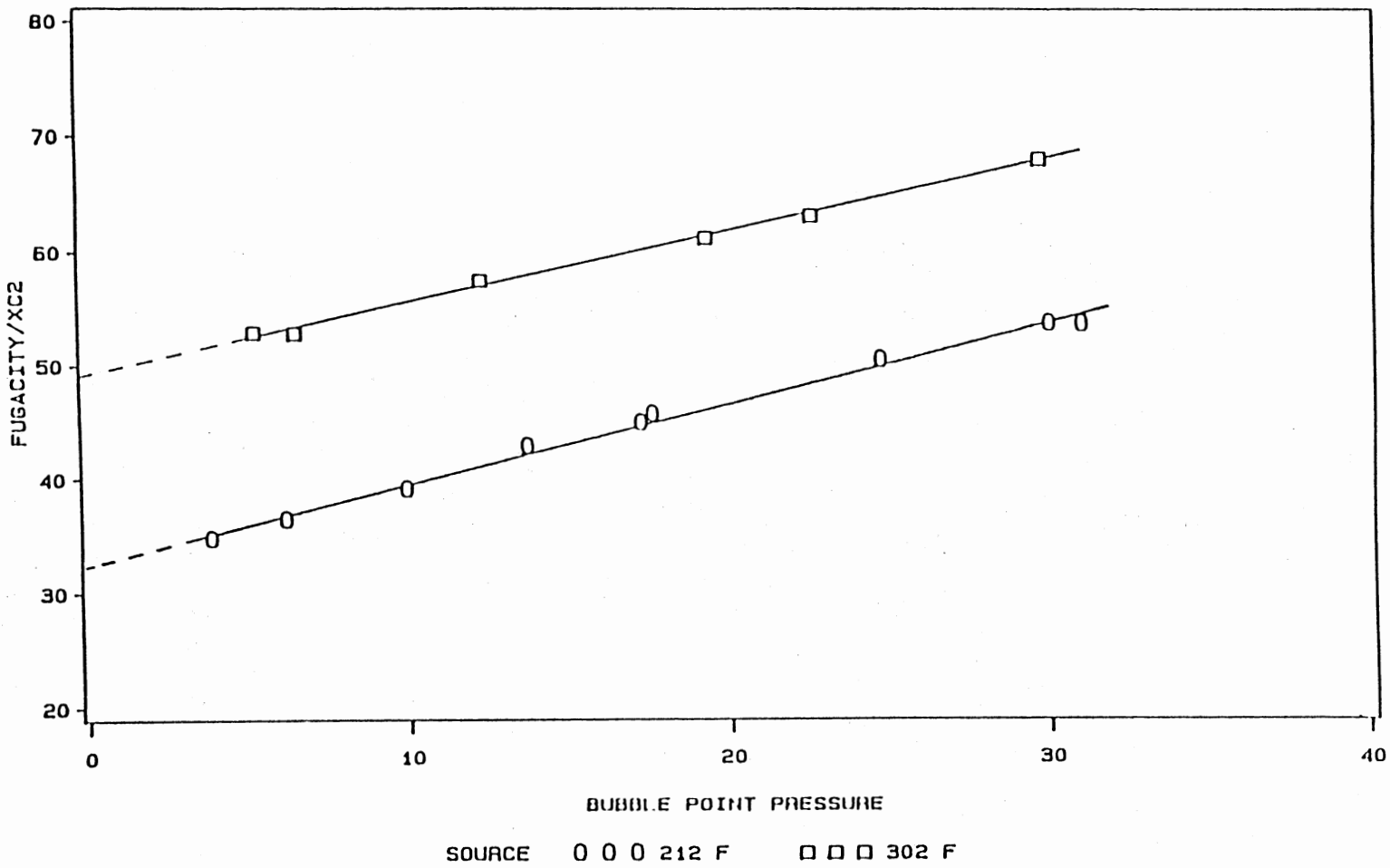

Figure 31. K-K Plots for Ethane + n-Tetratetracontane.

TABLE XXXIV

COMPARISONS OF HENRY'S CONSTANTS
FOR ETHANE + N-PARAFFIN SYSTEMS

CN	TEMP(K)	THIS WORK H (BAR)	LITERATURE H (BAR)	SOURCE
20	373.2	56.5	55.7	40
28	373.2	47.4	48.6	40
			46.1	41
36	373.2	40.8	41.5	40
			38.5	41

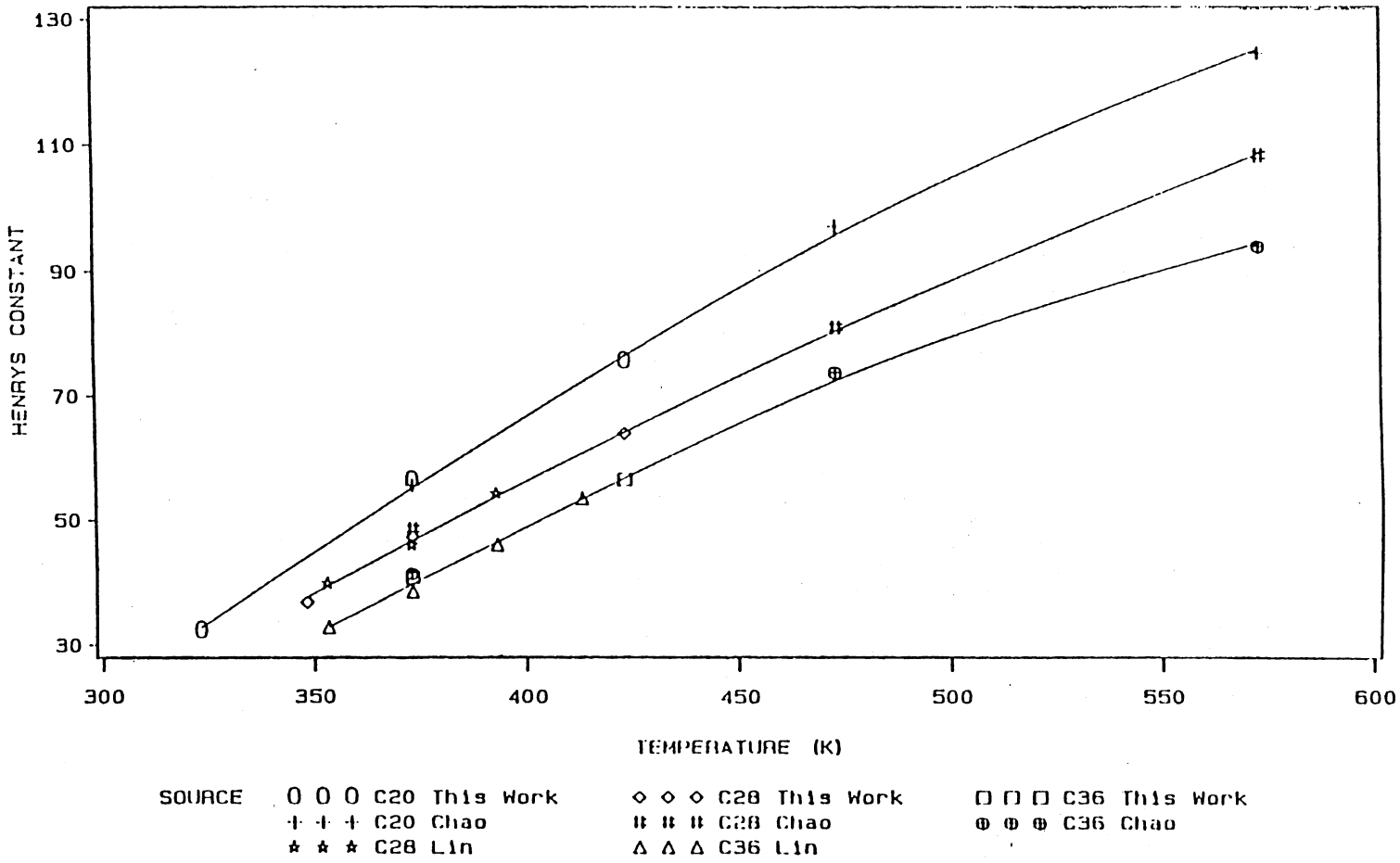

Figure 32. Comparisons of Henry's Constants for Ethane + n-Paraffins.

CHAPTER X

CONCLUSIONS AND RECOMMENDATIONS

This study includes the experimental determination of solubility data for CO2 + benzene at 40 C, and ethane + n-hexane, n-eicosane, n-hexatriacontane, and n-tetratetracontane at temperatures from 50 C to 150 C. The data were employed to determine EOS binary interaction parameters and Henry's constants. A study of the general behavior of ethane + n-paraffins systems was also performed. Based on this work, the following conclusions and recommendations are made:

Conclusions

1) The solubility of CO2 in benzene at 40 C has been measured with precision in the mole fractions of 0.002. These data are consistent with other investigators, leading to the conclusion that the apparatus and procedures used in this study are reliable.

2) Ethane solubilities in selected paraffins have been measured at temperatures ranging from 50 C to 150 C and pressures from 53.4 psia to 783.0 psia; uncertainty in the measured pressures are less then 2 psia, and mole fractions are measured to within 0.004.

3) The data on ethane binary systems are represented

adequately by both the SRK and P-R equations of state. The fit using these EOS becomes increasingly better as more specific interaction parameters are used. The addition of a second interaction parameter, Dij, improved the quality of fit. The most specific use of Cij and Dij yielded an overall RMSE error of 0.27 bar.

4) Both Cij and Dij show a dependence on solvent size for solvents smaller than C10. However, Dij seems to become constant at high solvent molecular weights and would be adequately represented by a constant value of -0.02. For the heavier hydrocarbon solvents, Cij shows variation with molecular size, but its functional dependence changes depending on whether one or two parameters are used.

5) Both Cij and Dij show some dependence on temperature. However, Dij appears to be a more consistent function then does Cij. It seems unlikely that a proper correlation can be developed expressing Cij as a function of temperature until a more complete range of data is collected.

6) The apparatus works well. The short time required for the system to come to equilibrium indicates that there is substantially less dead space in the cell than in previous studies. Reconstruction of the apparatus has simplified the necessary maintenance.

Recommendations

1) Further studies should be conducted on ethane + paraffins to complement the work already done. These new

studies should include a wider range of temperatures for existing data, as well as the study of different solvents with ethane. Such studies will increase the existing data base and could be used to establish correlations for Cij and Dij as functions of temperature and solvent size.

2) Other solutes (e.g. N2, CH4) should be investigated with n-paraffins. By comparing data from different solutes a refinement of the correlations proposed above might be possible.

3) A new equilibrium cell should be developed that further minimizes dead space. Such a cell has been suggested by Gasem. The cell would be in the shape of an inverted "U", and by making injections from the bottom it would be possible to almost eliminate dead space. Further investigation into this cell is needed.

4) A stirring mechanism should be added to the storage vessel to help with the degasing procedures as well as cleanup.

SELECTED REFERENCES

1. Anderson, J. M., "High Pressure Solubilities of Carbon Dioxide in Benzene, Cyclohexane, Naphthalene and Trans-Decalin", M.S. Thesis, Oklahoma State University, Stillwater, OK. (1985).

2. Bufkin, B. A., "High Pressure Solubilities of Carbon Dioxide and Ethane in Selected Paraffinic, Naphthenic and Aromatic Solvents", M.S. Thesis, Oklahoma State University, Stillwater, OK. (1986).

3. Gasem, K. A. M., "Binary Vapor-Liquid Equilibrium for Carbon Dioxide + Heavy Normal Paraffins", Ph.D. Dissertation, Oklahoma State University, Stillwater, OK. (1986).

4. Kim, C.-H., P. Vimalchand, and M. D. Donohue, "Vapor-Liquid Equilibria for Binary Mixtures of Carbon Dioxide with Benzene, Toluene, and P-Xylene", Fluid Phase Equilibria 31, 299 (1986).

5. Gupta, M. K., Y.-H. Li, B. J. Hulsey, and Robert L. Robinson, Jr., "Phase Equilibrium for Carbon Dioxide-Benzene at 313.2, 353.2, and 393.2K", J. Chem. Eng. Data 27, 55 (1982).

6. Ohgaki, K., and T. Katayama, "Isothermal Vapor-Liquid Equilibrium Data for Binary Systems Containing Carbon Dioxide at High Pressures: Methanol-Carbon Dioxide, n-Hexane-Carbon Dioxide, and Benzene-Carbon Dioxide", J. Chem. Eng. Data 10, 307 (1965).

7. Orbey, H., "Vapor-Liquid Equilibria of Carbon Dioxide-Hydrocarbon Systems at Moderately High Pressure", Ph.D. Thesis, McGill University, Montreal (1983).

8. Matschke, D. E., and G. Thodos, "Vapor-Liquid Equilibria in the Ethane-Propane System", J. Chem. Eng. Data 7, 232 (1962).

9. Mehra, V. S., and G. Thodos, "Vapor-Liquid Equilibrium in the Ethane-n-Butane System", J. Chem. Eng. Data 10, 307 (1965).

10. Reamer, H. H., B. H. Sage, and W. N. Lacey, "Phase Equilbria in Hydrocarbon Systems", J. Chem. Eng. Data 5, 44 (1960).

11. Zais, E. J., and I. H. Silberberg, "Vapor-Liquid Equilibria in the Ethane-n-Hexane System", J. Chem. Eng. Data 15, 253 (1970).

12. Mehra, V. S., and G. Thodos, "Vapor-Liquid Equilibrium in the Ethane-n-Heptane System", J. Chem. Eng. Data 10, 211 (1965).

13. Rodriques, A. B. J., D. S. McCaffrey, Jr., and J. P. Kohn, "Heterogeneous Phase and Volumetric Equilibrium in the Ethane-n-Octane System", J. Chem. Eng. Data 13, 164 (1968).

14. Robinson, R. L. Jr., J. M. Anderson, M. W. Barrick, B. A. Bufkin, and C. H. Ross, "Phase Behavior of Coal Fluids: Data for Correlation Development", DE-FG22-83PC60039-12, Final Report, Department of Energy, January (1987).

15. Lee, K. H., and J. P. Kohn, "Heterogeneous Phase Equilibrium in the Ethane-n-Dodecane System", J. Chem. Eng. Data 14, 292 (1969).

16. Meskel-Lesante, M. D. Richon, and H. Renon,"New Variable Volume Cell for Determining Vapor-Liquid Equilibria and Saturated Liquid Molar Volumes by the Static Method", Ind. Eng. Chem. Fund. 20, 284 (1981).

17. Wichterle, I., et. al, J. Chem. Eng. Data. 17, 13 (1972).

18. Parikh, J. S., R. F. Bukacek, L. Graham, and S. Liepziger, "Dew and Bubble Point Measurements for a Methane-Ethane-Propane Mixture", J. Chem. Eng. Data 29, 301 (1984).

19. Liave, F. M., K. D. Luks, and J. P. Kohn, "Three-Phase Liquid-Liquid-Vapor Equilibria in the Methane+ Ethane+n-Hexane and Methane+Ethane+n-Heptane Systems", J. Chem. Eng. Data 31, 418 (1986).

20. Van Horn, L. D., and R. Kobayashi, "Vapor-Liquid Equilibria of Light Hydrocarbons at Low Temperatures and Elevated Pressures in Hydrocarbon Solvents: Methane-Propane-n-Heptane, Methane-Ethane-n-Heptane, and Methane-Propane-Toluene Systems", J. Chem. Eng. Data 12, 294 (1967).

21. Lhotak, V., et. al, Fluid Phase Equilibria. 12, 307 (1983).

22. Uchytil, P.,and I. Wichterle, "Liquid-Vapor Critical Region of the Most Volatile Component of a Ternary System", Fluid Phase Equilibria 15, 209 (1983).

23. Dingrani, J. G.,and G. Thodos, " Vapor-Liquid Equilibrium Behavior of the Ethane-n-Butane-n-Hexane System", Can. J. Chem. Eng. 56, 616 (1978).

24. Mehra, V. S., and G. Thodos, "Vapor-Liquid Equilibrium Constants for the Ethane-n-Butane-n-Heptane System at 300 and 350 F", J. Chem. Eng. Data 13, 155 (1968).

25. Eubank, P. T., et. al, "A Review of Experimental Techniques for Vapor Liquid Equilibria at High Pressure", H. Knapp and S. I. Sandler (Editors), Int. Conf. on Phase Equilibria and Fluid Properties in Chemical Industry, Dechema, Frankfurt, Part II, 675 (1980).

26. Li, Y. H., K. H. Dillard, and Robert L. Robinson, Jr., "Vapor-Liquid Phase Equilibrium for Carbon Dioxide-n-Hexane at 40, 80, and 120 C", J. Chem. Eng. Data 26, 53 (1981)

27. Malanowski, S., "Experimental Methods for Vapor-Liquid Equilibria. II Dew- and Bubble-Point Method", Fluid Phase Equilibria 9, 311 (1968).

28. Ng, H., S. S. -S. Huang, and D. B. Robinson, "Equilibrium Phase Properties of Selected m-Xylene Binary Systems. m-Xylene-Methane and m-Xylene-Carbon Dioxide", J. Chem. Eng. Data 27, 119 (1982).

29. Rousseaux, P., D. Richon, and H. Renon, "A Static Method of Determination of Vapour-Liquid Equilibria and Saturated Liquid Molar Volumes at High Temperatures Using a New Variable-Volume Cell", Fluid Phase Equilibria 11, 153 (1983).

30. Prausnitz, J. M., Molecular Thermodynamics of Fluid-Phase Equilibria, Prentice-Hall, Englewood Cliffs, N.J. (1969).

31. Robinson, R. L., "Review of Phase Equilibrium Thermodynamics", Class Notes, Cheng 5843, Oklahoma State University, (1987).

32. Soave, G., "Equilibrium Constants from a Modified Redlich- Kwong Equation of State", Chem. Eng. Sci., 27 (1972).

33. Robinson, D. B., "A New Two-Constant Equation of State", Ind. Eng. Chem. Fundam., 15 (1976).

34. Ross, C. H., "Solubilities of Ethane in Selected Hydrocarbon Solvents", M.S. Report, Oklahoma State University, Stillwater Oklahoma (1987).

35. Barrick, M. W., "High Pressure Solubility of Carbon Dioxide in Aromatic Solvents Benzene, Naphthalene, Phenanthrene, and Pyrene", M.S. Thesis, Oklahoma State University, Stillwater Oklahoma (1985).

36. Ely, H. F., et. al, NBS Technical Notes, 1039 (1981).

37. Krichevsky, I. R., and J. S. Kasarnozsky, "Thermodynamical Calculations of Solubilities of Nitrogen and Hydrogen in Water at High Pressures", J. Am. Chem. Soc. 57, 2168 (1935).

38. Goodwin, R., "Thermophsical Properties of Ethane, from 90 to 600 K at Pressures to 700 Bar", NBS Technical Note 684, U.S. National Bureau of Standards, Washington D.C. (1977).

39. Van Ness, H. C., Classical Thermodynamics of Nonelectrolyte Solutions with Applications to Phase Equilibria, McGraw-Hill, New York (1982).

40. Chao, K. C., Final Report to the Department of Energy, Contract No. DE-AC22-84PC70024, Purdue University, West Lafayette, IN (1987).

41. Lin, P. J., and J. F. Parcher, "Direct Gas Chromatographic Determination of the Solubilities of Light Gasses in Liquids. Henry's Law Constants for Eleven Gasses in n-Hexadecane, n-Octacosane, and n-Hexatriacontane", J. Chromatographic Sci. 20, 33 (1982).

APPENDIX

STATISTICS USED IN THIS STUDY

TABLE XXXV

STATISTICS USED IN THIS STUDY

Statistic	Definition	Description
$\bar{X}$	$\frac{\sum_{n} X_i}{n}$	The arithmetic average of n observations.
DEV	$(X_{cal}-X_{exp})$	Deviation of a calculated value for a variable from the experimentally observed one.
AAD	$\frac{\sum_{n} \lvert DEV \rvert}{n}$	The arithmetic average of the absolute values of the deviations of n observations.
BIAS	$\frac{\sum_{n} DEV}{n}$	The arithmetic average of the deviations of n observations.
RMSE	$(\frac{\sum_{n} DEV^2}{n})^{1/2}$	The standard deviation of n observations. It is the square root of the mean of the squared deviations.

VITA

Aaron M. Raff

Candidate for the Degree of

Master of Science

Thesis: EXPERIMENTAL DETERMINATION OF THE SOLUBILITIES OF ETHANE IN SELECTED N-PARAFFIN SOLVENTS

Major Field: Chemical Engineering

Biographical:

Personal Data: Born in New York City, New York, May 27, 1964, the son of Lionel M. and Murna J. Raff.

Education: Graduated from Stillwater High School, Stillwater, Oklahoma, in May 1982; Received Bachelor of Science in Chemical Engineering from Oklahoma State University in May, 1986; completed requirements for the Master of Science degree at Oklahoma State University in May 1989.

Professional Experience: Research Assistant, Department of Chemical Engineering, Oklahoma State University, September, 1986, to October 1988.